

测光数据处理

黄样(中国科学院大学)

huangyang@ucas.ac.cn

2023/06/13

目录

- 大规模巡天简史
- 准备知识（不完备）
- 探测器性能标定
- 天测与测光
- 流量定标
- Pipeline in Python: all in all

大规模巡天简史

人眼时代



1609 – 1850s

照相底片时代



1898 Pleiades negative, drying rack, and darkroom tray

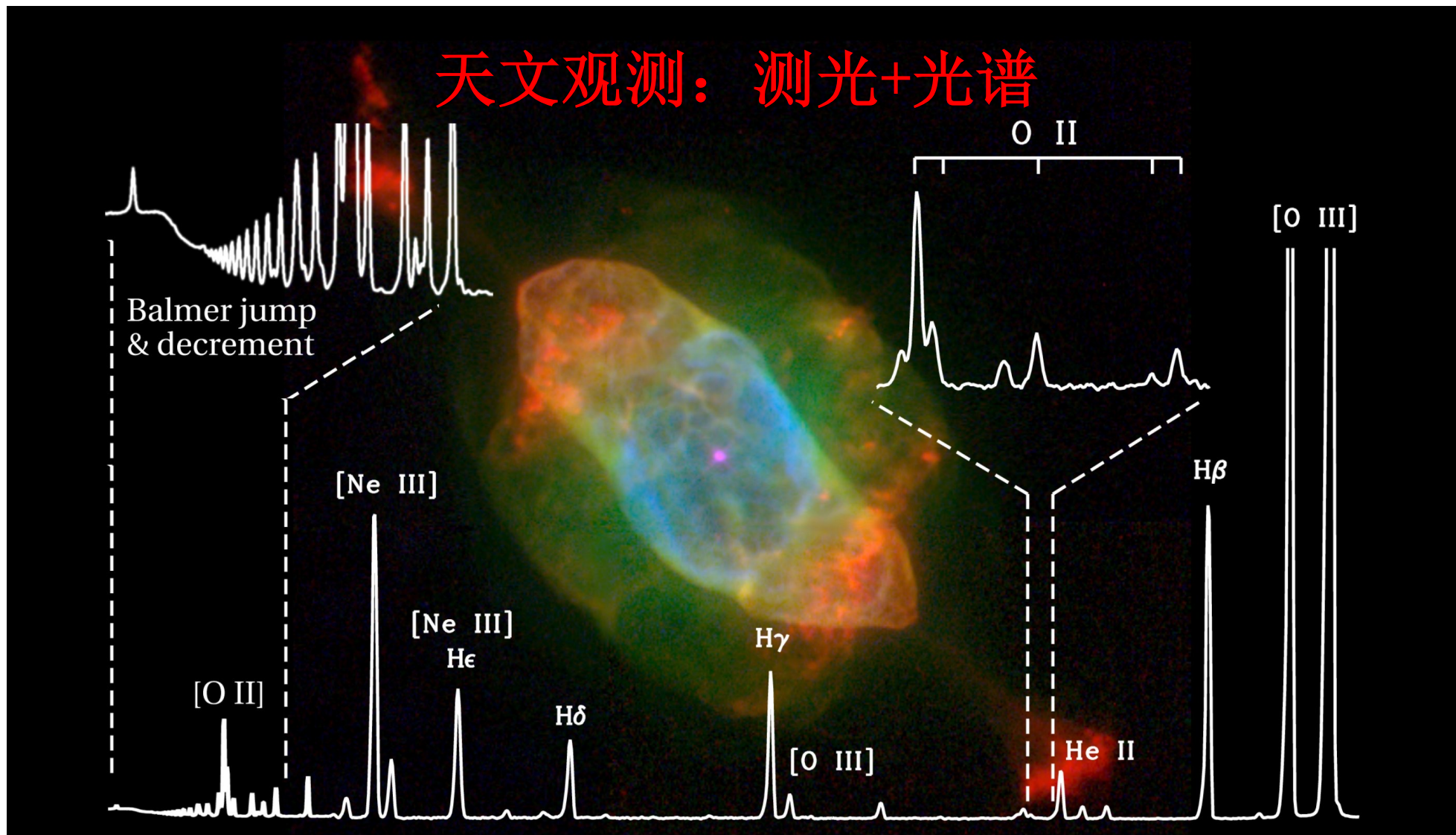
1850s – 1980s

数字化时代

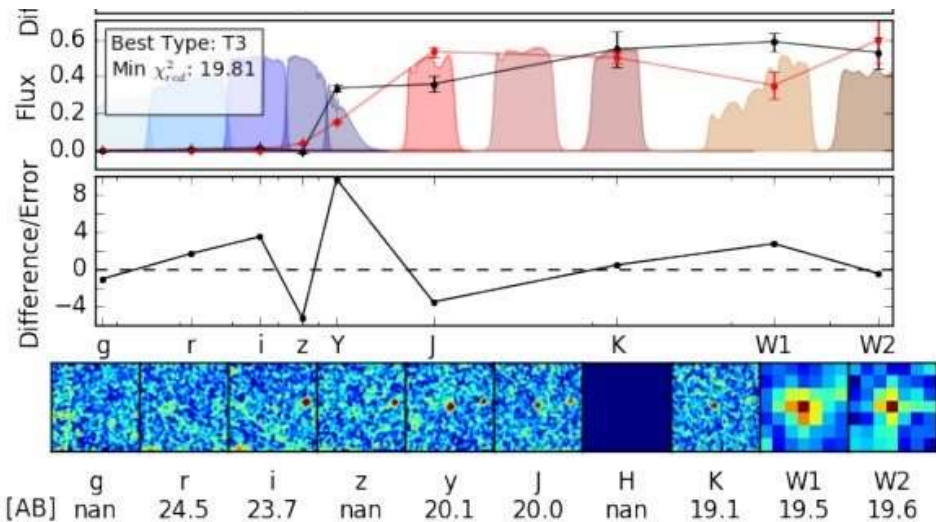


1980s – present

大规模巡天简史

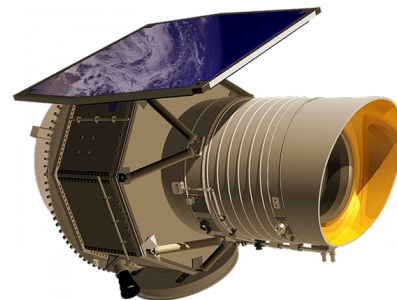
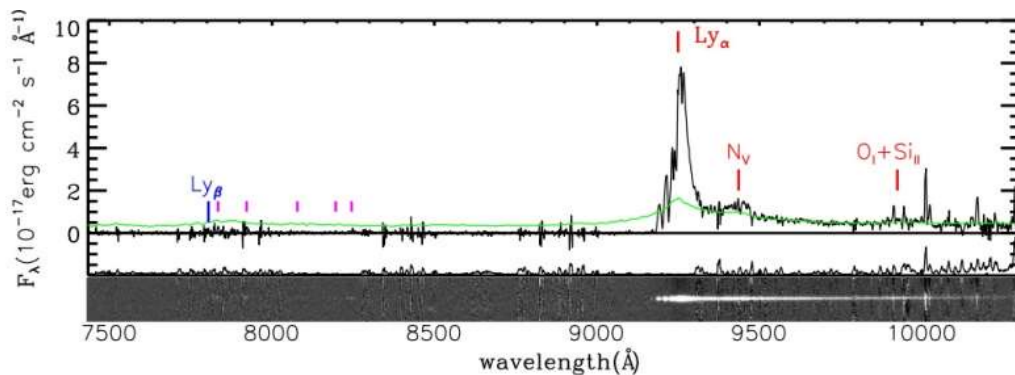


大规模巡天简史

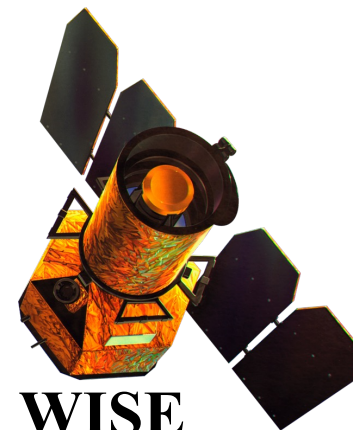


多波段星等

天体红移、化学组成



Galex



WISE



DESI



PS1



SDSS

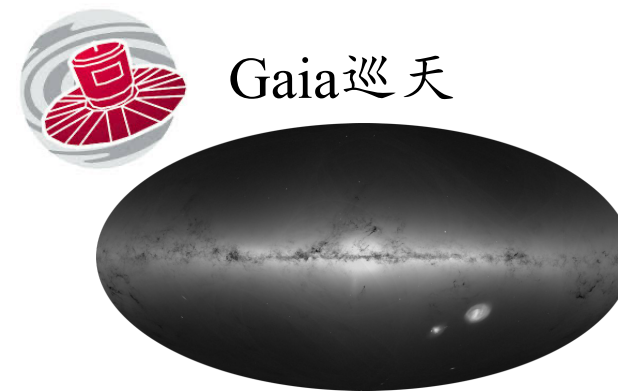
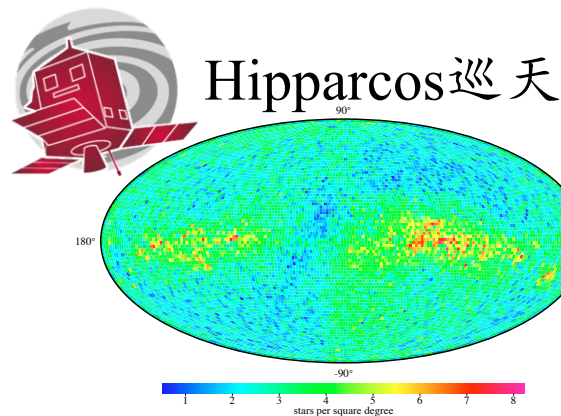
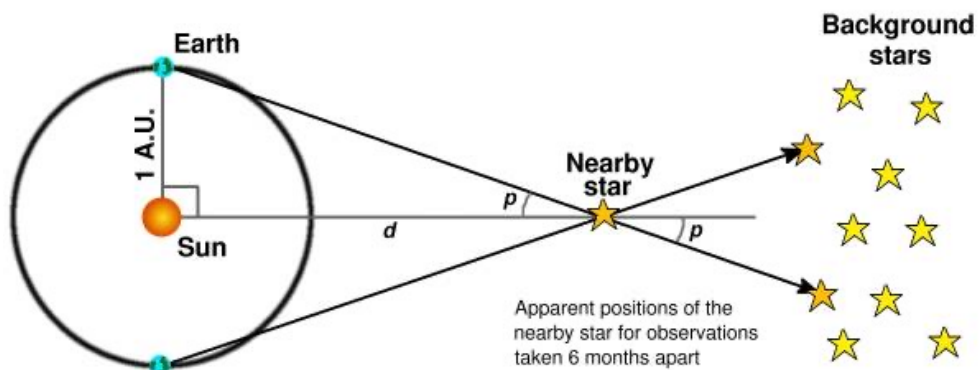


2MASS



SkyMapper

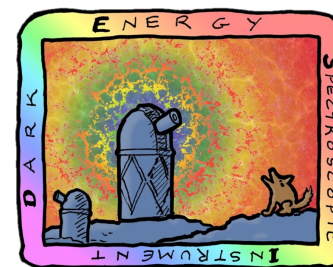
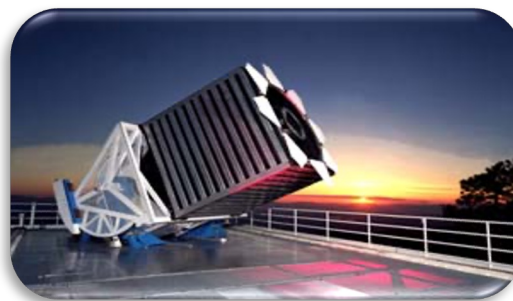
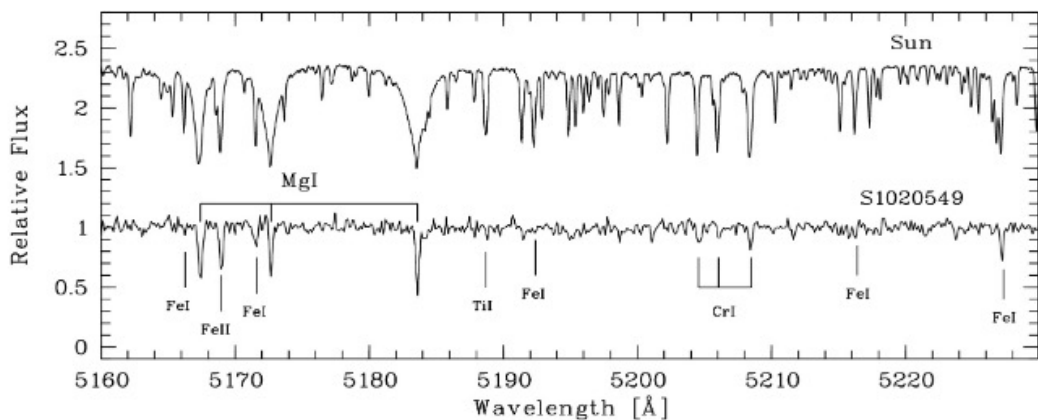
大规模巡天简史



天体位置、自行、视差

天体视向速度、化学组成

完备相空间
信息：三维
位置、三维
速度+年龄+Z

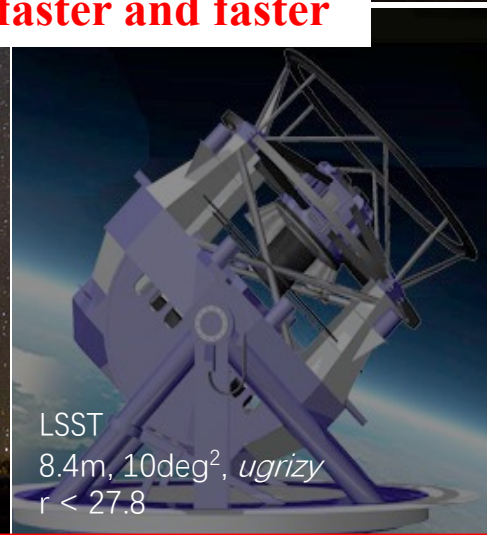
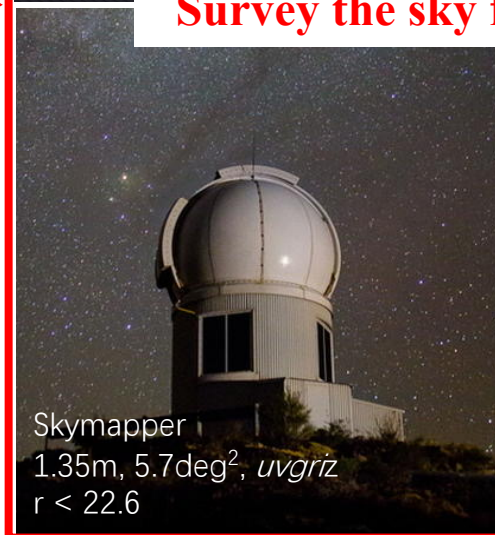
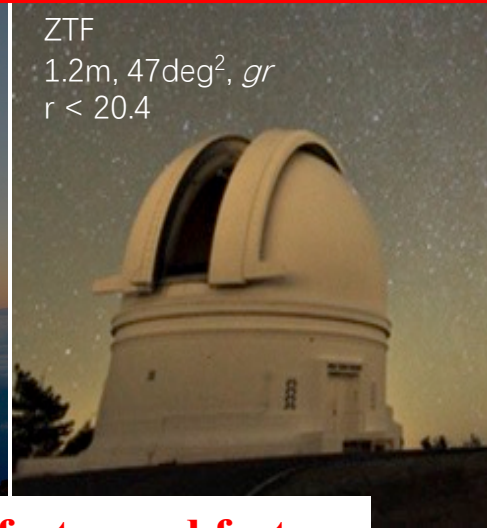


大规模巡天简史

拍照片

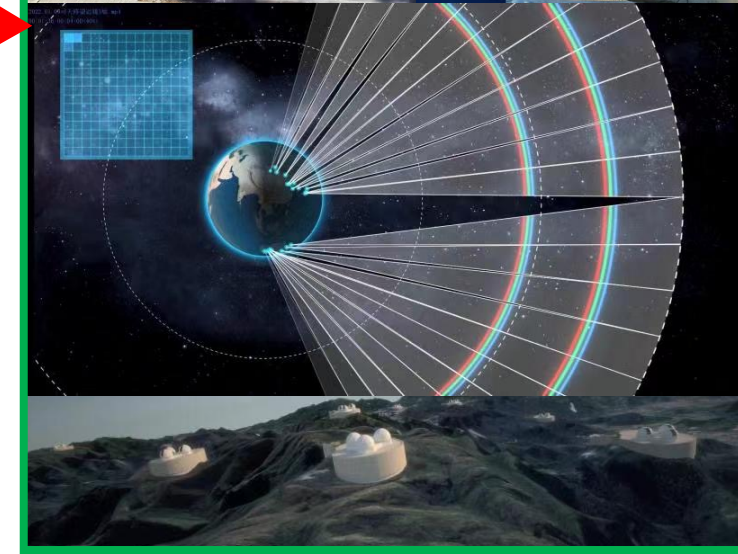
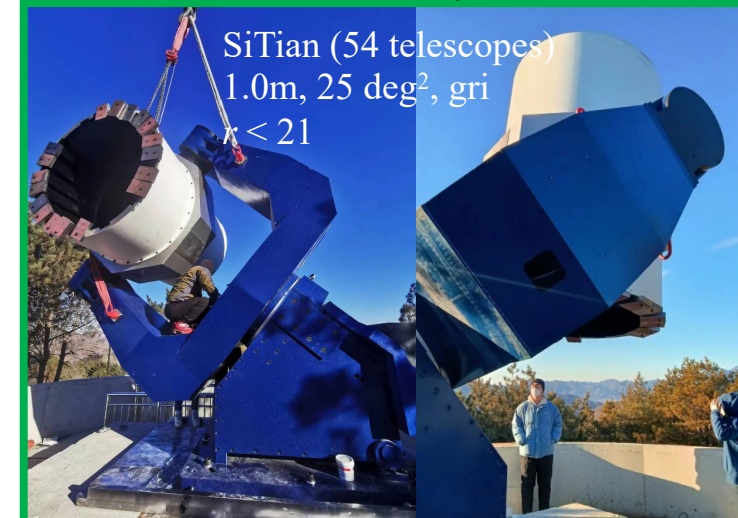


拍动图



Survey the sky faster and faster

拍电影



大规模巡天简史

自然科学基金委《天文学十四五及中长期规划》景益鹏+

多信使天文学：使用引力波、中微子、宇宙线等**非电磁手段**来研究致密天体性质、丈量宇宙时空、追踪剧烈天体物理过程、**检验基本物理规律**

时域天文学：采用多波段、多时标方式研究**动态宇宙**，通过**重复观测**来揭示宇宙中各类天体的变化，**发现和探索新天体**、揭示未知的新现象、新规律

行星大科学：关乎生命起源的行星大科学，是集系外行星、太阳系行星、天体生物学、天体化学、地质学研究方法于一体的高度交叉学科，旨在探索行星与**生命的起源和演化**

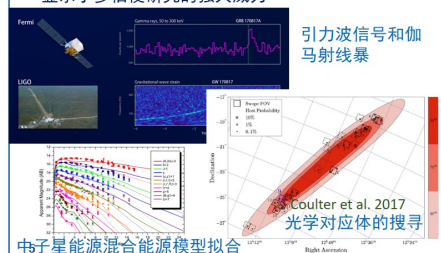
多波段、手段联合观测：不同侧面、不同类型天体更加全面的信息

大天区面积深度巡天：覆盖尽可能多的天体类型和数量

高频采样、长期持续监测：暂现源和变源的长期/短时标的变化特点

引力波暴电磁对应体：

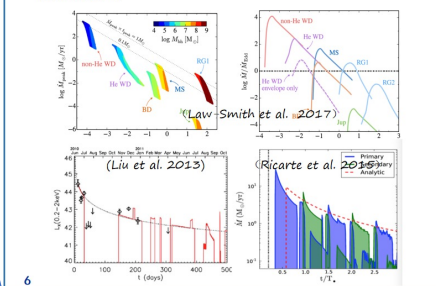
- 2017年，人类再次从一对中子星的并合事件中，首次实现了**引力波和多波段电磁波的联合探测**
- 有力推动了**短伽马射线暴起源**和**宇宙中超铁元素（如金、银、铀等）起源**等重大科学问题的解决，显示了多信使研究的强大威力



+ + +

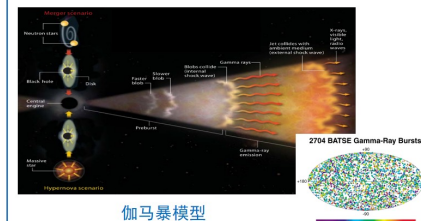
黑洞潮汐撕裂恒星事件 (TDE)

- 发生概率低
- 科学意义显著**：理解超大质量黑洞 (SMBHs) 的起源及其宇宙学成长历史、黑洞吸积物理、引力波多信使观测等



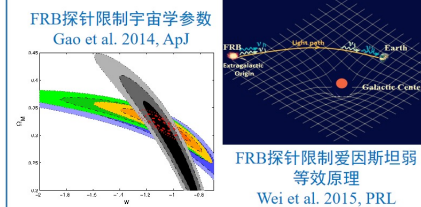
超新星与伽马射线暴：

- 超新星是大质量恒星在演化末期经历的剧烈爆炸，反映恒星演化最后时刻的空间结构和物理性质
- 伽马射线暴是宇宙中最为剧烈的恒星尺度爆发现象，是**研究早期宇宙的探针**，可用于探索第一代/早期恒星、早期金属丰度、宇宙再电离等



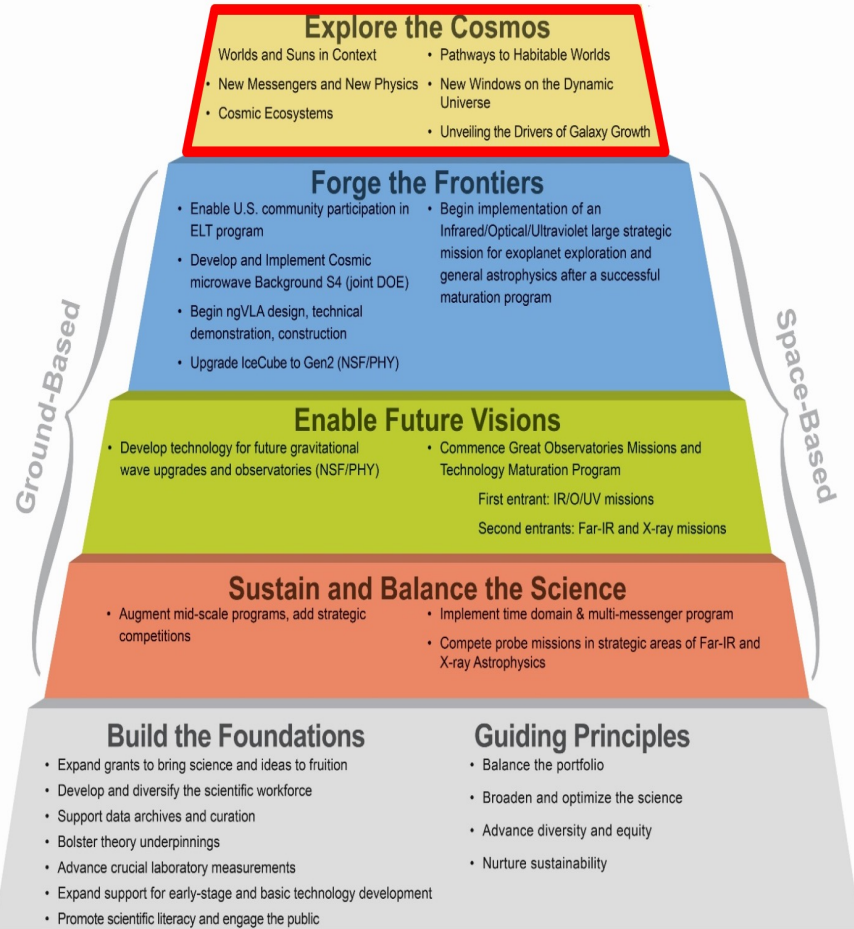
快速射电暴 (FRB)

- 一种持续时间仅为数毫秒的爆发性、脉冲式射电辐射天文现象，瞬时辐射流量可达数十央斯基 (Jy)
- 全新的天体物理现象，起源未知**
- 是从无线电到高能伽马射线，甚至中微子、引力波天文台的探测对象，是从**时域天文学到干涉成像多课题的研究目标**



大规模巡天简史

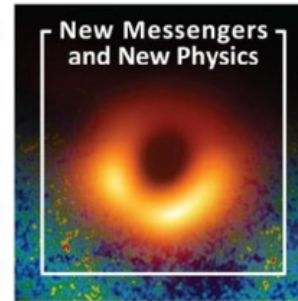
Realizing the Astro2020 Program: Pathways From Foundations to Frontiers



Priority Area: Pathways to Habitable Worlds

We are on a path to exploring worlds resembling Earth and answering the question: "Are we alone?" The task for the next decades will be finding the easiest of such planets to characterize, and then studying them in detail, searching for signatures of life.

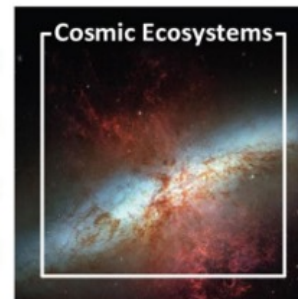
系外行星及宜居性
宿主恒星活动性
系外行星生命信号



Priority Area: New Windows on the Dynamic Universe

The New Windows on the Dynamic Universe priority area involves using light in all its forms, gravitational waves, and neutrinos to study cosmic explosions on all scales and the mergers of compact objects

动态宇宙新窗口
多信使多波段
瞬变天体
致密天体

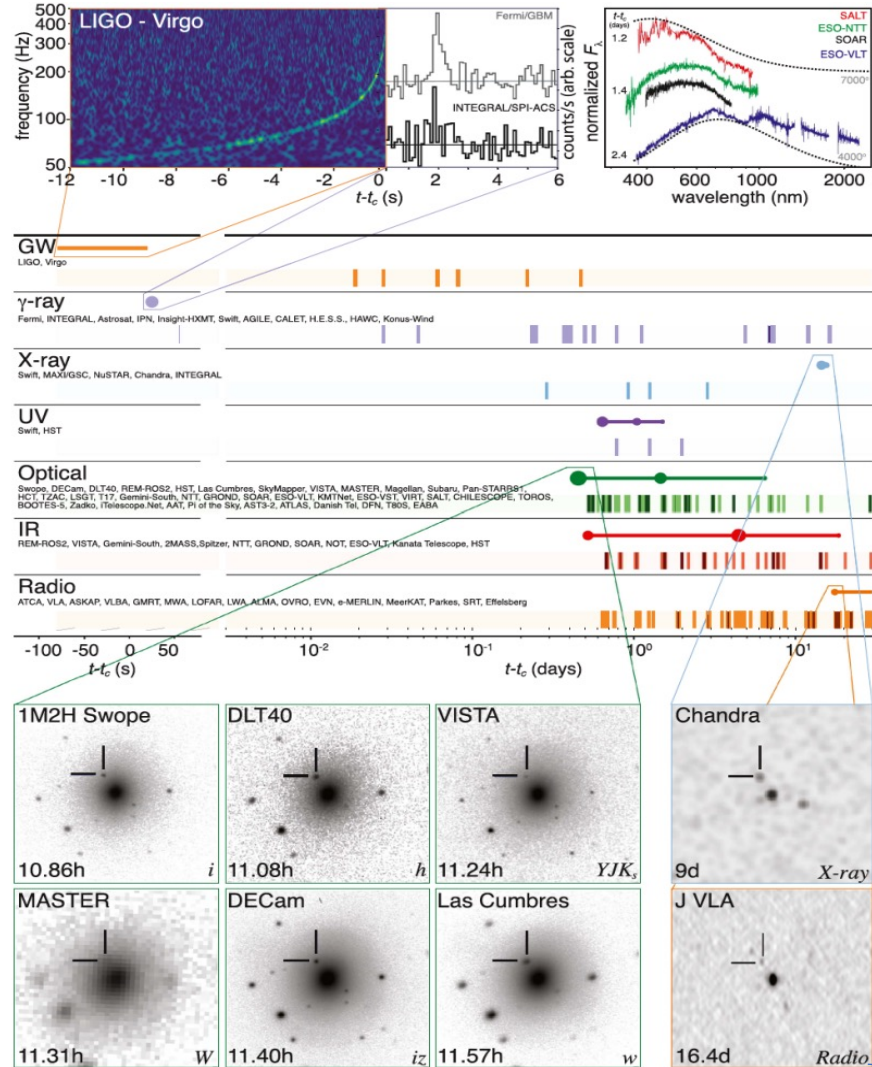


Priority Area: Unveiling the Drivers of Galaxy Growth

The priority area involves unveiling the drivers of galaxy growth, focusing on processes affecting galactic scales

驱动星系生长
黑洞星系共同
演化等

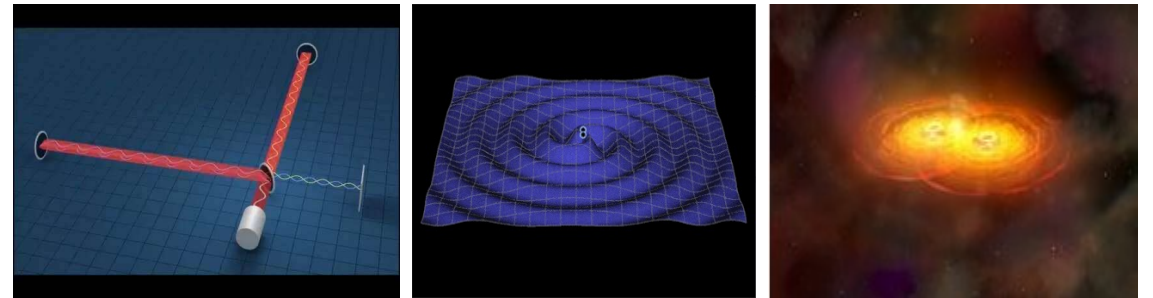
大规模巡天简史



引力波探测获2017年 诺贝尔物理学奖



-> **引力波天文学**：致密天体并合之电磁对应体



GW170817的电磁对应体观测

- **光学发现**：11小时后探测到←1米Swope巡天
- **触发后随光学光谱**：1天之后获取
- 探测到后期光变和光谱可以由中子星重元素衰变解释，但反应更关键物理的早期信息被丢失，因此无法区分最核心追求的致密天体模型！
- **问题**：需要五个小时内的极早期光变来区分模型！

大规模巡天简史

特点:

天去覆盖: 单次曝光>1平方度

数据量: **GB->TB** 每晚

探测器: **CCD/CMOS**

要求:

处理模式: 全自动

实效性: 数分钟模式 (变源瞬变源) / 离线模式

精度要求: 1-3%/毫星等

大规模巡天简史

Volume: 数据量大

Variety: 种类繁多（图像、时序、不同层级的星表等）

Value: 我们想要的最有价值的信息

Velocity: 时效性（真正的挑战）-- 分钟量级

Veracity: 怎样在大海捞针下捞到针

What happened?
What is happening?

What will happen?
What will it happen?

What should we do?
Why should I do it?



我们需要在几十台司天望远镜不停拍摄的同时作上述判断与决定

准备知识

Noises of CCD photometry

$$\frac{S}{N} = \frac{N_*}{\sqrt{N_* + n_{pix} (N_{sky} + N_D + N_{RD}^2)}}$$

N_* : the total number of photons collected from the object of interest

n_{pix} : the total number of pixels under the object of interest; for ground based telescope, $n_{pix} =$

$\frac{\pi r^2}{pixel\ size}$ (r given by the typical seeing)

N_{sky} : the total number of photons per pixel from the sky background

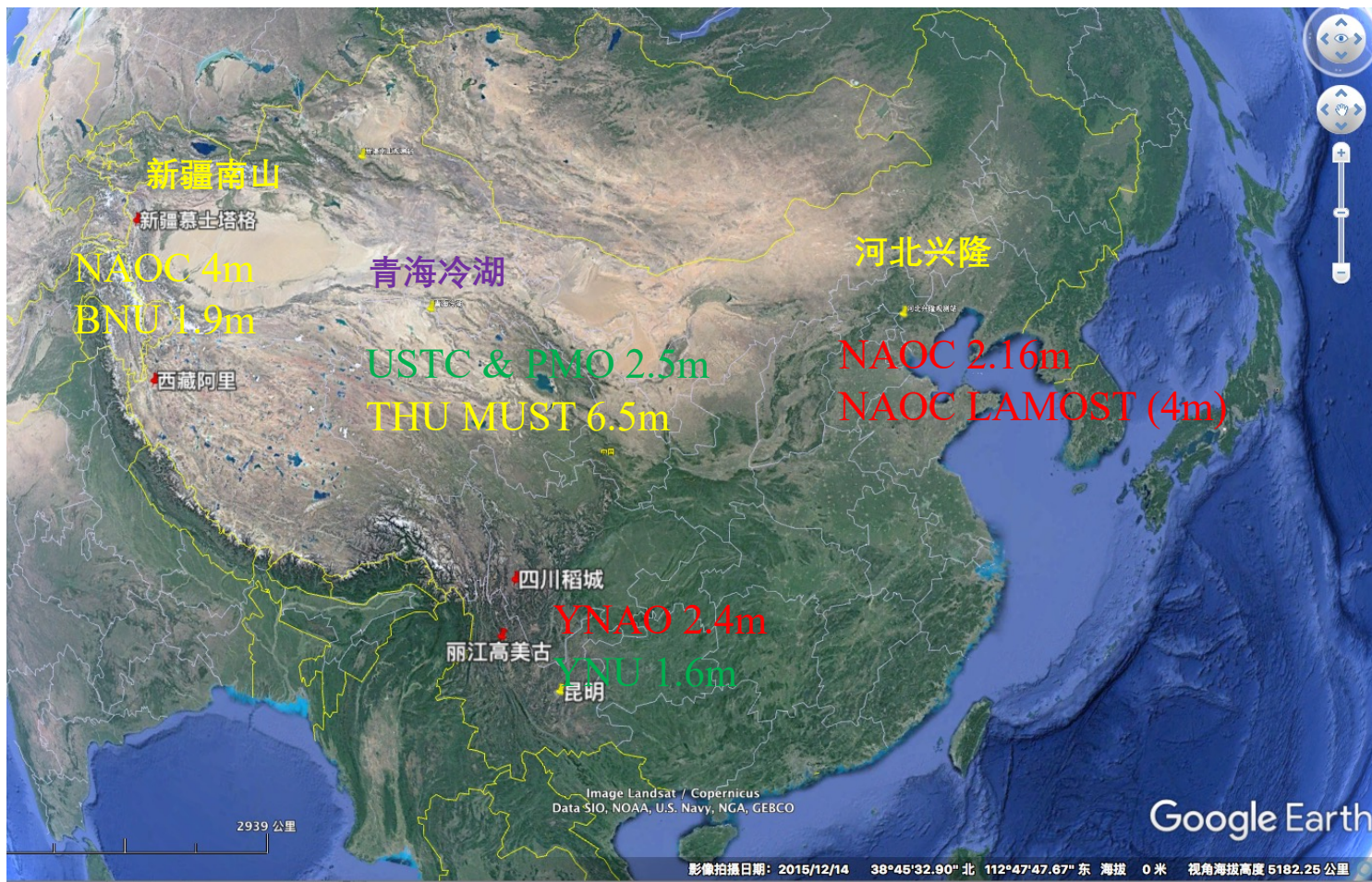
N_D : the total number of dark current electrons per pixel

N_{RD}^2 : the total number of electrons per pixel resulting from the read noise

Those noises are determined by the **site station** and **camera properties** and can not be **reduced more** once the station and camera been chosen!

准备知识

一流台址



准备知识

一流台址

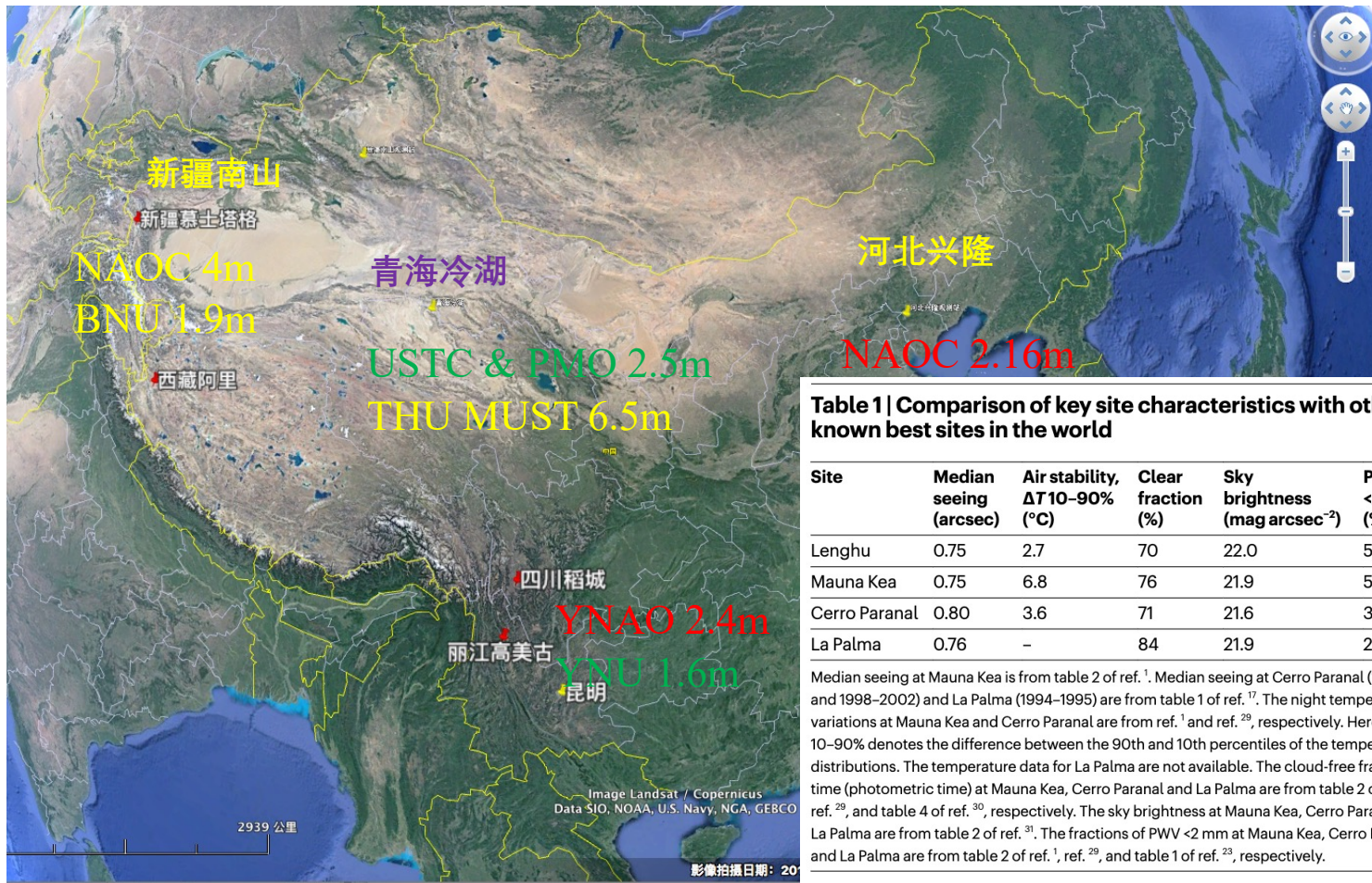
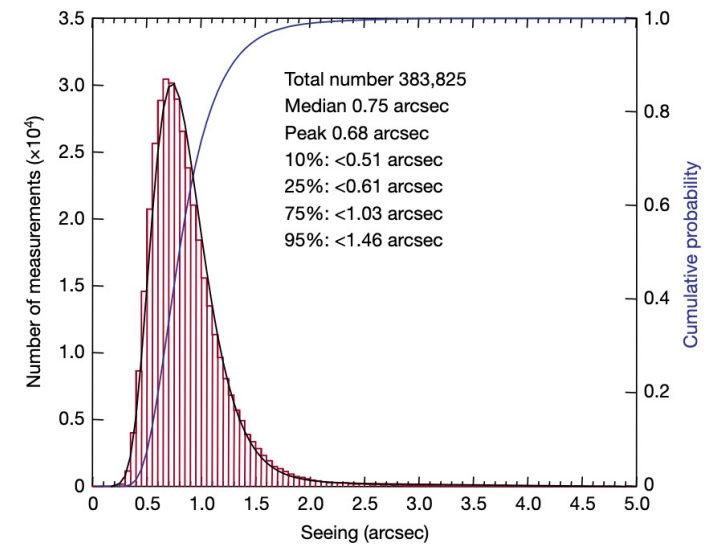


Table 1 | Comparison of key site characteristics with other known best sites in the world

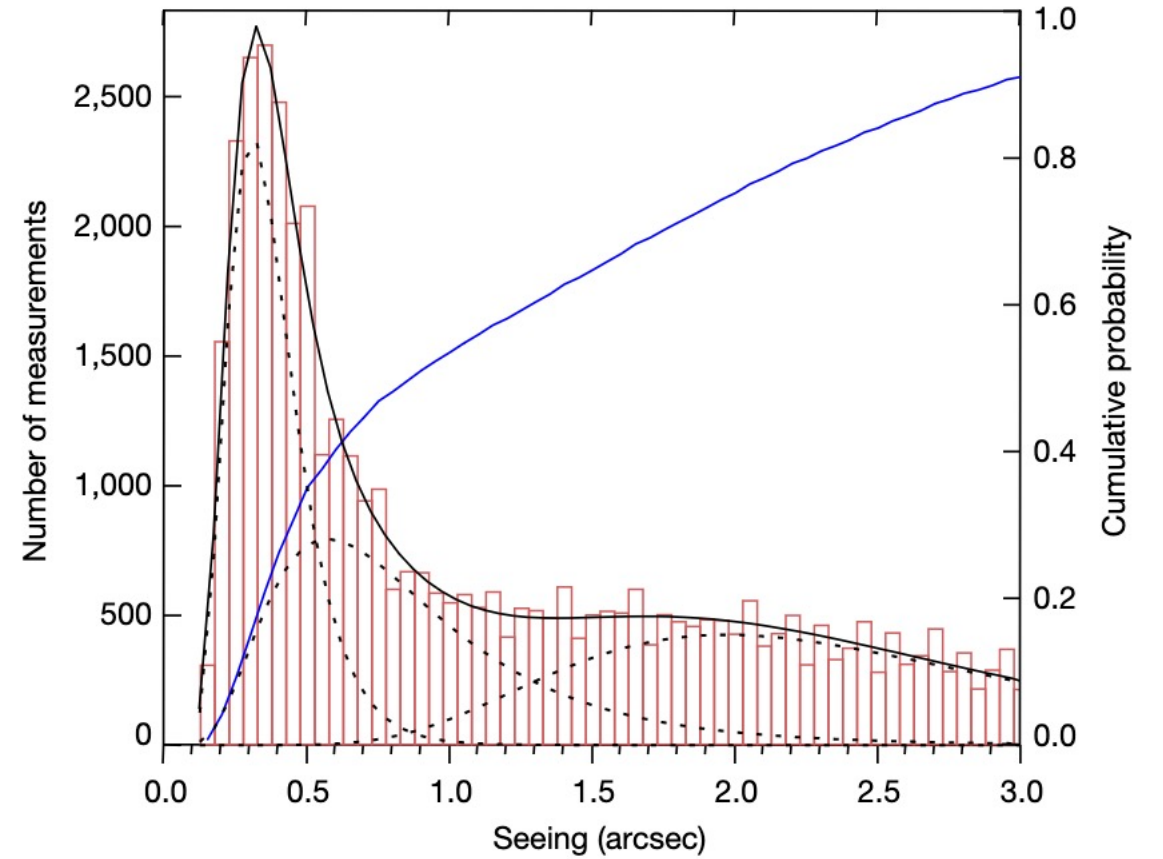
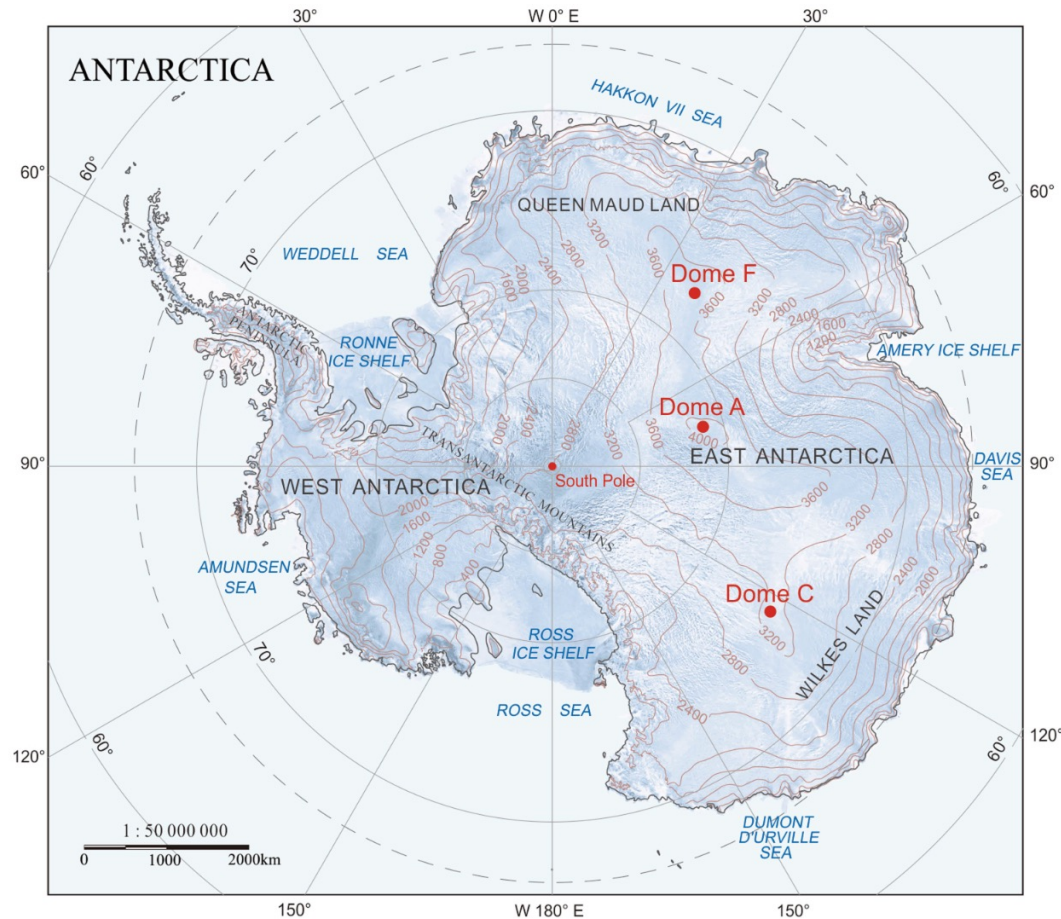
Site	Median seeing (arcsec)	Air stability, $\Delta T_{10-90\%}$ ($^{\circ}\text{C}$)	Clear fraction (%)	Sky brightness (mag arcsec $^{-2}$)	PWV <2 mm (%)
Lenghu	0.75	2.7	70	22.0	55
Mauna Kea	0.75	6.8	76	21.9	54
Cerro Paranal	0.80	3.6	71	21.6	36
La Palma	0.76	-	84	21.9	21

Median seeing at Mauna Kea is from table 2 of ref. ¹. Median seeing at Cerro Paranal (1989–1995 and 1998–2002) and La Palma (1994–1995) are from table 1 of ref. ¹⁷. The night temperature variations at Mauna Kea and Cerro Paranal are from ref. ¹ and ref. ²⁹, respectively. Here, $\Delta T_{10-90\%}$ denotes the difference between the 90th and 10th percentiles of the temperature distributions. The temperature data for La Palma are not available. The cloud-free fractions of time (photometric time) at Mauna Kea, Cerro Paranal and La Palma are from table 2 of ref. ¹, ref. ²⁹, and table 4 of ref. ³⁰, respectively. The sky brightness at Mauna Kea, Cerro Paranal and La Palma are from table 2 of ref. ³¹. The fractions of PWV <2 mm at Mauna Kea, Cerro Paranal and La Palma are from table 2 of ref. ¹, ref. ²⁹, and table 1 of ref. ²³, respectively.



准备知识

一流台址



Ma et al. 2020

准备知识

<https://sites.astro.caltech.edu/~george/ay122/Bessel2005ARAA43p293.pdf>

STANDARD PHOTOMETRIC SYSTEMS

Michael S. Bessell

*Research School of Astronomy and Astrophysics, The Australian National University,
Weston, ACT 2611, Australia; email: bessell@mso.anu.edu.au*

TABLE 1 Wavelengths (\AA) and widths (\AA) of broad-band systems

UBVRI		Washington		SDSS		Hipparcos		WFPC2						
λ_{eff}	$\Delta\lambda$	λ_{eff}	$\Delta\lambda$	λ_{eff}	$\Delta\lambda$	λ_{eff}	$\Delta\lambda$	λ_{eff}	$\Delta\lambda$					
<i>U</i>	3663	650	<i>C</i>	3982	1070	<i>u'</i>	3596	570	<i>H_P</i>	5170	2300	F336	3448	340
<i>B</i>	4361	890	<i>M</i>	5075	970	<i>g'</i>	4639	1280	<i>B_T</i>	4217	670	F439	4300	720
<i>V</i>	5448	840	<i>T₁</i>	6389	770	<i>r'</i>	6122	1150	<i>V_T</i>	5272	1000	F555	5323	1550
<i>R</i>	6407	1580	<i>T₂</i>	8051	1420	<i>i'</i>	7439	1230				F675	6667	1230
<i>I</i>	7980	1540				<i>z'</i>	8896	1070				F814	7872	1460

准备知识

Homework #1

SUMMARY PERFORMANCE (Typical)

Number of pixels	9216 (H) × 9232 (V)
Pixel size	10 μm square
Image area	92.2 mm × 92.4 mm
Outputs	16
Package size	98.5 × 93.7 mm
Package format	Silicon carbide with two flexi connectors
Focal plane height, above base	20.0 mm
Connectors	Two 51-way micro-D
Flatness	20 μm (peak to valley)
Amplifier sensitivity	7.5 μV/e ⁻
Read-out noise	4 e ⁻ at 0.5 MHz 2.5 e ⁻ at 50 kHz
Maximum pixel data rate	3 MHz
Charge storage (pixel full well)	90,000 e ⁻
Dark signal	4 e ⁻ /pixel/hour (at -100 °C)

CCD290-99 Sensor designed by e2v

XingLong Station:

Background: $V = 21.0 \text{ mag/srcsec}^2$

Atmospheric extinction: $kV = 0.35 \text{ mag/airmass}$

Telescope efficiency: 40% (assumed)

Aperture: 1m in diameter

Pixel scale: 0.6 arcsec/pixel

Seeing: 1.5 arcsec

	DD silicon Astro Multi-2	Standard silicon Astro Multi-2	Pixel Response Non-Uniformity PRNU (1 σ)
Wavelength (nm)	Minimum QE (%)	Minimum QE (%)	Maximum PRNU (%)
350	30	30	-
400	75	75	3
500	75	75	-
650	80	80	3
900	50	25	5

*Limiting magnitude?
(5sigma; @1.2 airmass)*

@ 2s

@ 20s

@ 200s

And which one dominates the error?

准备知识

流量标准星

<https://www.eso.org/sci/observing/tools/standards/spectra.html>

Oke (1990) Spectrophotometric Standards

Oke (AJ, 99, 1621, 1990) has provided absolute spectral energy distributions covering the wavelength range 3200 to 9200Å in AB magnitudes for 25 stars. The measurements were made with the Double Beam Spectrograph of the [Hale 5m telescope](#). The reduced magnitudes are tabulated at 1Å intervals from 3300 to 4700Å and at 2Å intervals from 4700 to 9200Å. Comparison of the fluxes with those determined elsewhere showed that Oke's absolute magnitudes are systematically brighter by 0.04 mag. The magnitudes and fluxes plotted have been corrected for this effect. Colina & Bohlin (AJ, 1931, 1994) tabulate the differences between the original Oke fluxes, in terms of synthesized B and V magnitudes, and Landolt photometry for each star individually. The AB magnitudes were converted to flux (ergs/cm/cm/s/Å) using the formula

$$ABMAG = -2.5 \log_{10}(F_{\nu}) - 48.59$$

(Hamuy et al., PASP, 104, 533, 1992), where F_{ν} is in ergs/cm/cm/s/Hz.

Cautionary Note:

These data have larger uncertainties than tabulated in the following spectral regions:

- below 3400Å (atmospheric and instrument transmission);
- 4000–4500Å (CCD flaws);
- 4650–4800Å (overlap between orders, dichroic cut);
- telluric A and B bands (around 7615 and 6875Å respectively);
- above about 8500Å (second-order contamination).

No.	Name	alpha (2000)	delta	Sp.	V	AB
				Type	(5460Å)	
1	G158-100	00 33 54.3	-12 07 57	sdG	14.89	14.82
2	HZ 4	03 55 21.7	+09 47 19	DA4	14.52	14.47
3	G191B2B	05 05 30.6	+52 49 54	DAO	11.78	11.72
4	G193-74	07 53 27.4	+52 29 36	DC	15.70	15.58
5	BD+75d325	08 10 49.3	+74 57 57	O5p	9.54	9.52

准备知识

望远镜空间分辨本领：

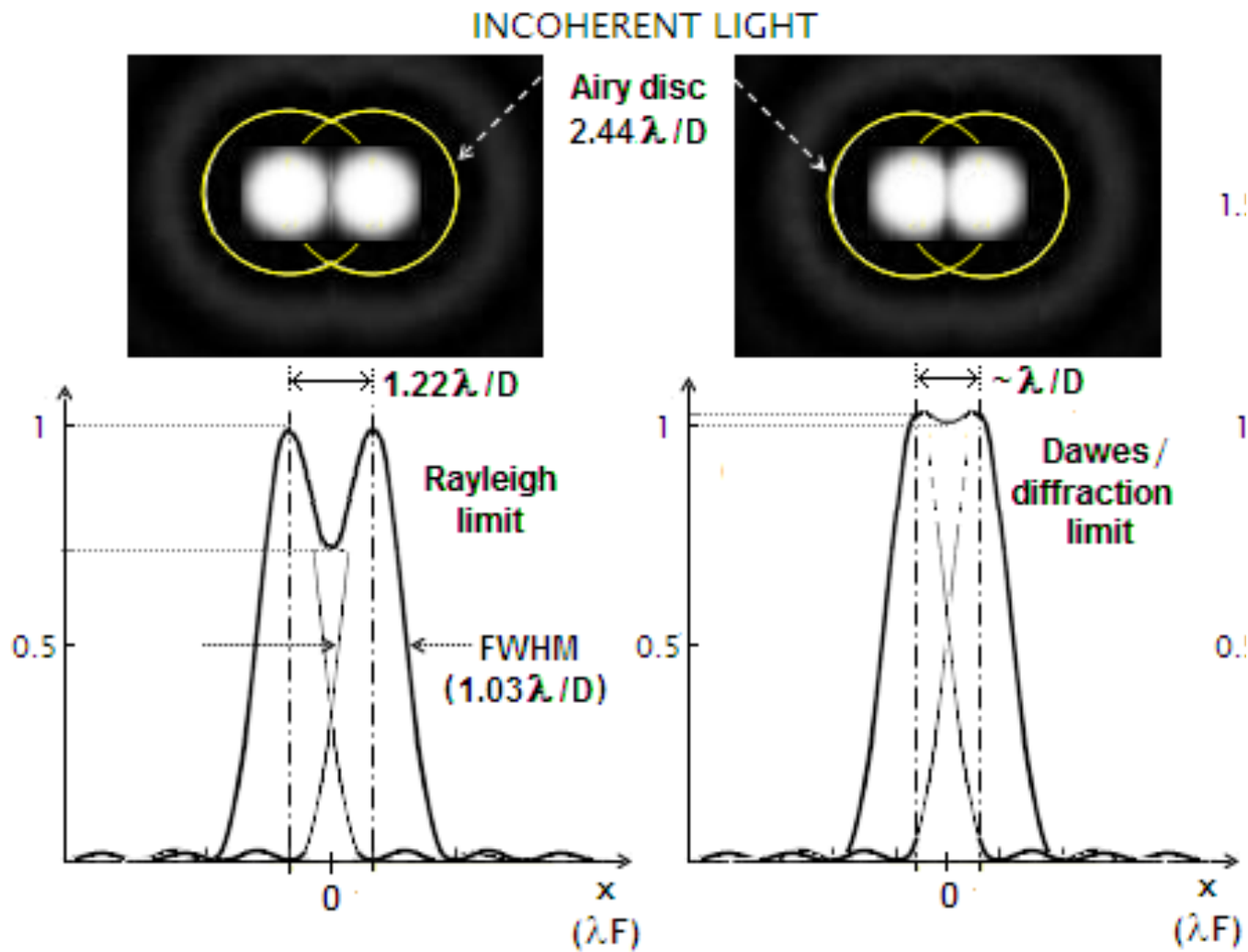
准备知识

望远镜空间分辨本领:

衍射极限

大气湍流

探测器采样
(焦面比例尺)



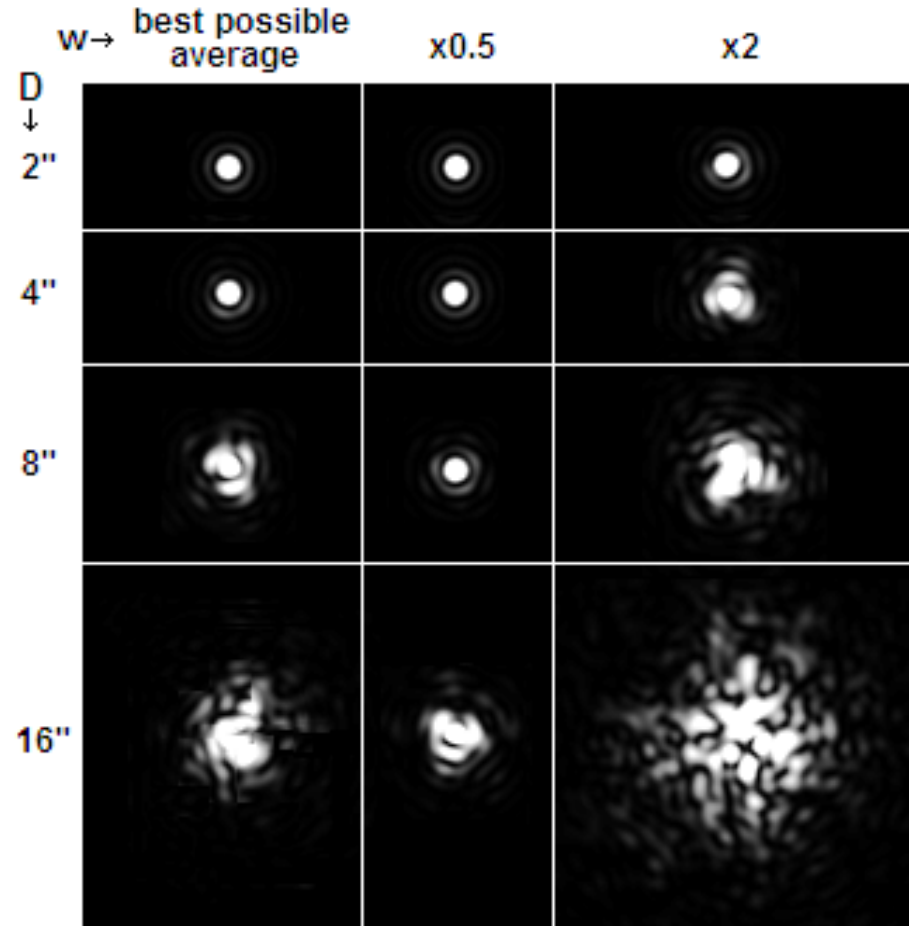
准备知识

望远镜空间分辨本领:

衍射极限

大气湍流

探测器采样
(焦面比例尺)



准备知识

望远镜空间分辨本领：

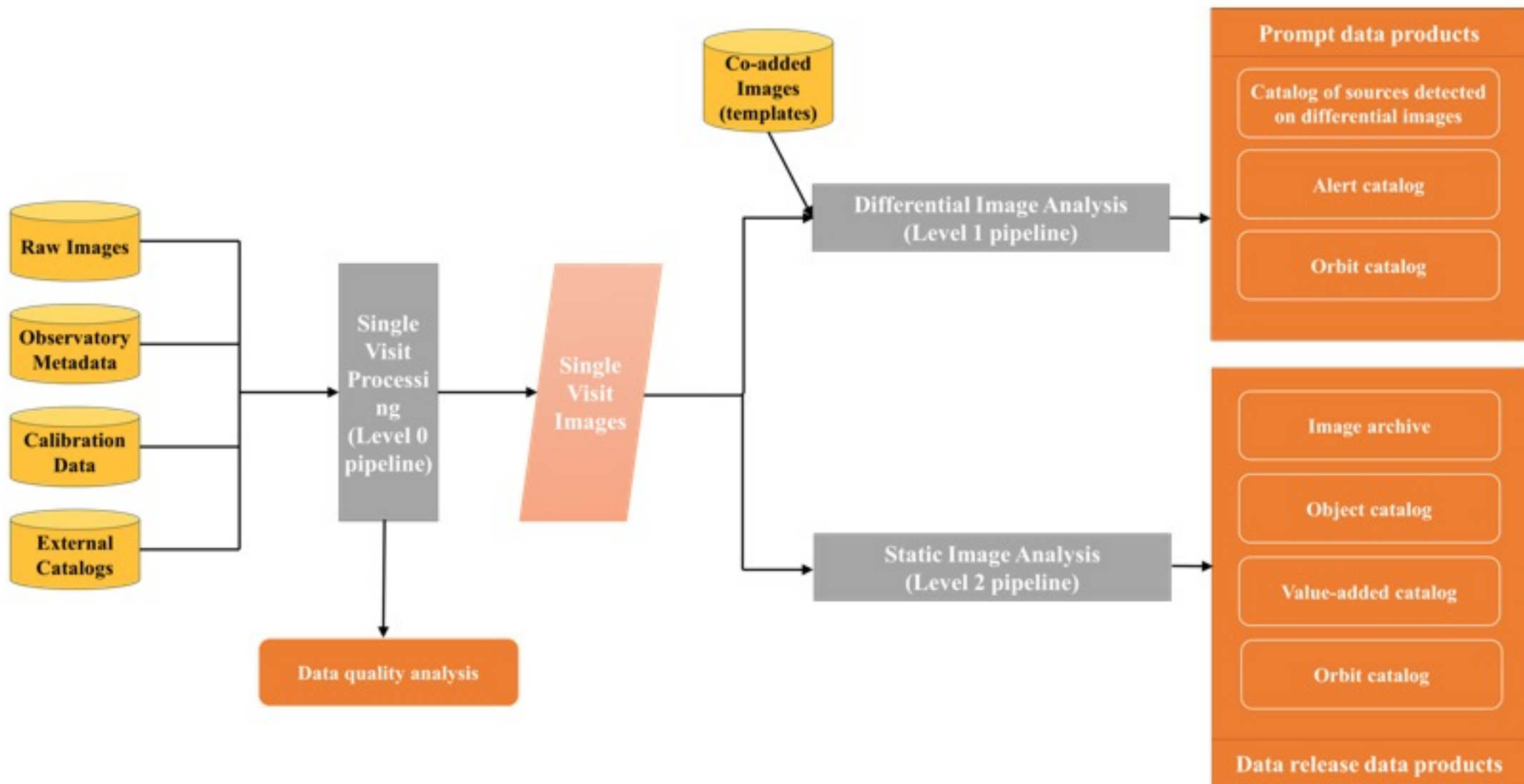
衍射极限

大气湍流

探测器采样
(焦面比例尺)

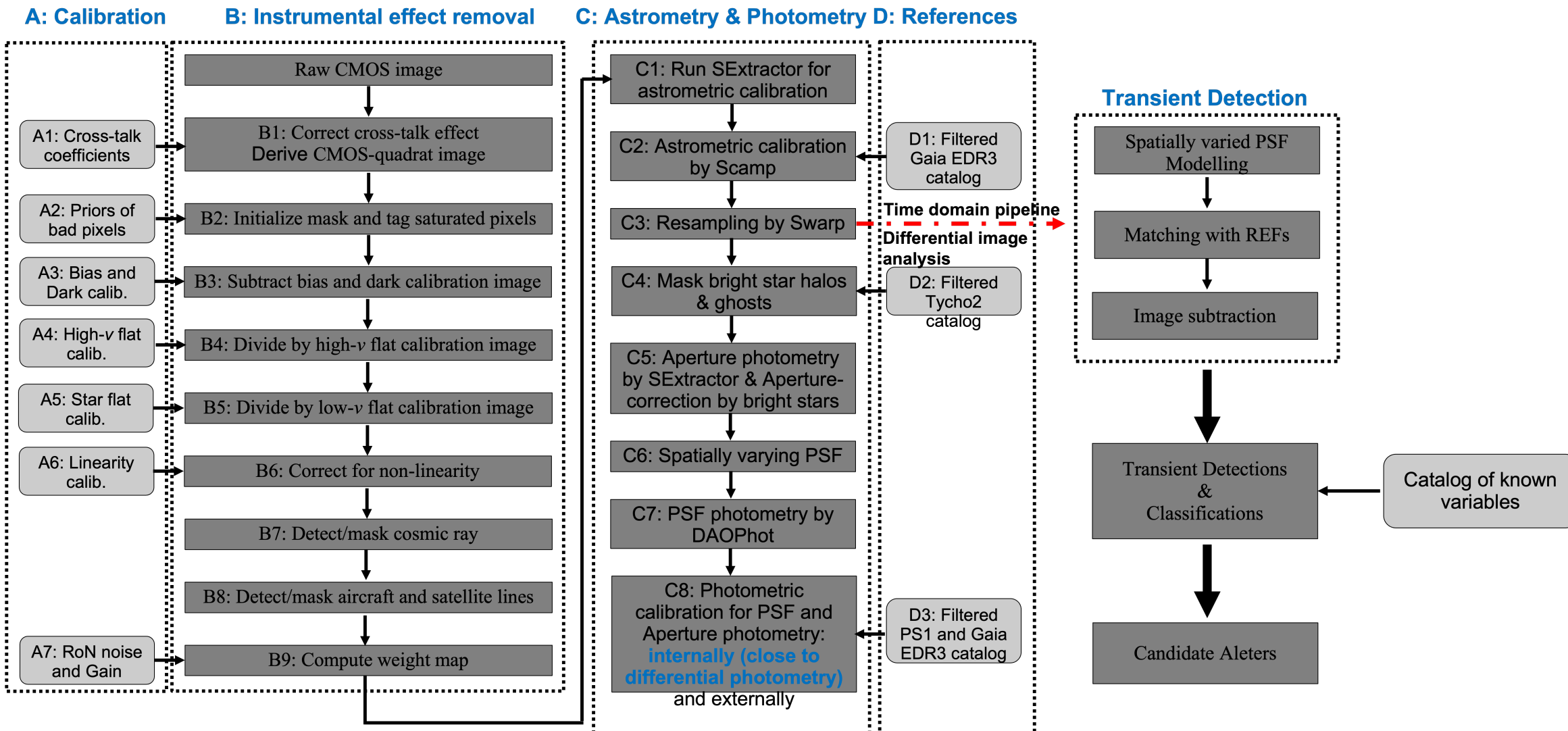


测光数据处理纵览



测光数据处理纵览

SiTian image Processing pipeline (STEP)



探测器性能标定

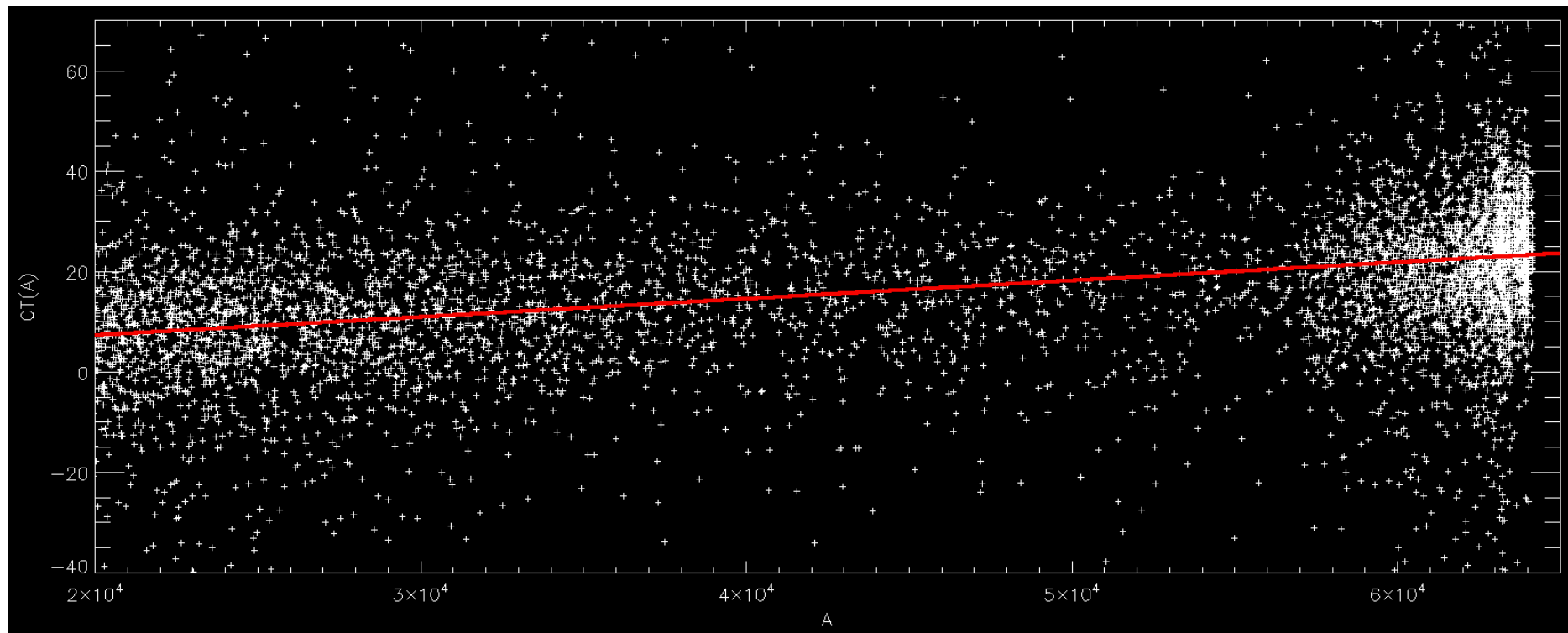
CCD Cross-talk:

BASS CCD #1 Four
amplifiers

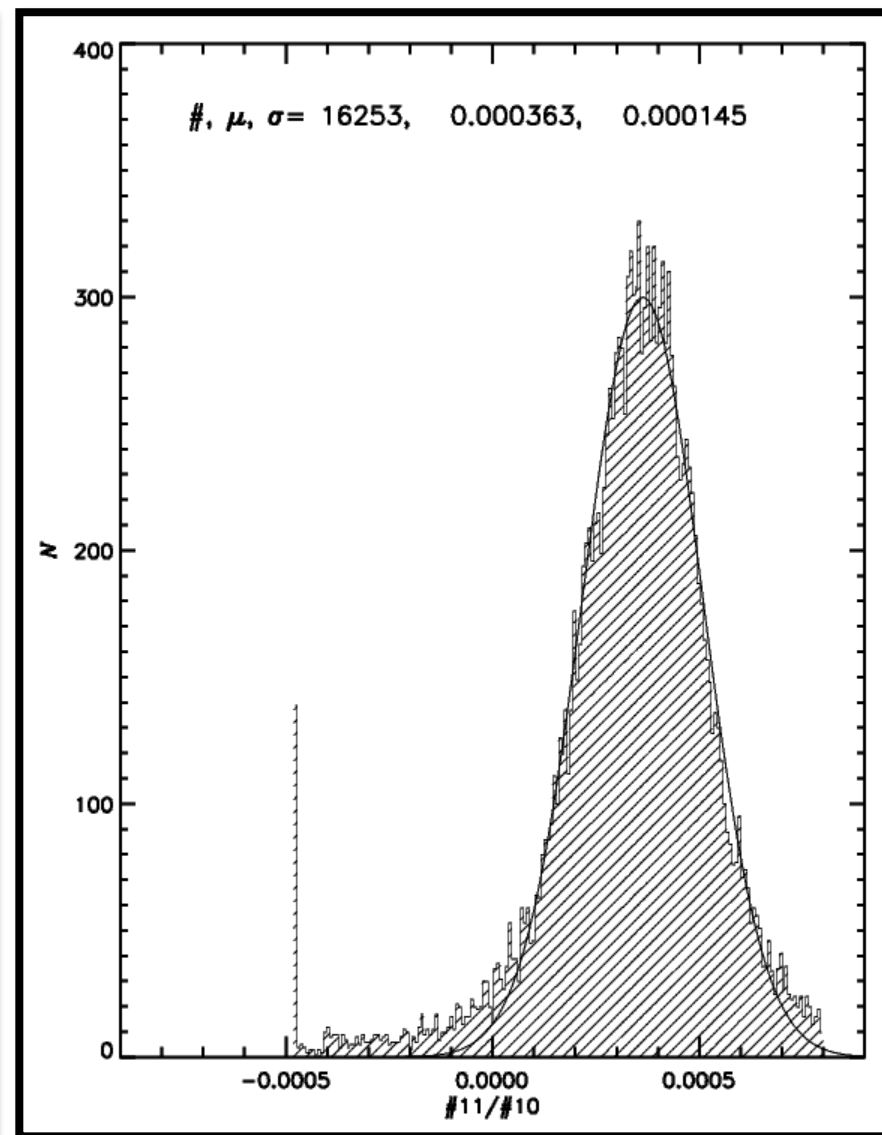
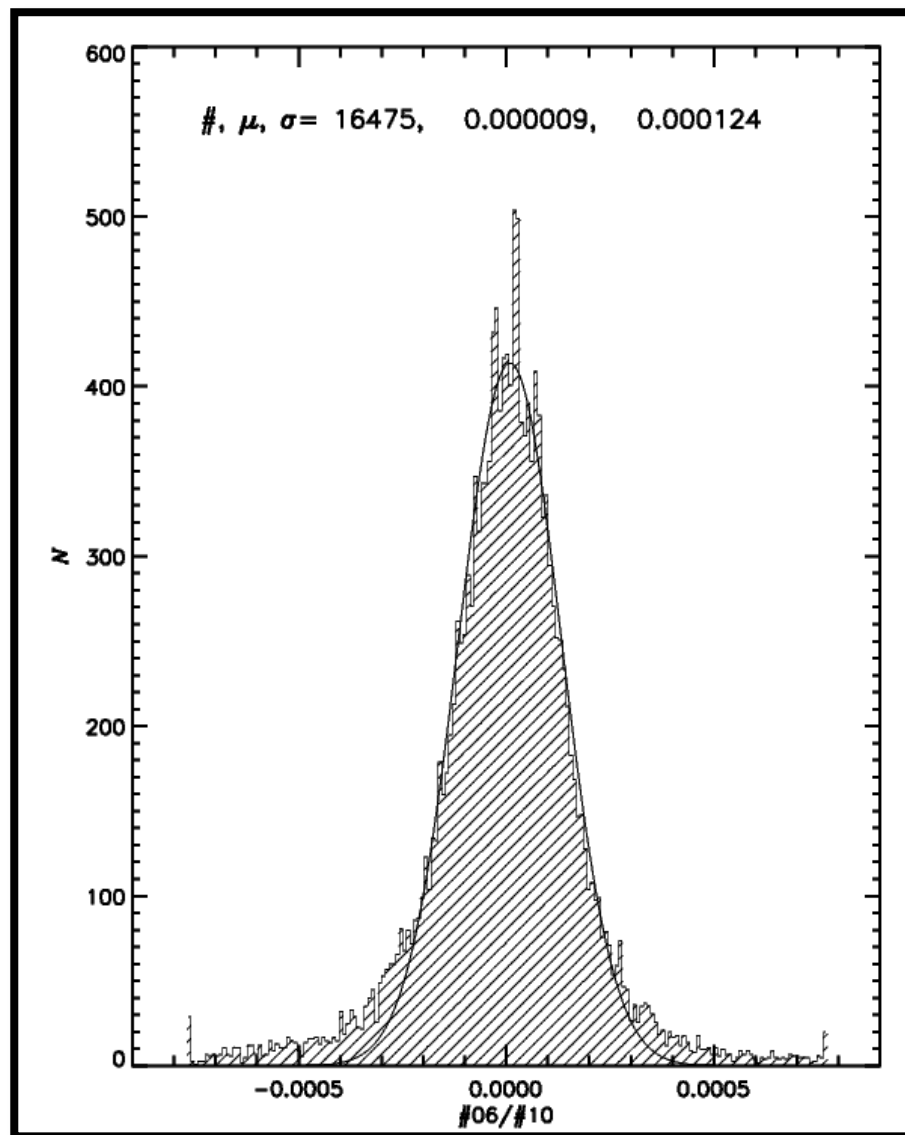
Cross-talk effect:
typically in the level of
1:1000 to 1:10000.



探测器性能标定



探测器性能标定



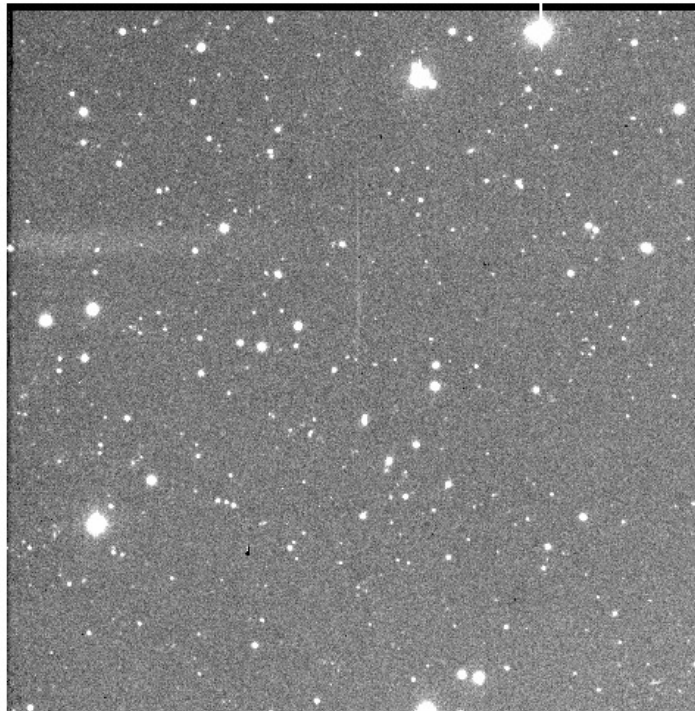
探测器性能标定

HDU	1	2	3	4	5	6	7	8	9	10	11	12	13	14	15	16
1	0	-23	-33	-30	1	2	2	2	1	-1	1	1	2	2	1	3
2	-17	0	-24	-23	1	1	2	3	1	0	1	1	2	3	3	3
3	-10	-8	0	-11	1	1	2	2	1	0	1	1	2	2	2	4
4	-11	-9	-11	0	2	-4	2	2	1	0	0	1	1	2	2	2
5	3	3	3	3	0	-33	-37	-27	2	-1	2	1	0	0	1	2
6	3	3	4	3	-10	0	-17	-14	3	2	4	3	1	1	1	2
7	3	3	3	3	-11	-14	0	-6	2	1	2	2	1	2	2	2
8	3	3	4	4	-9	-6	-5	0	1	3	4	2	0	1	1	1
9	3	2	3	2	1	1	2	2	0	-16	-23	-19	3	3	2	2
10	2	1	2	1	0	1	1	1	-31	0	-40	-32	2	2	2	2
11	3	2	2	1	0	-1	1	1	-25	-16	0	-17	2	2	1	2
12	3	2	3	2	1	1	2	2	-15	-11	-8	0	-2	1	2	1
13	4	3	4	3	-1	0	1	1	-9	0	1	3	0	-24	-26	-22
14	4	3	4	3	0	1	1	2	-9	1	1	-2	-24	0	-26	-22
15	4	4	5	4	1	1	1	2	-11	0	1	3	-13	-10	0	-5
16	5	5	5	5	-1	1	1	2	-7	-3	-1	0	-15	-14	-12	0

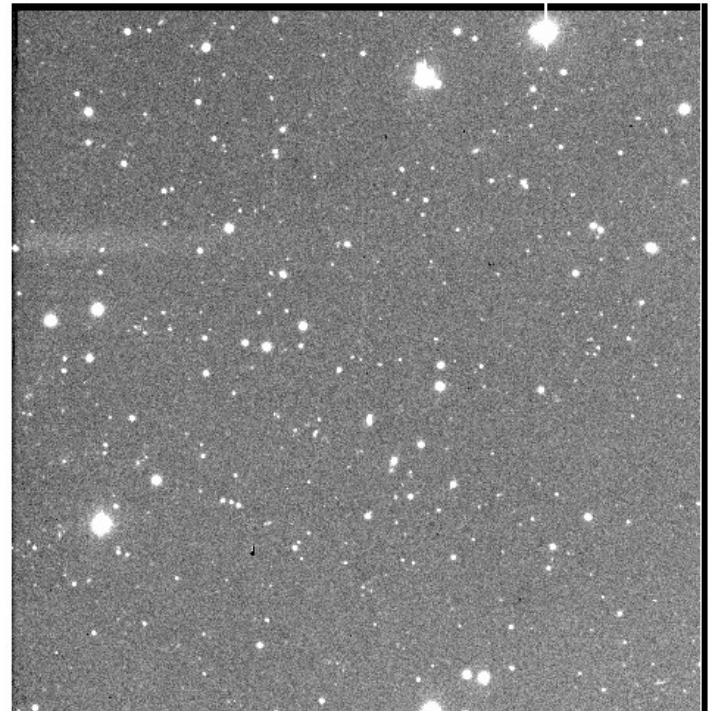
Note. The scale is 10^{-5} .

探测器性能标定

Before



After



探测器性能标定

CCD RoN & Gain:

$$\sigma_{\text{ADU}} = \frac{\text{Readout noise}}{\text{Gain}}$$

$$\sigma_{\text{ADU}} = \frac{\sqrt{\langle F \rangle \cdot \text{Gain}}}{\text{Gain}}$$

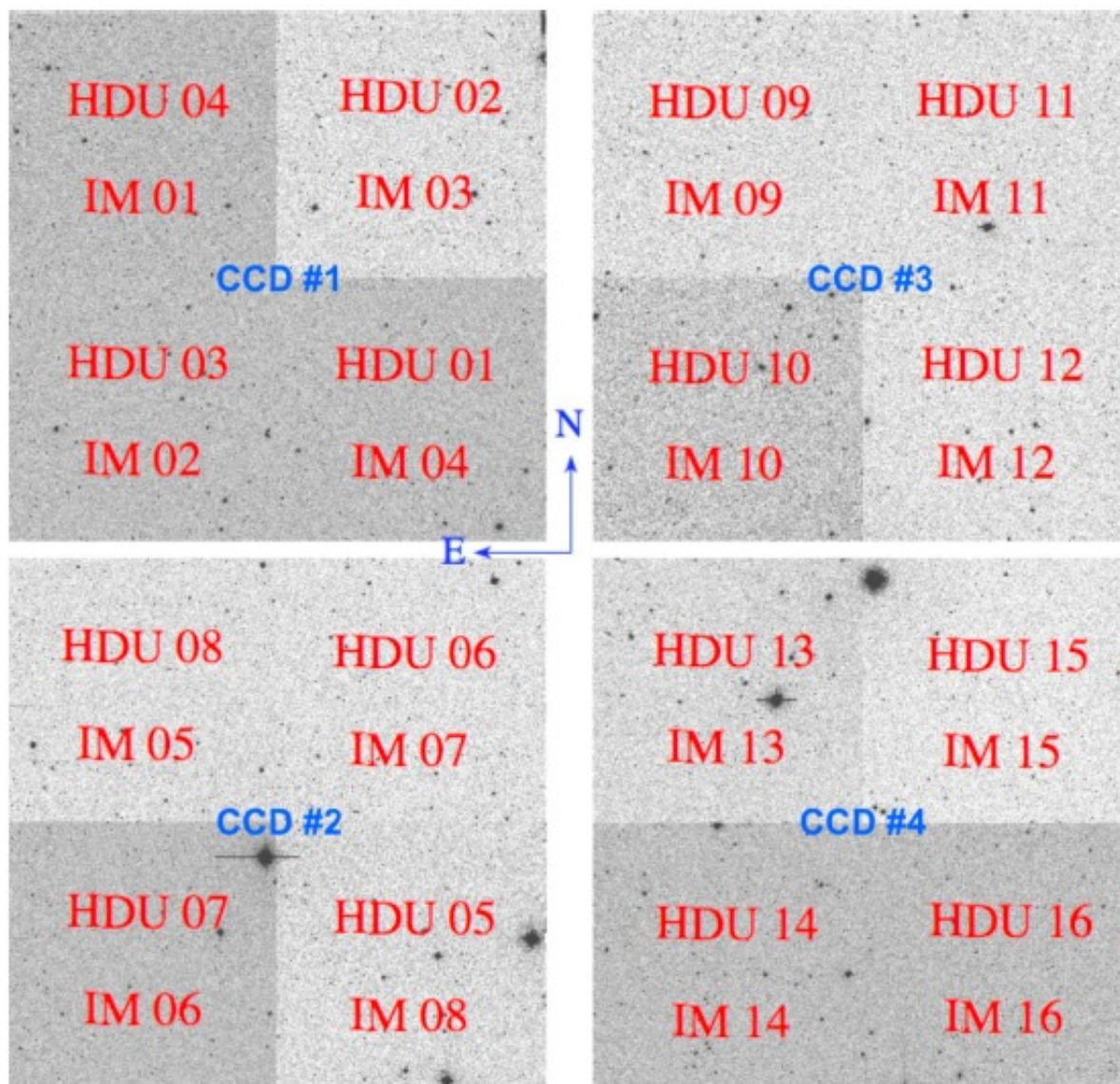
探测器性能标定

CCD RoN & Gain:

$$\text{Gain} = \frac{(\langle F1 \rangle + \langle F2 \rangle) - (\langle B1 \rangle + \langle B2 \rangle)}{\sigma_{F1-F2}^2 - \sigma_{B1-B2}^2}$$

$$\text{Readout noise} = \frac{\text{Gain} \cdot \sigma_{B1-B2}}{\sqrt{2}}$$

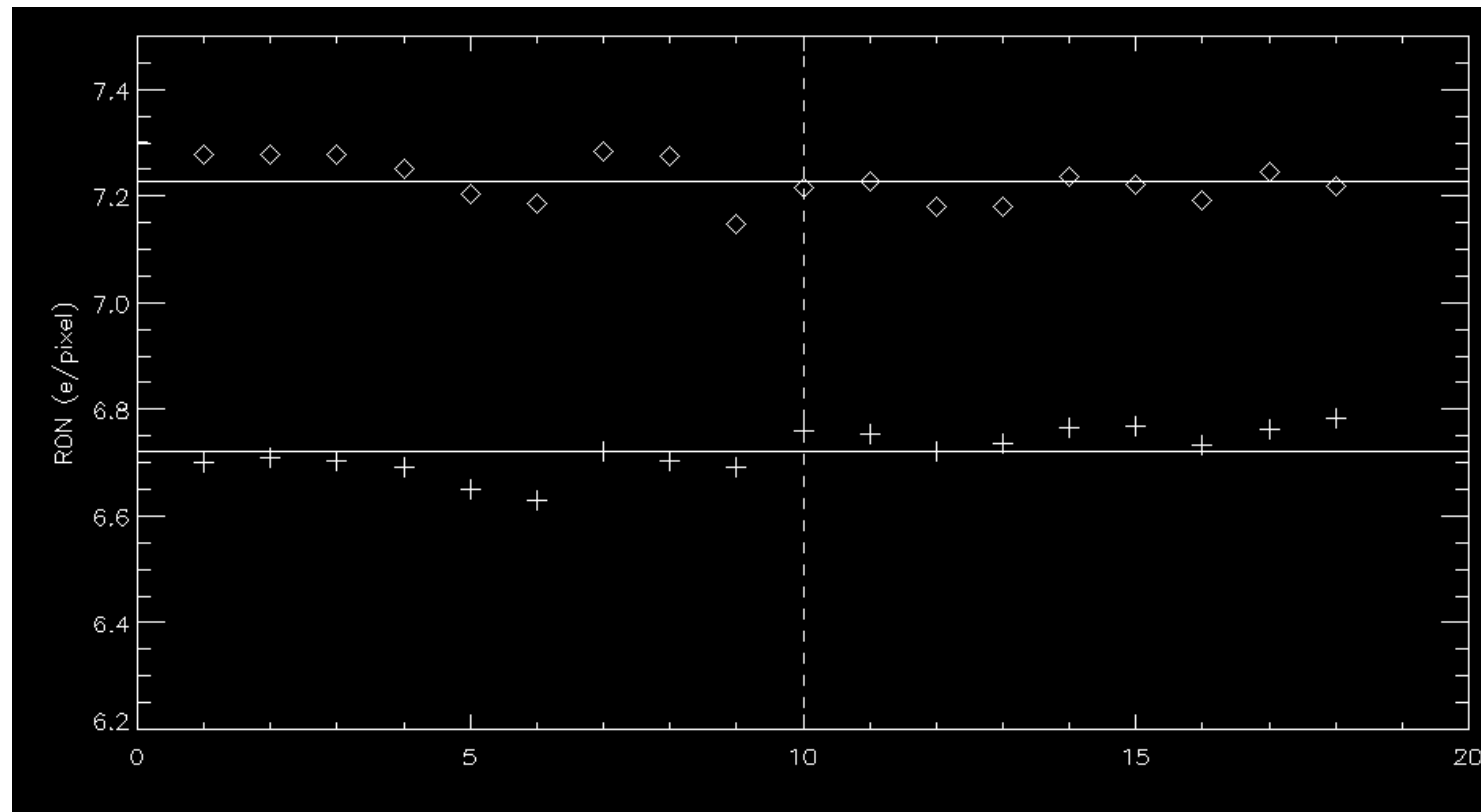
探测器性能标定



探测器性能标定

Readout noise

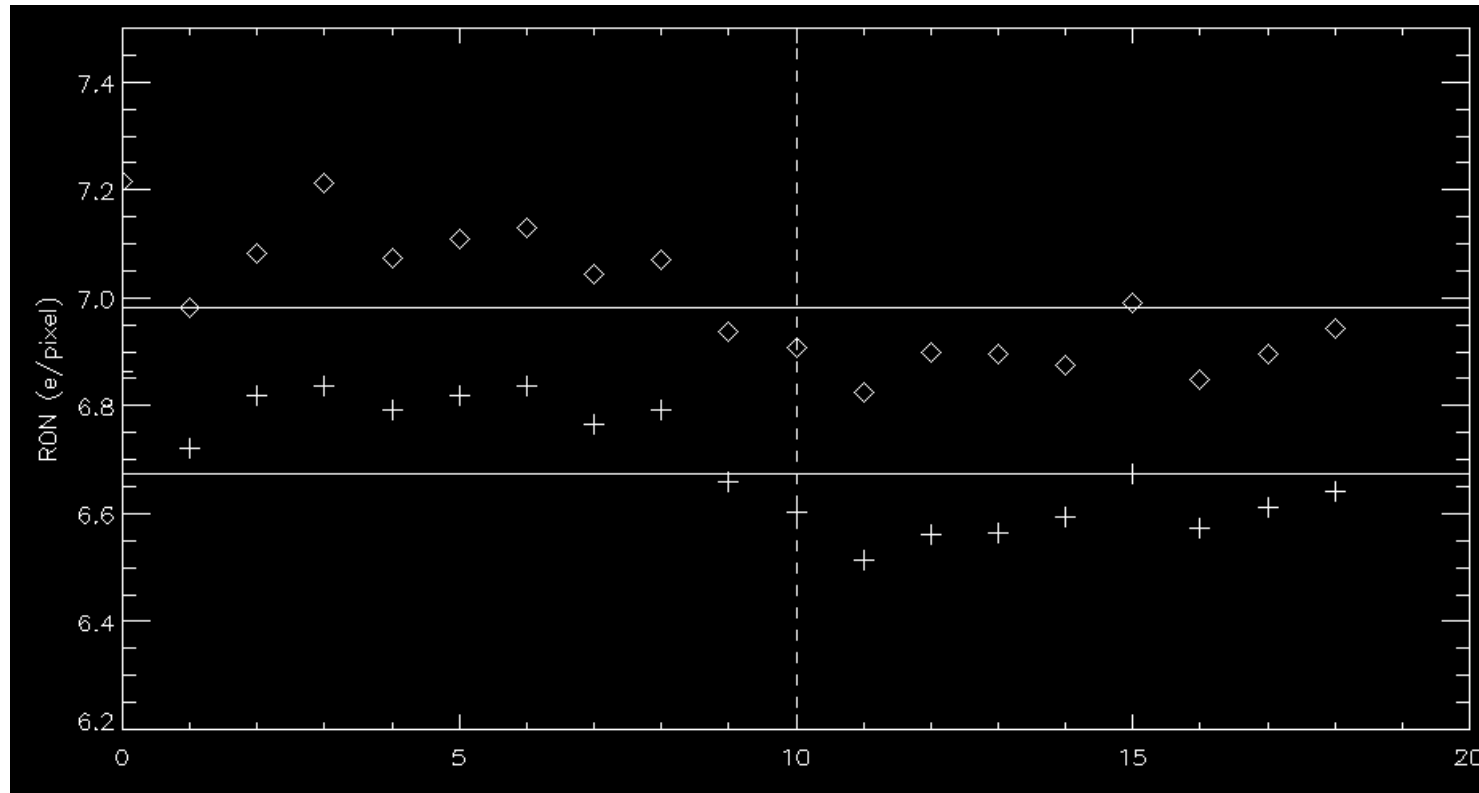
20160207



探测器性能标定

Readout noise

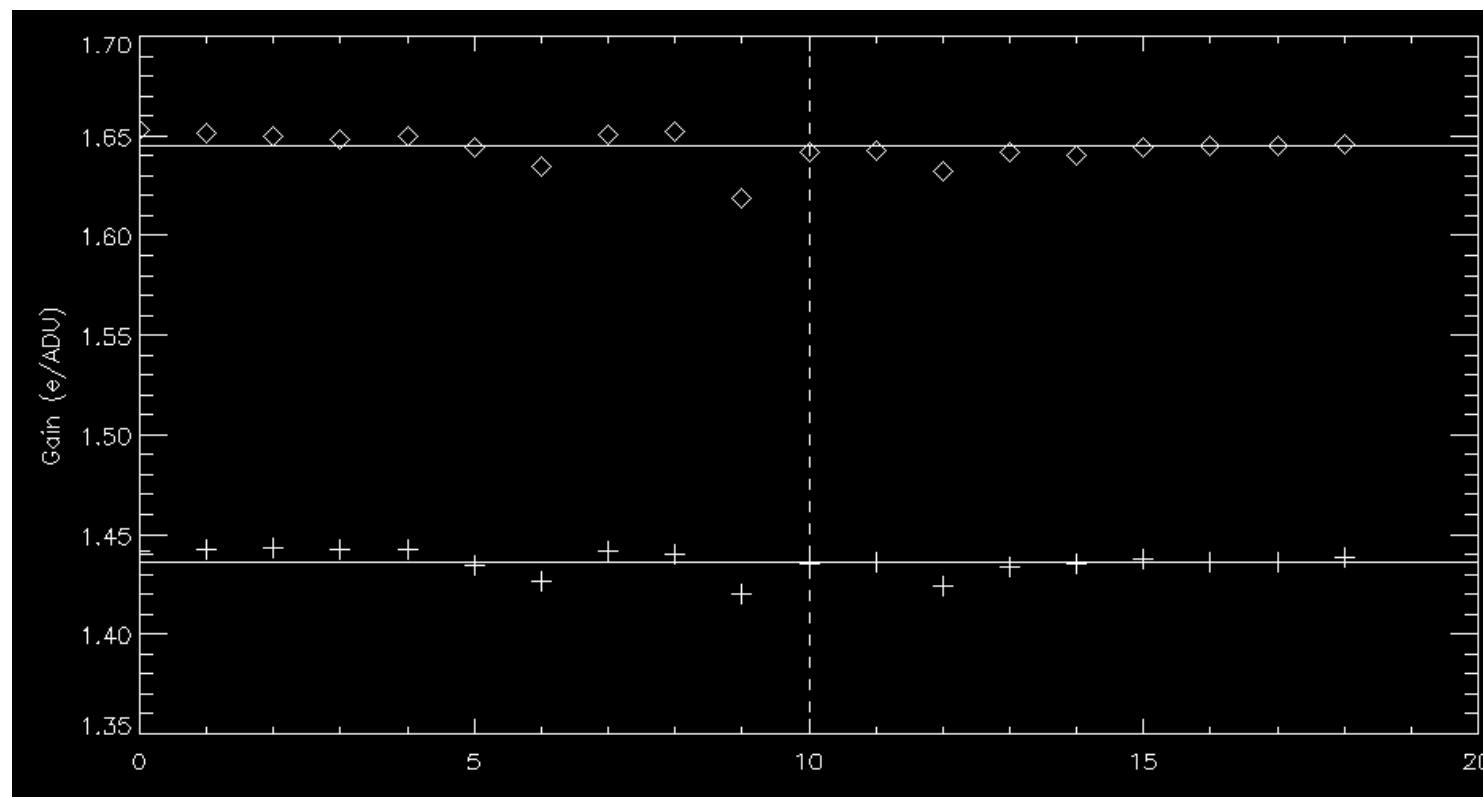
20160204



探测器性能标定

Gain

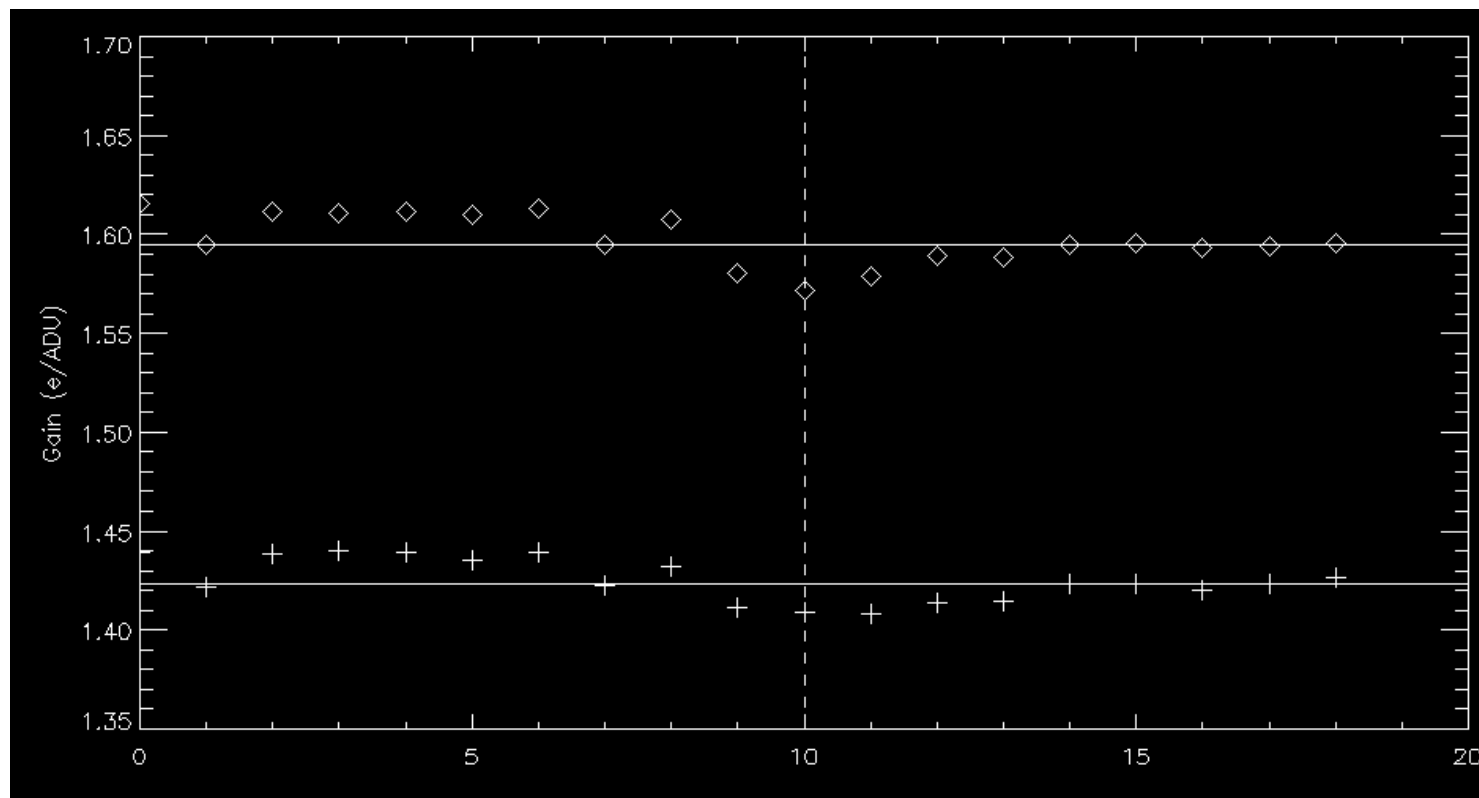
20160207



探测器性能标定

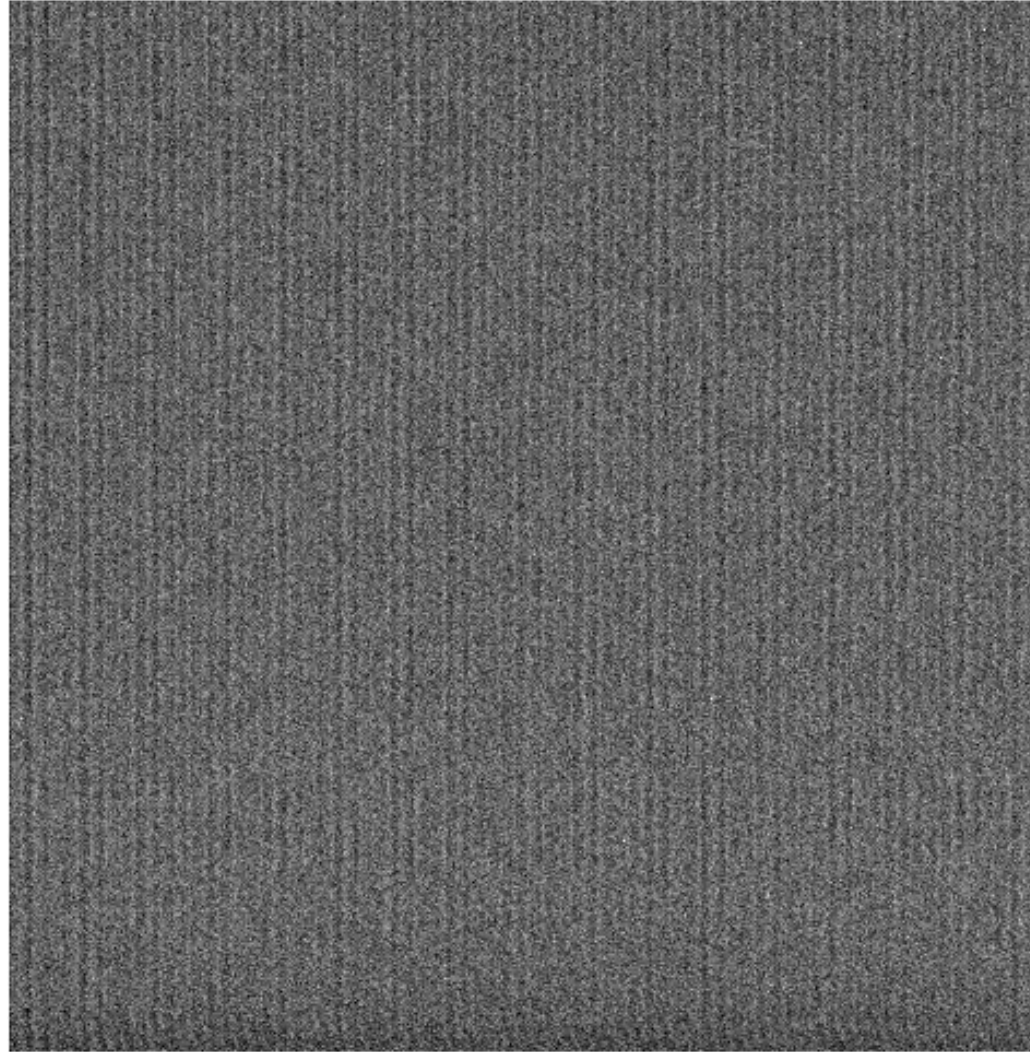
Gain

20160204



探测器性能标定

Bias (X, t)



探测器性能标定

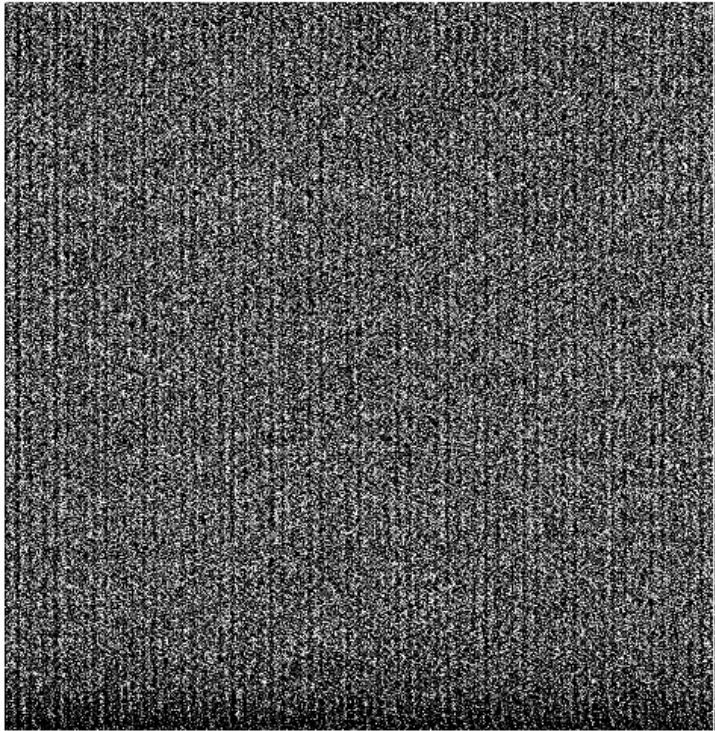
Overscan(s)

Overscans can monitor the time variations of the median bias and also roughly monitor the large-scale pattern variations along the X/Y direction.

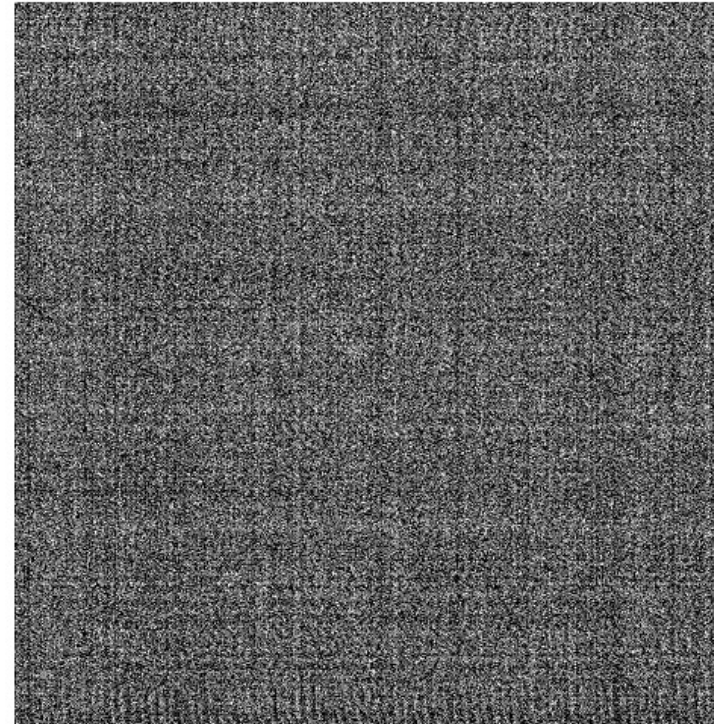
探测器性能标定

Overscan(s)

Bias

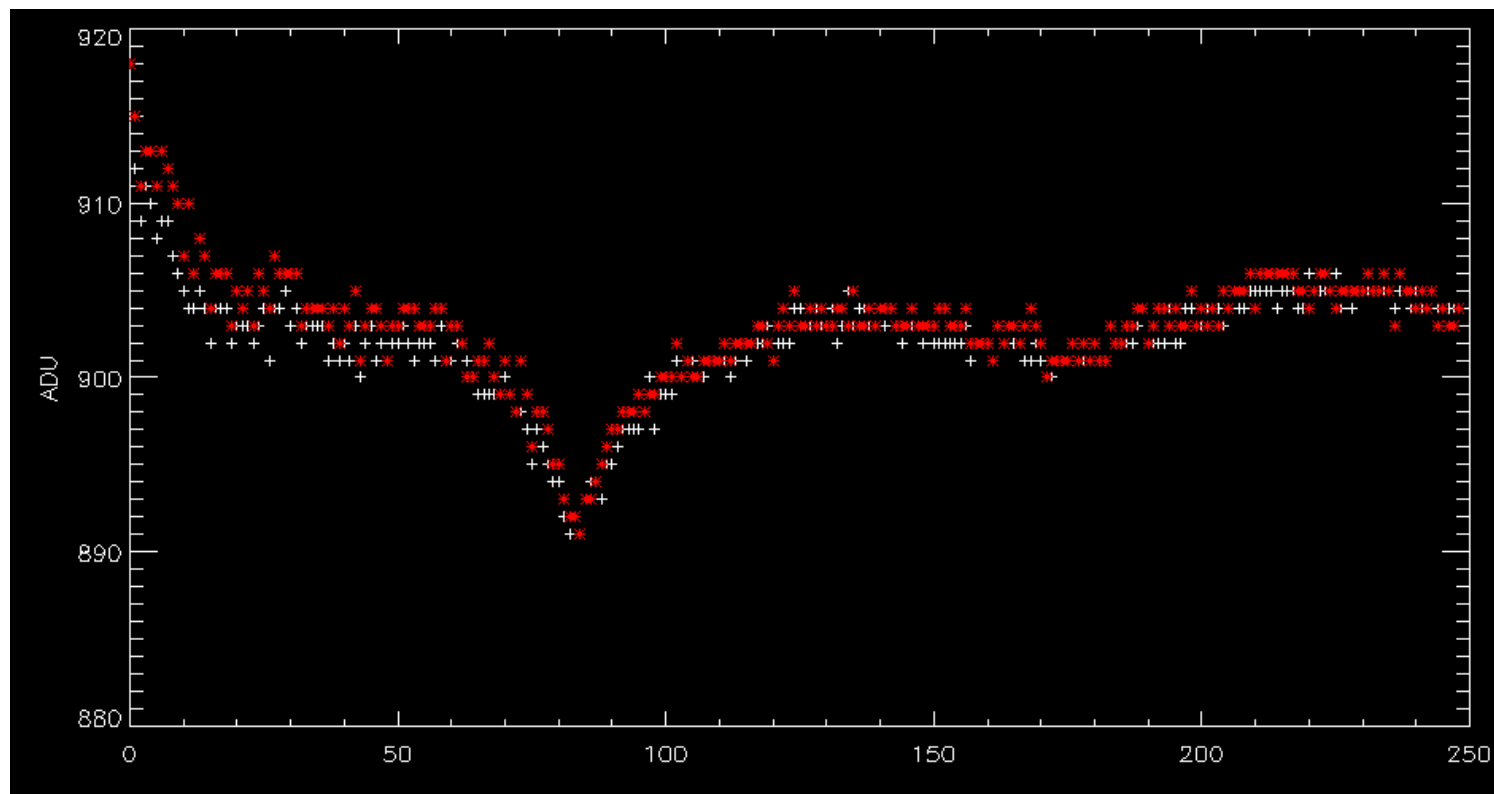


Bias - overscan



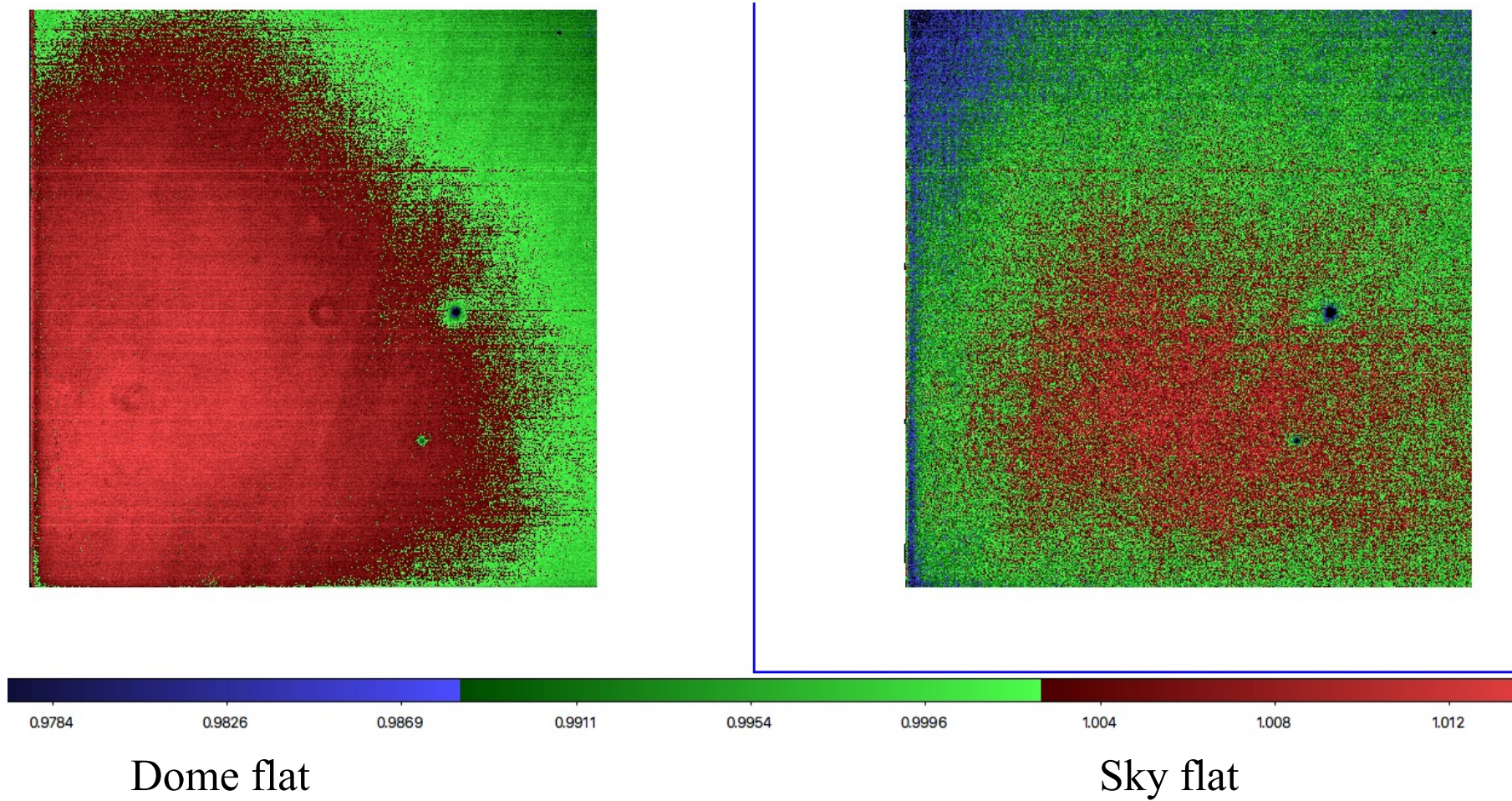
探测器性能标定

Overscan(s)



探测器性能标定

Flat: small (QE) + large (dust, vignetting) spatial variations

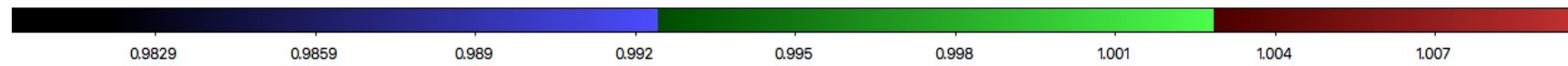
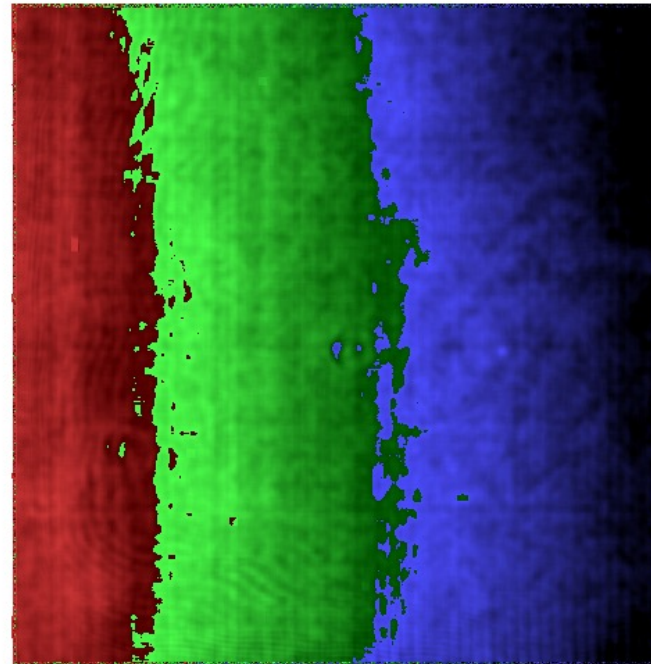


探测器性能标定

Flat: small (QE) + large (dust, vignetting) spatial variations

Dome: $S * L * I$

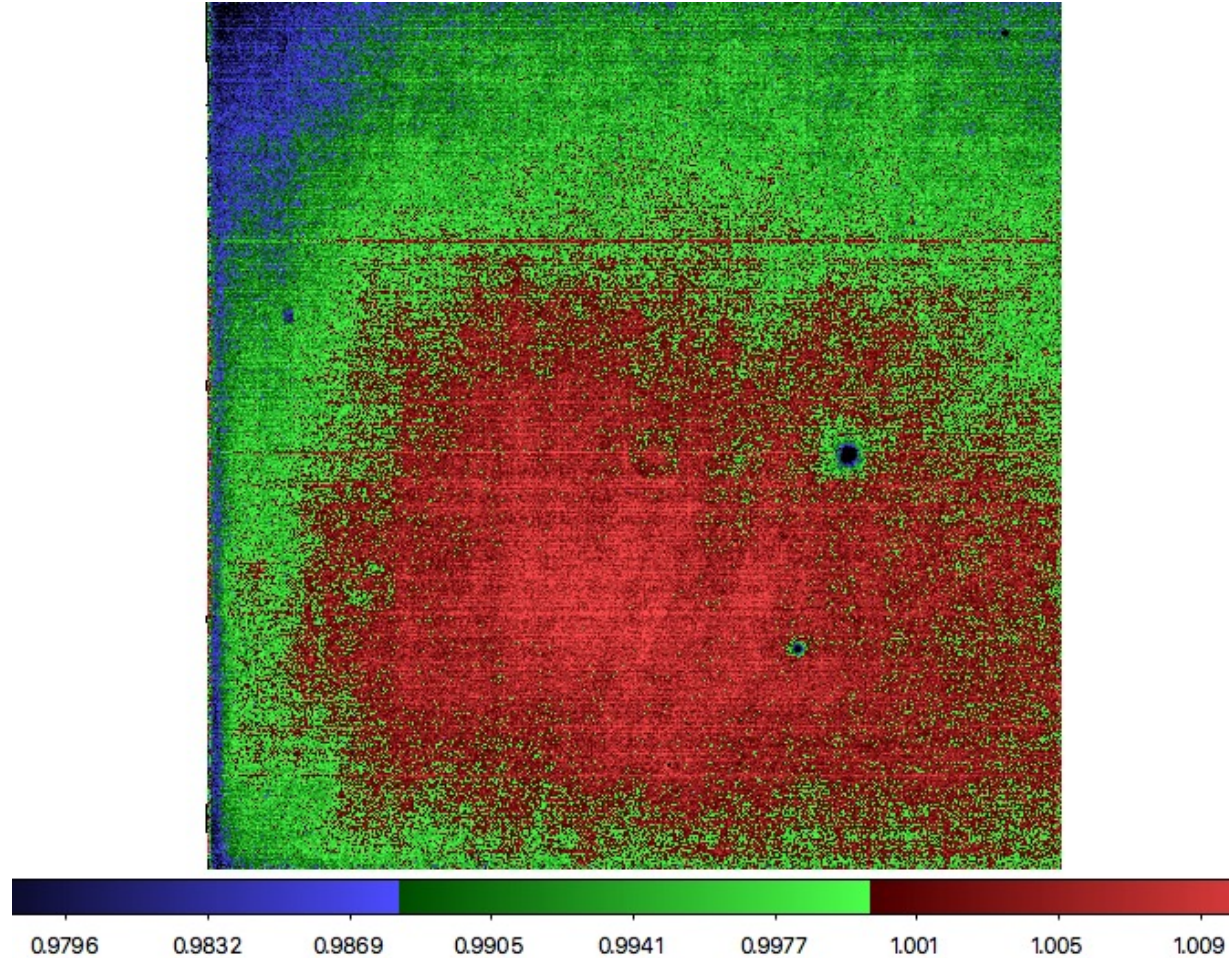
Sky: $S \text{ (low SNR)} * L$



Dome/Sky

探测器性能标定

Flat: small (QE) + large (dust, vignetting) spatial variations



Dome/Smooth(Dome/Sky) Flat

探测器性能标定

Wavelength (& positional)-dependent instrumental response function

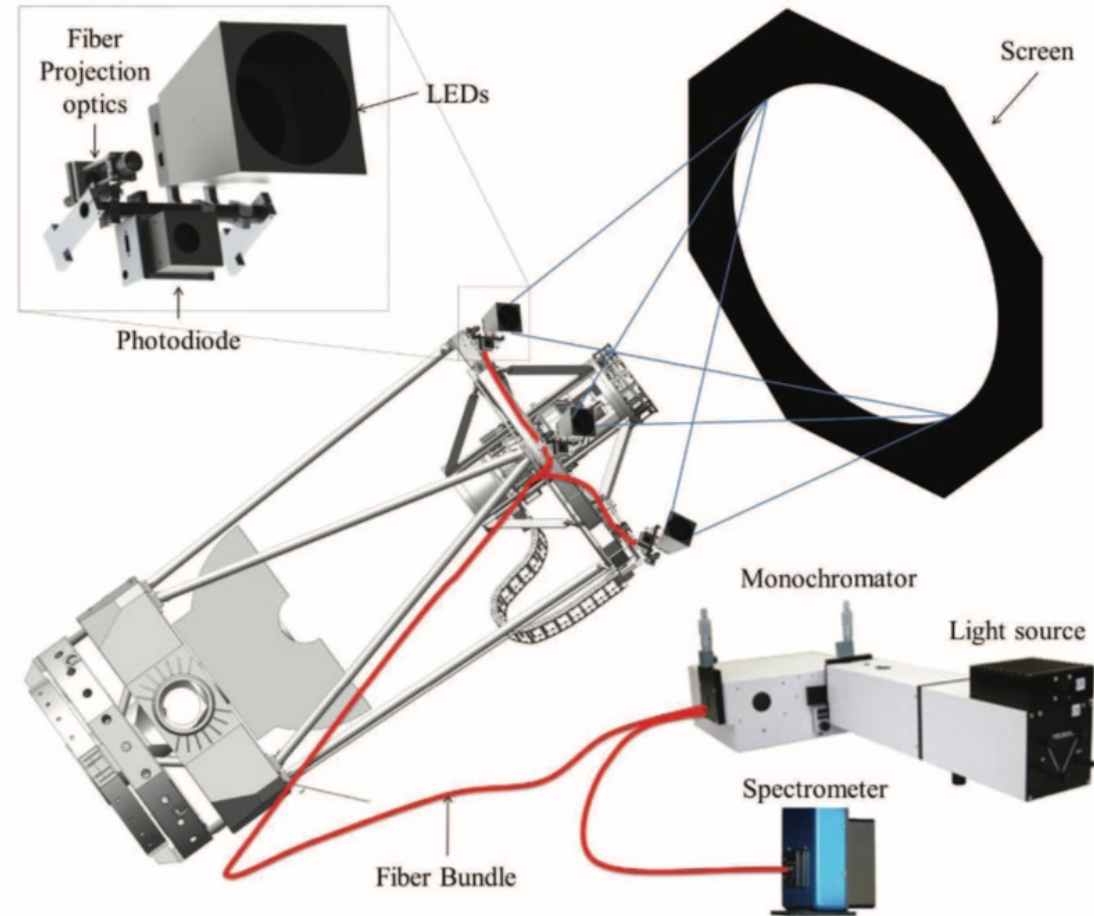
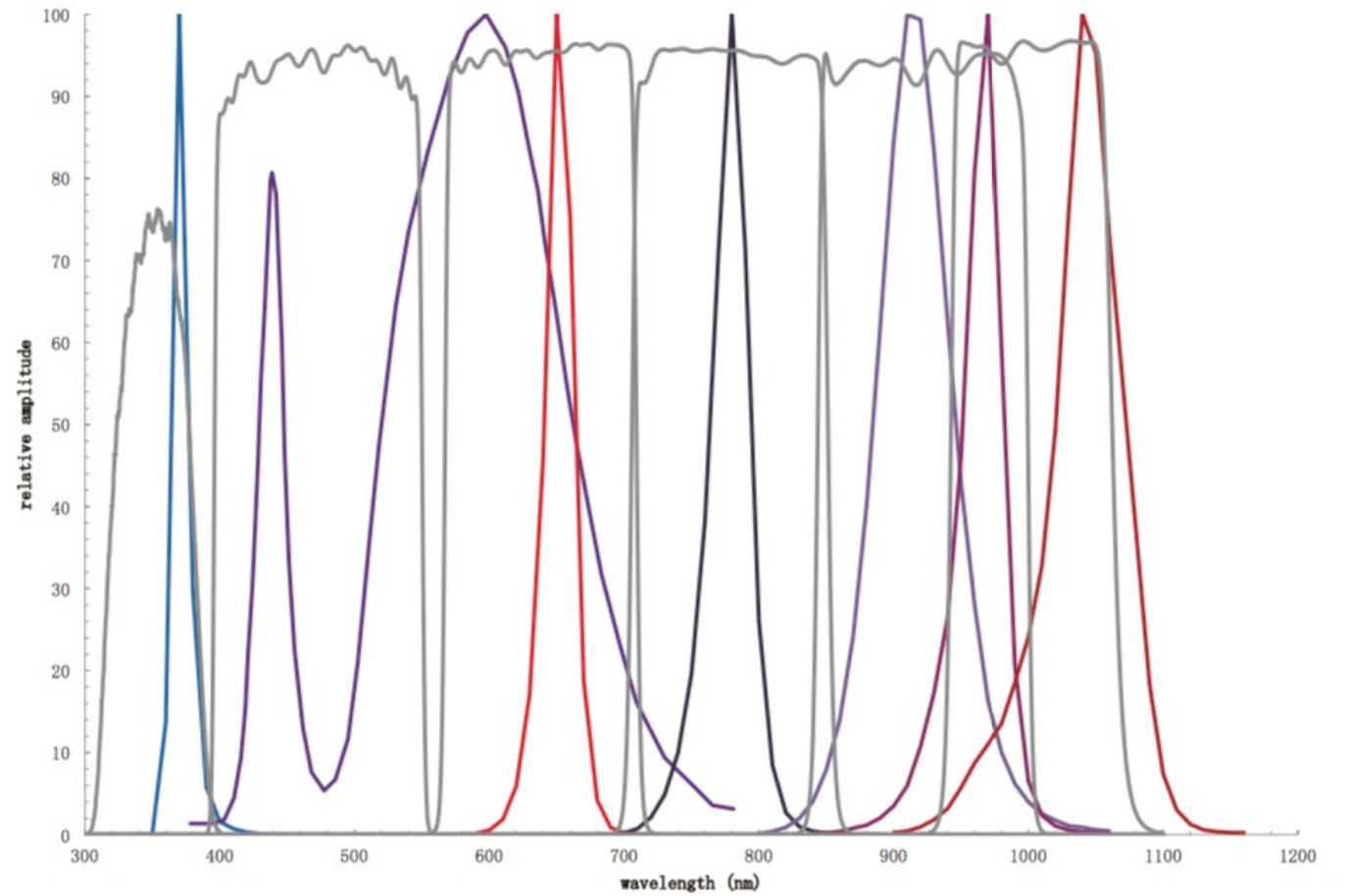


Figure 1. Schematic drawing of the DECal system.

探测器性能标定

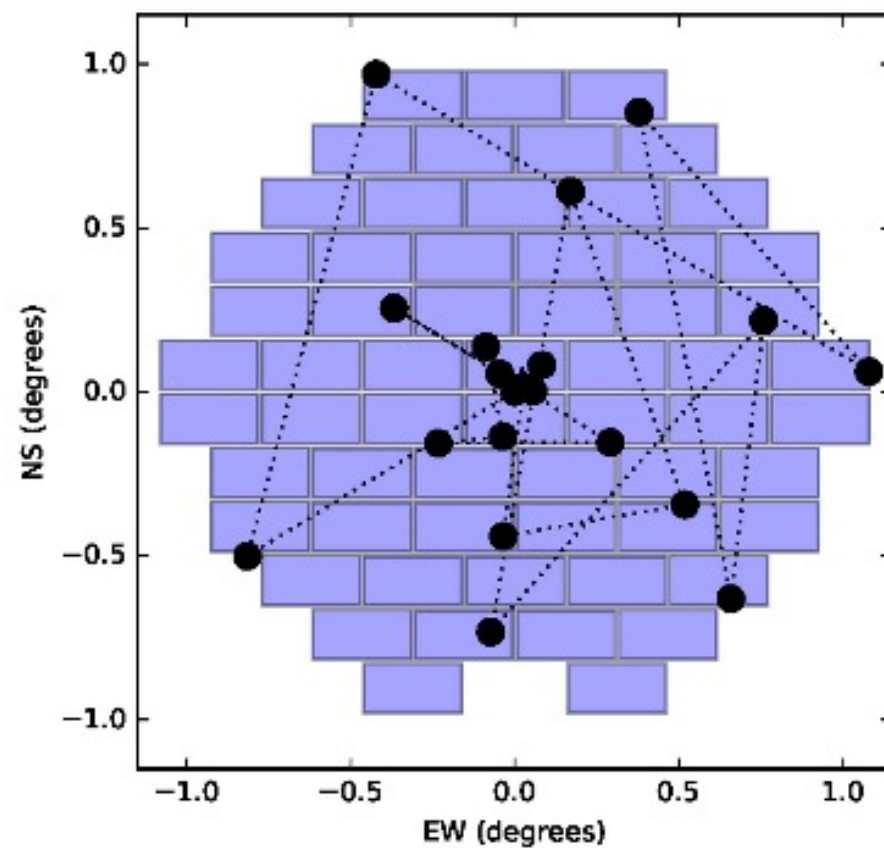
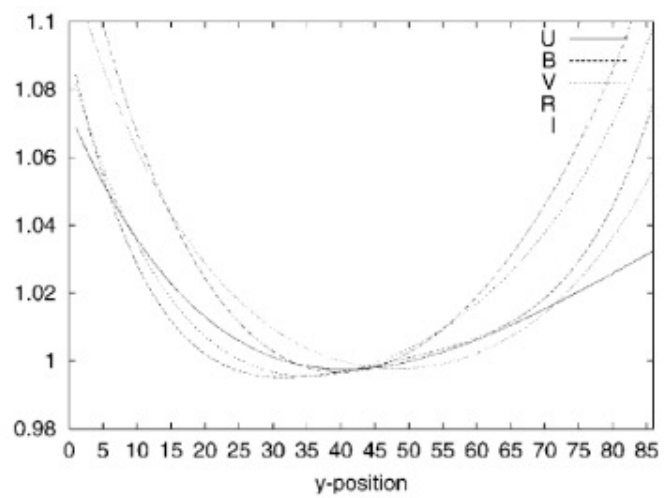
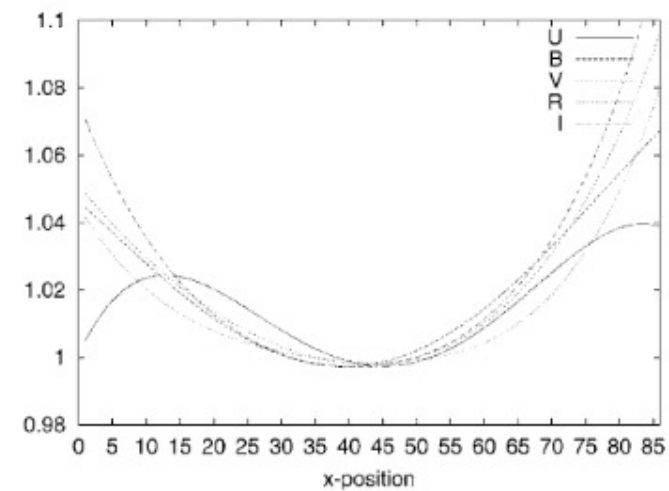
Flat-fielding strategy



Marshall et al. 2013

探测器性能标定

“Star flats” (Manfroid 1995, 1996)

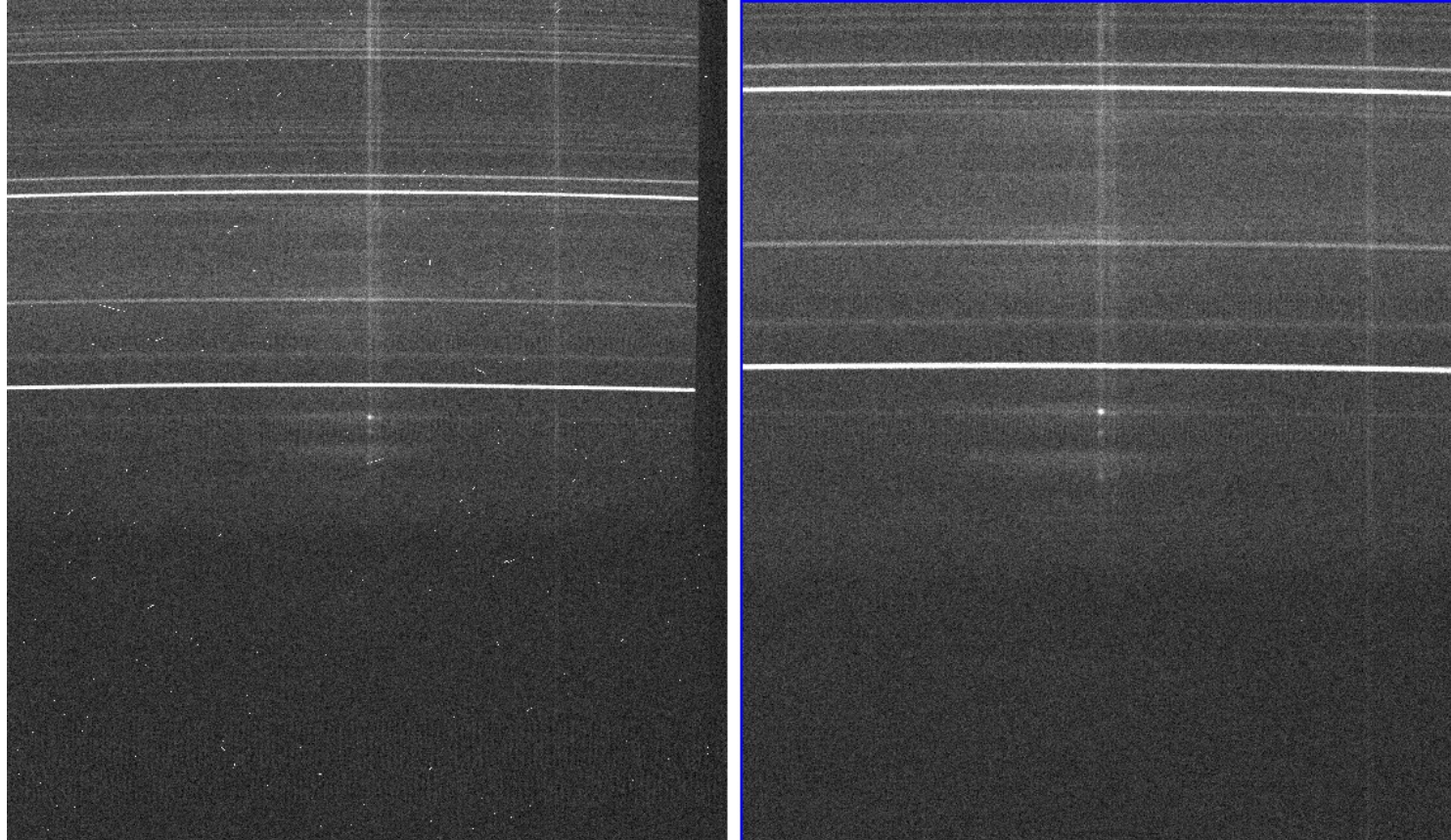


探测器性能标定

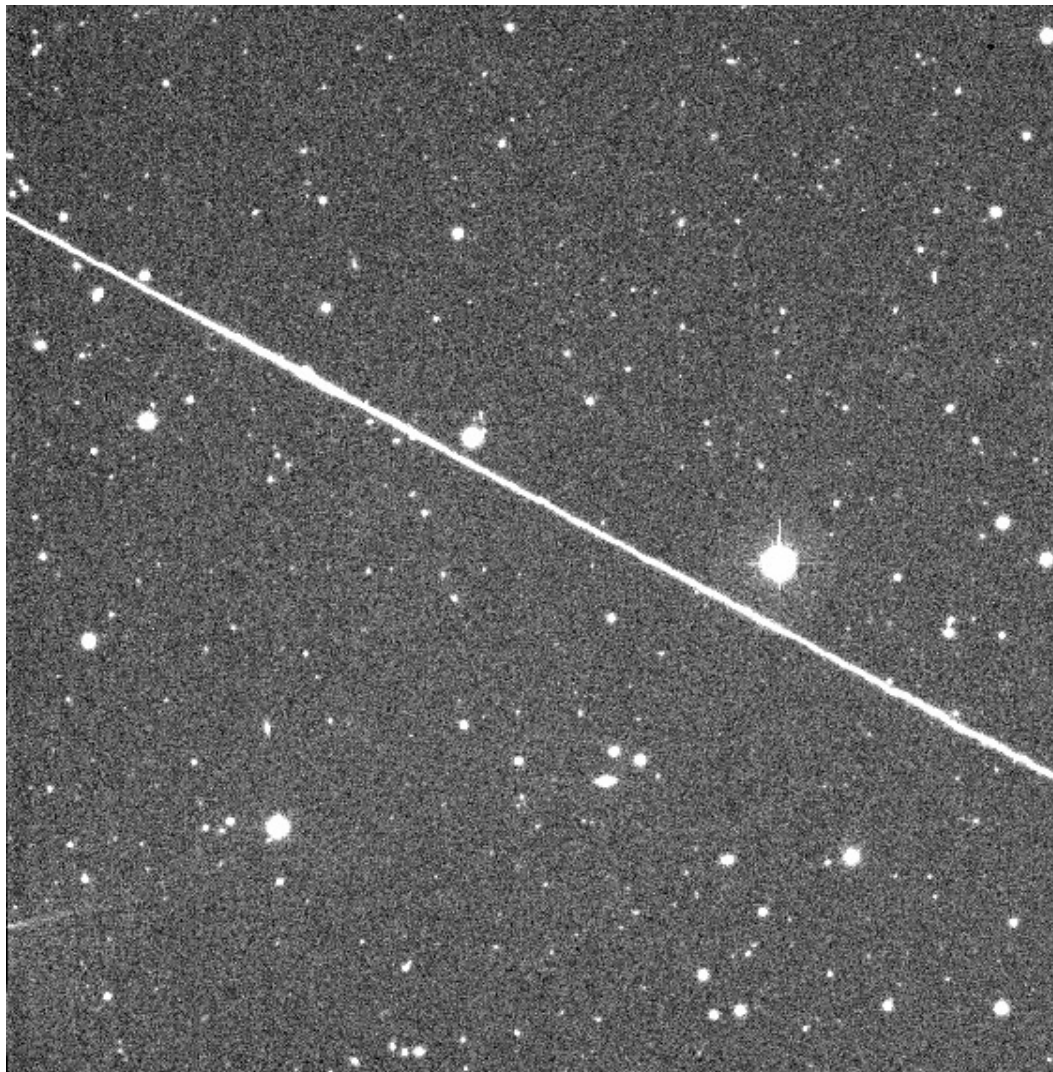
Multi-visits (including different bands): comparison or sigma-clipping

Single visit: median filter (2-3 s/frame)

Cosmic rays



探测器性能标定



Hough transformation (Hough 1962)

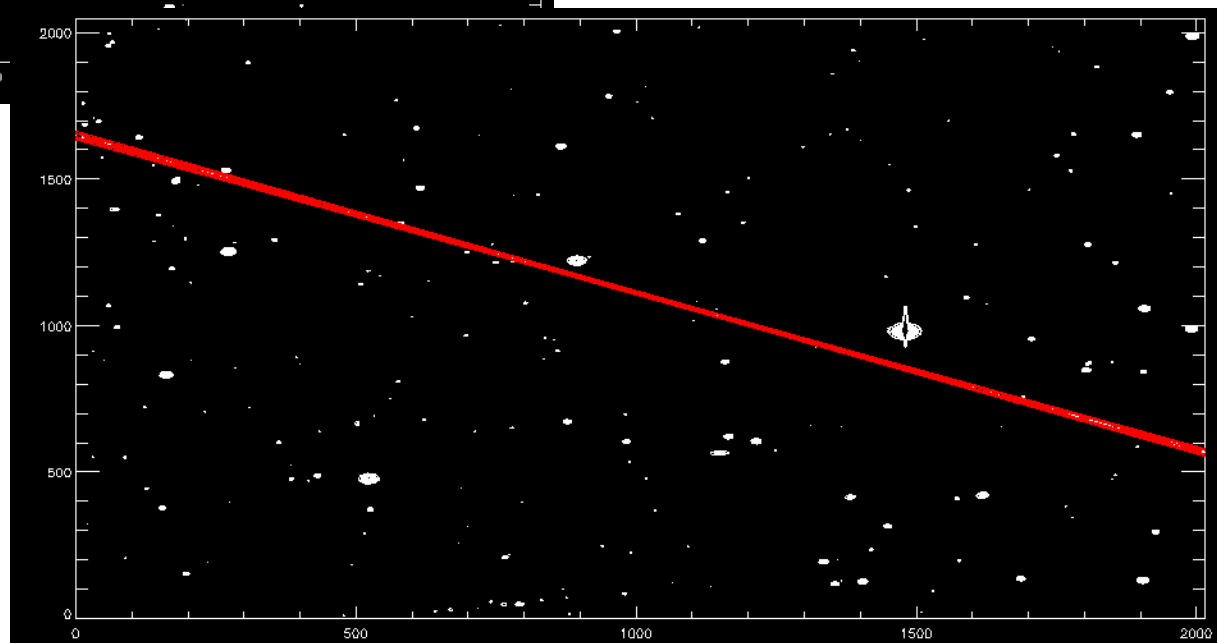
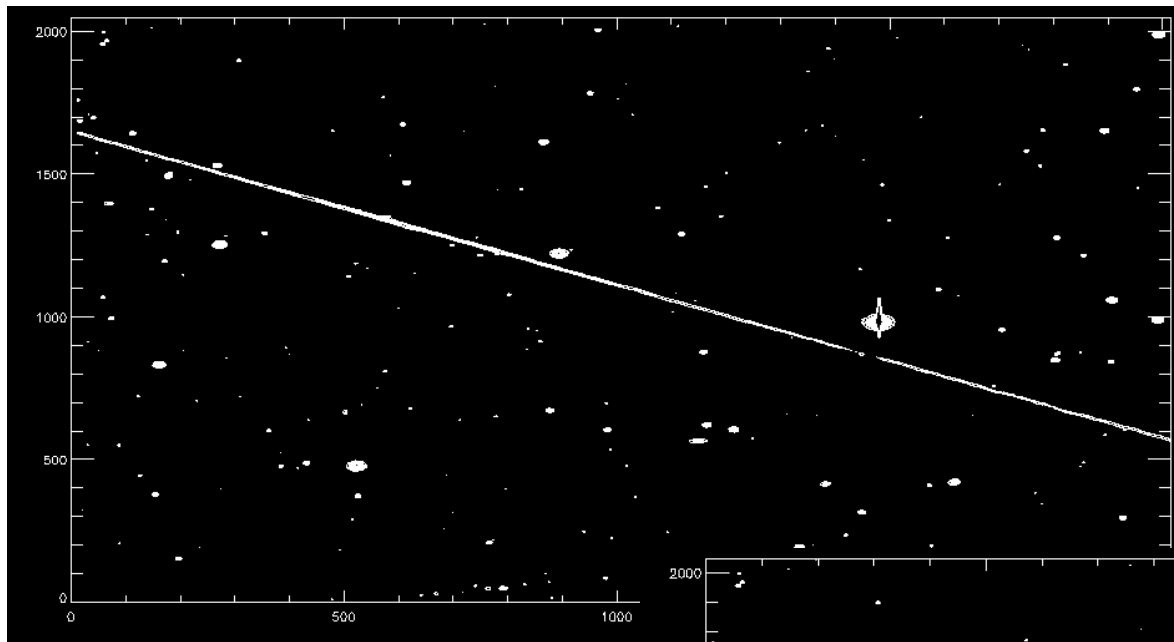
$$y = a \cdot x + b$$

$$r = x \cdot \cos \theta + y \cdot \sin \theta \Leftrightarrow$$

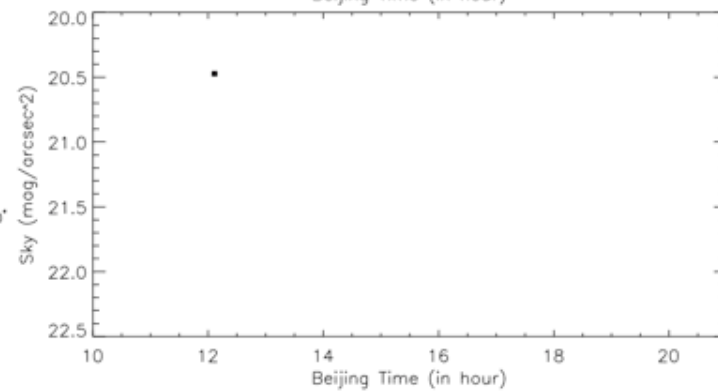
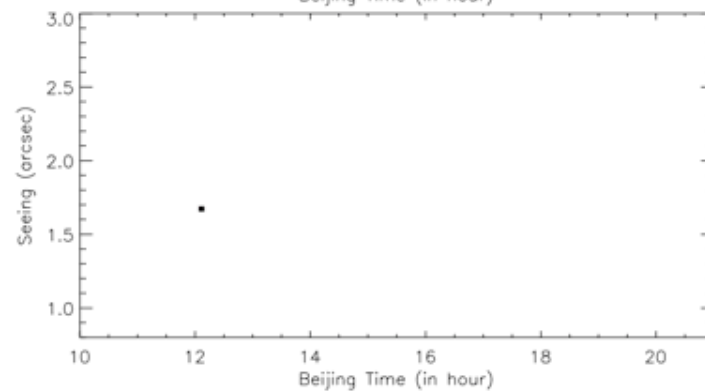
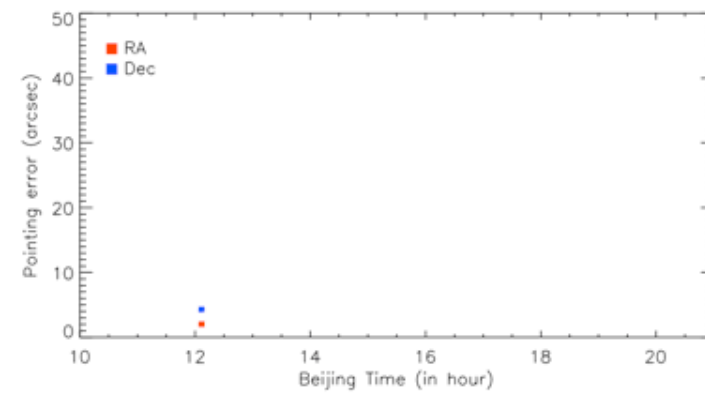
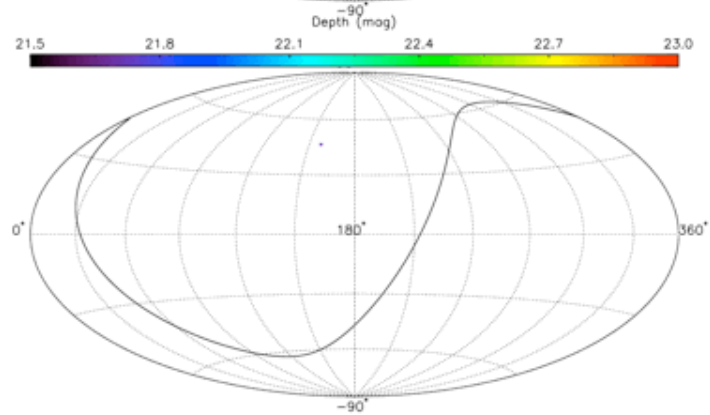
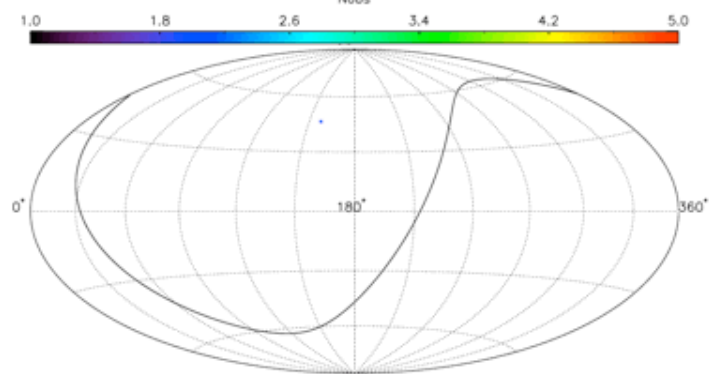
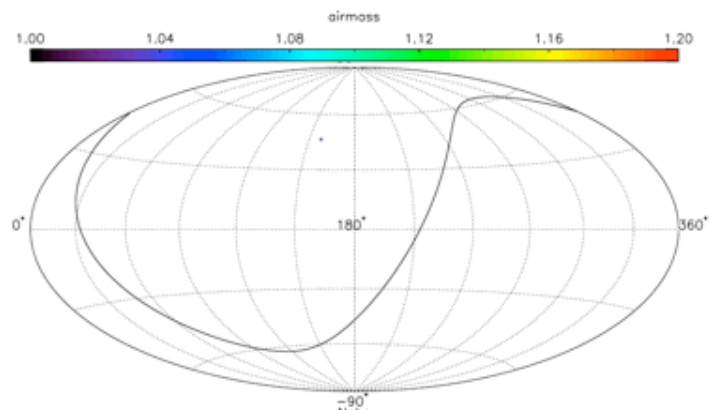
$$y = -\frac{\cos \theta}{\sin \theta} \cdot x + \frac{r}{\sin \theta}$$

Satellite lines

探测器性能标定

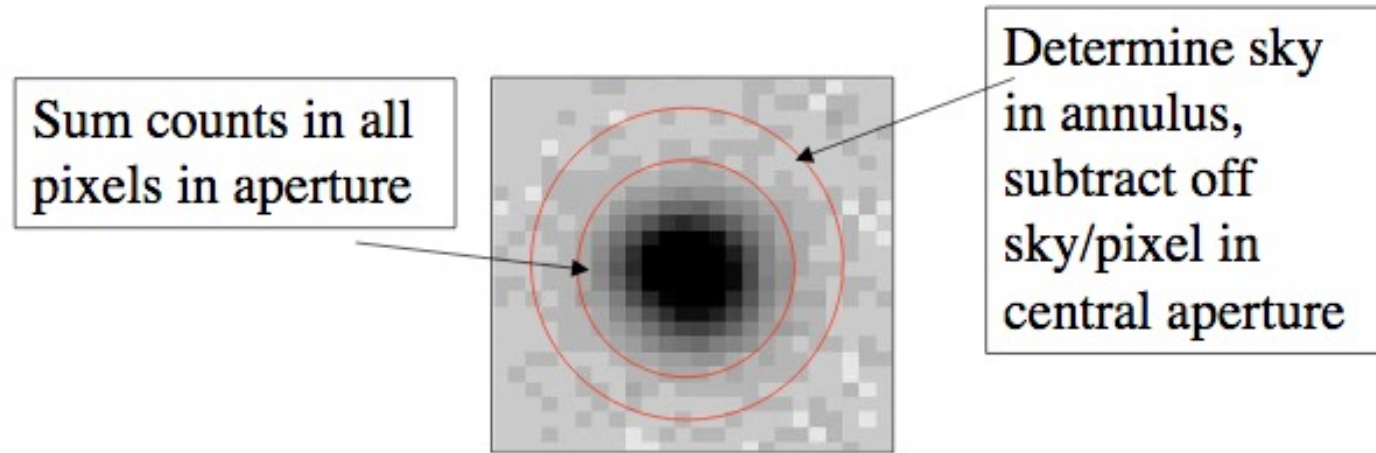


天测与测光



天测与测光

Aperture Photometry



References:

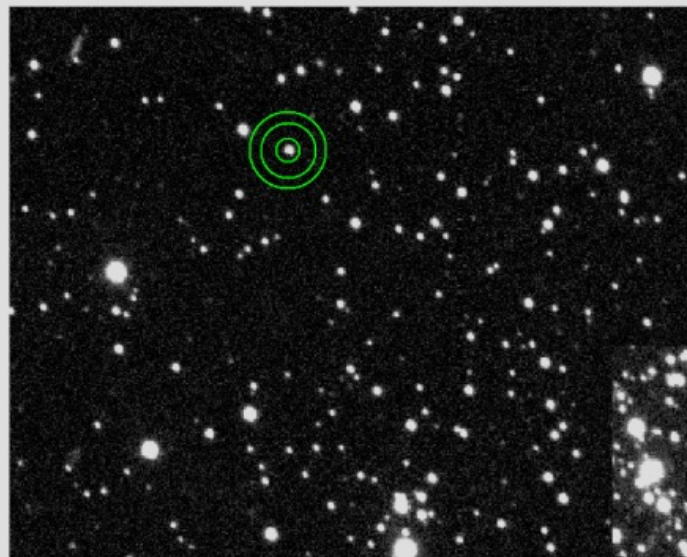
Da Costa, 1992, ASP Conf Ser 23

Stetson, 1987, PASP, 99, 191

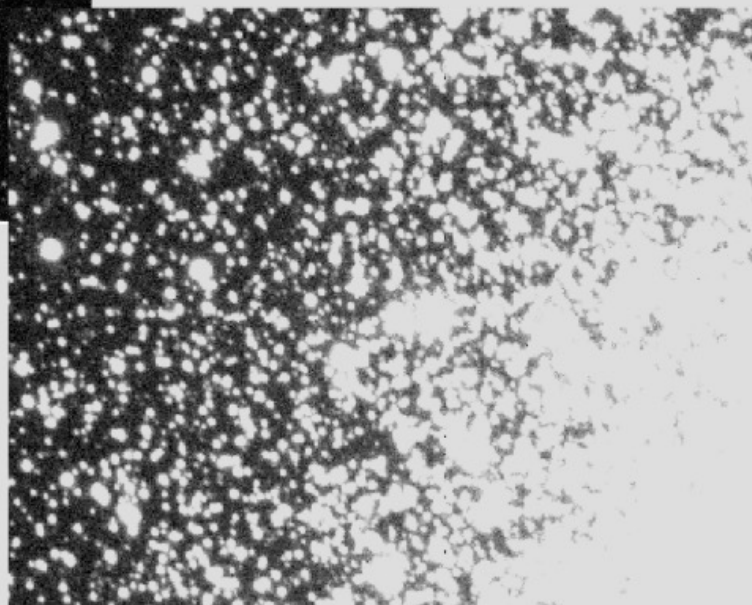
Stetson, 1990, PASP, 102, 932

天测与测光

Aperture Photometry



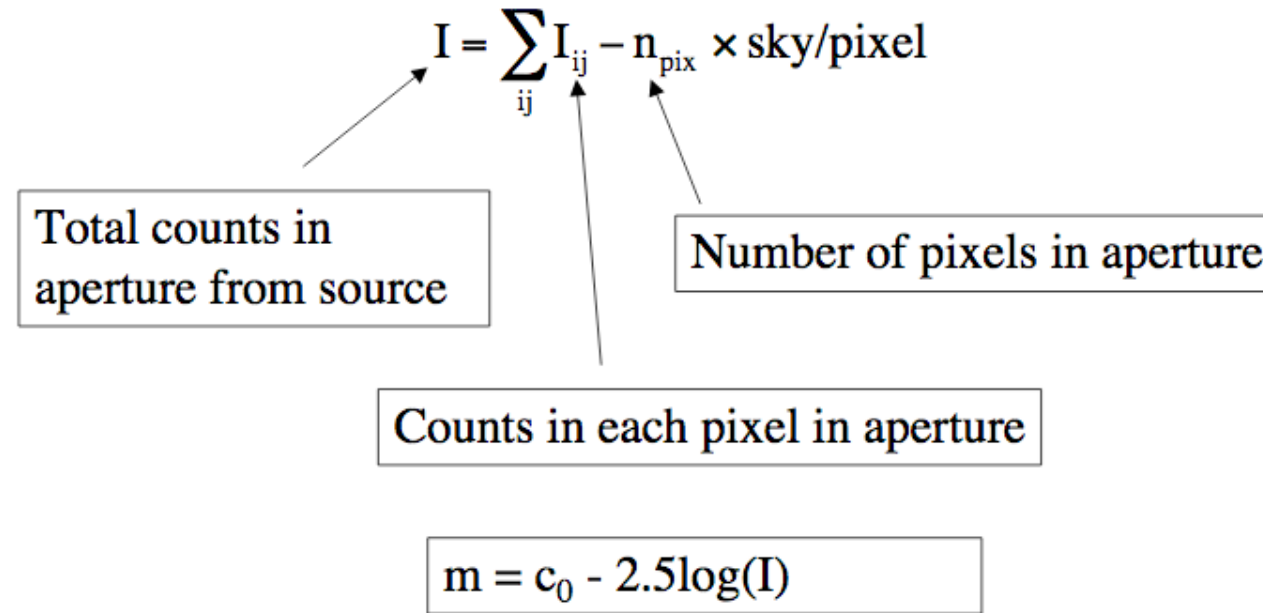
Aperture photometry good here.



Aperture photometry not so good here!

天测与测光

Aperture Photometry

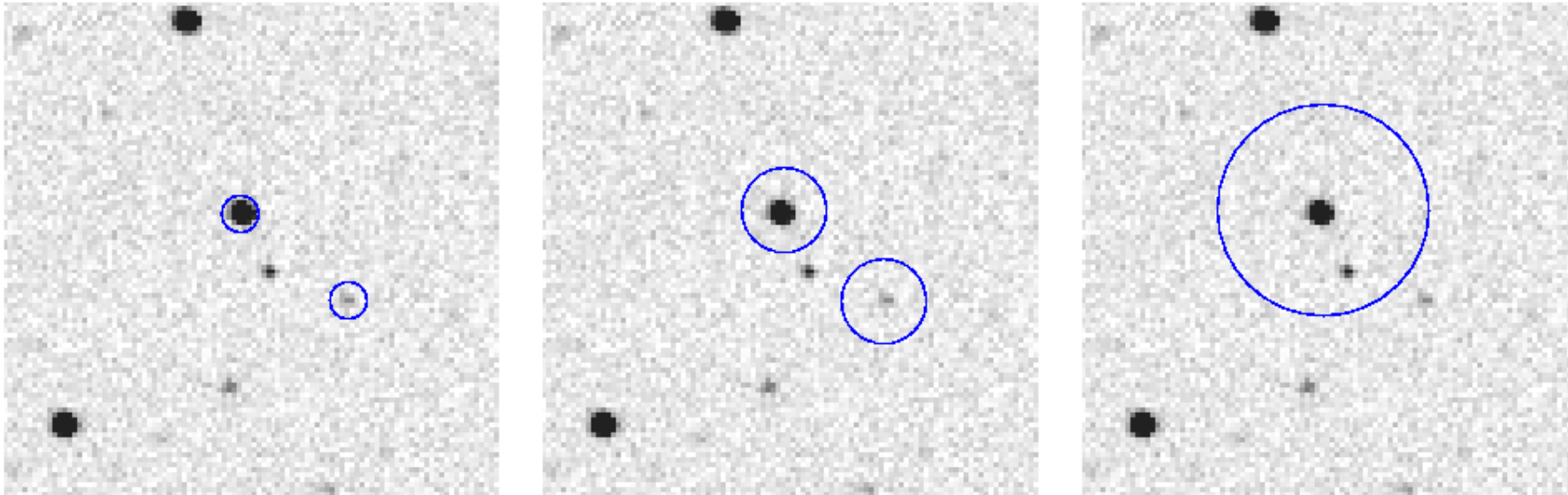


Center
Sky background
Aperture radius

天测与测光

Aperture Photometry

Selecting the right aperture

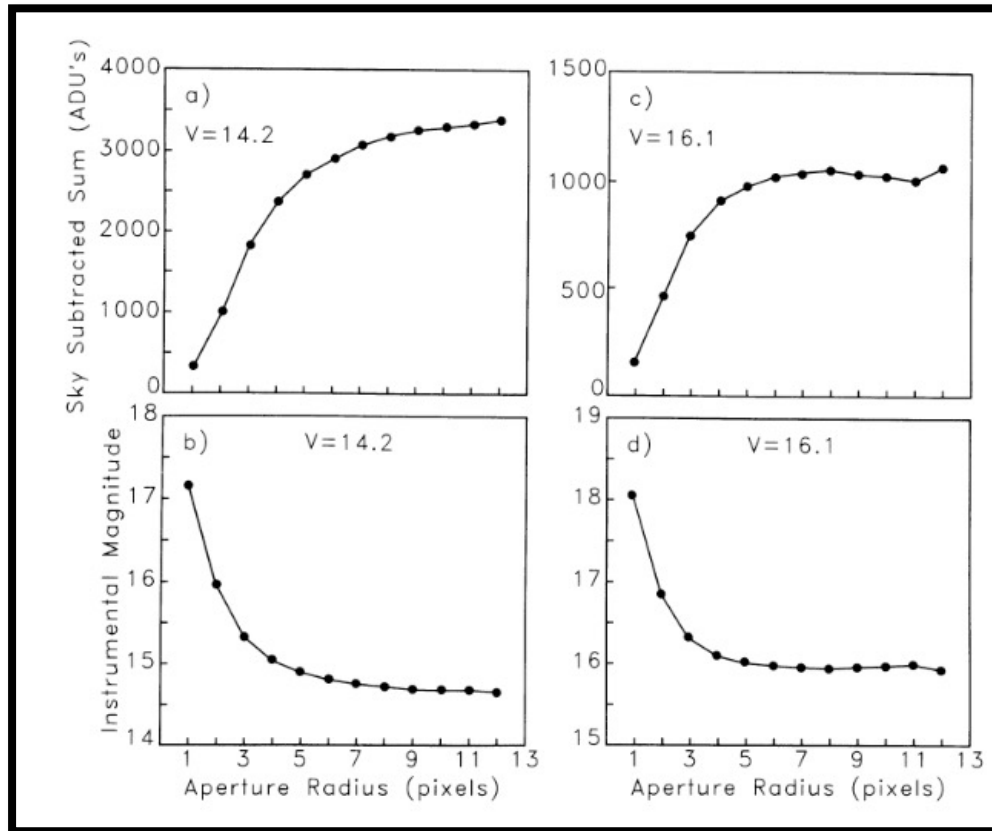


- Too small: not enough to include the whole stellar light
- Too big: too many “noise pixels”

天测与测光

Aperture Photometry

CCD Equation: Signal-to-Noise



0.4 arcsec pixel scale
1.2 arcsec FWHM seeing
Howell 1989

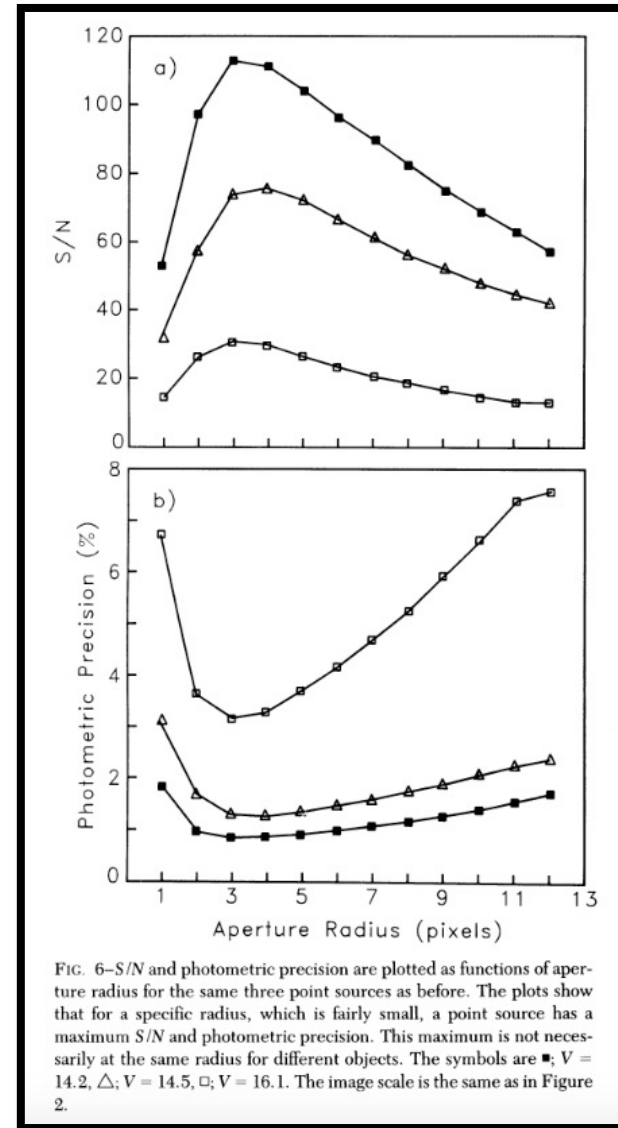
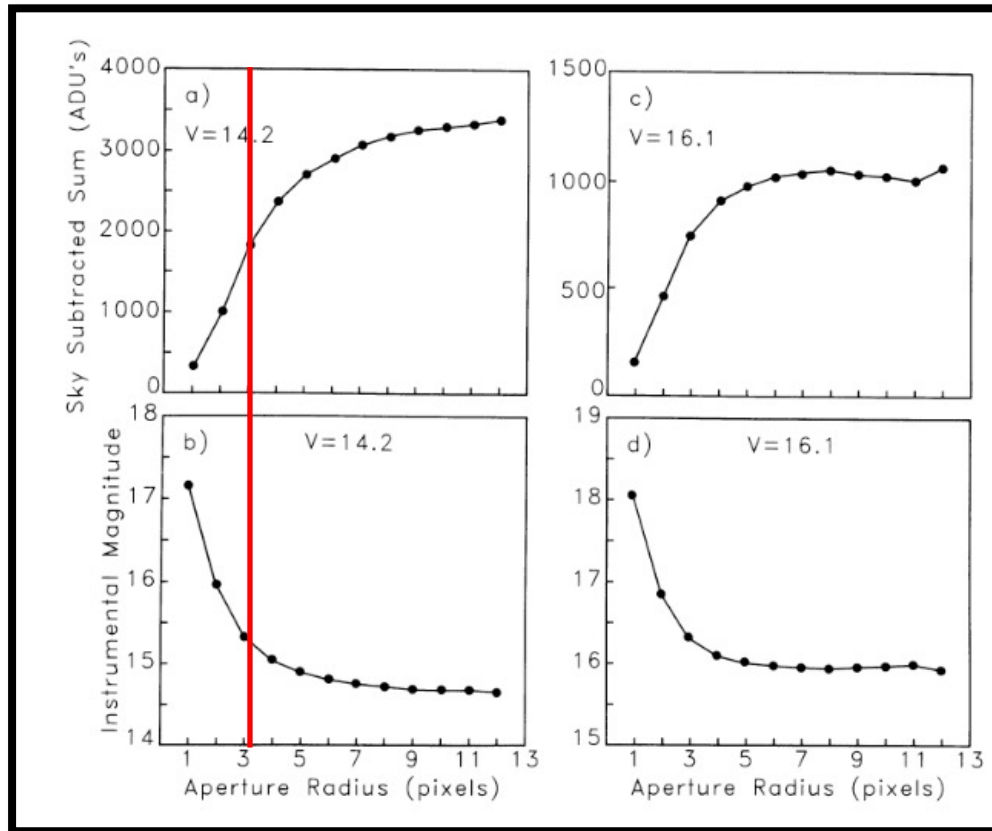


FIG. 6—S/N and photometric precision are plotted as functions of aperture radius for the same three point sources as before. The plots show that for a specific radius, which is fairly small, a point source has a maximum S/N and photometric precision. This maximum is not necessarily at the same radius for different objects. The symbols are ■, V = 14.2, △, V = 14.5, □, V = 16.1. The image scale is the same as in Figure 2.

天测与测光

Aperture Photometry

CCD Equation: Signal-to-Noise



0.4 arcsec pixel scale
1.2 arcsec FWHM seeing
Howell 1989

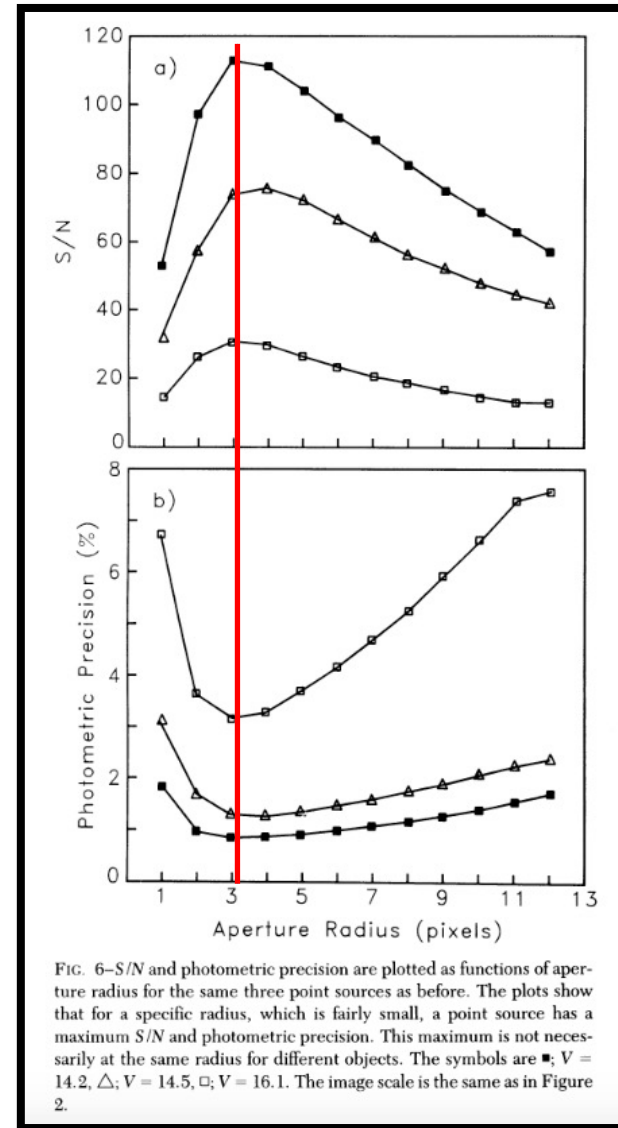
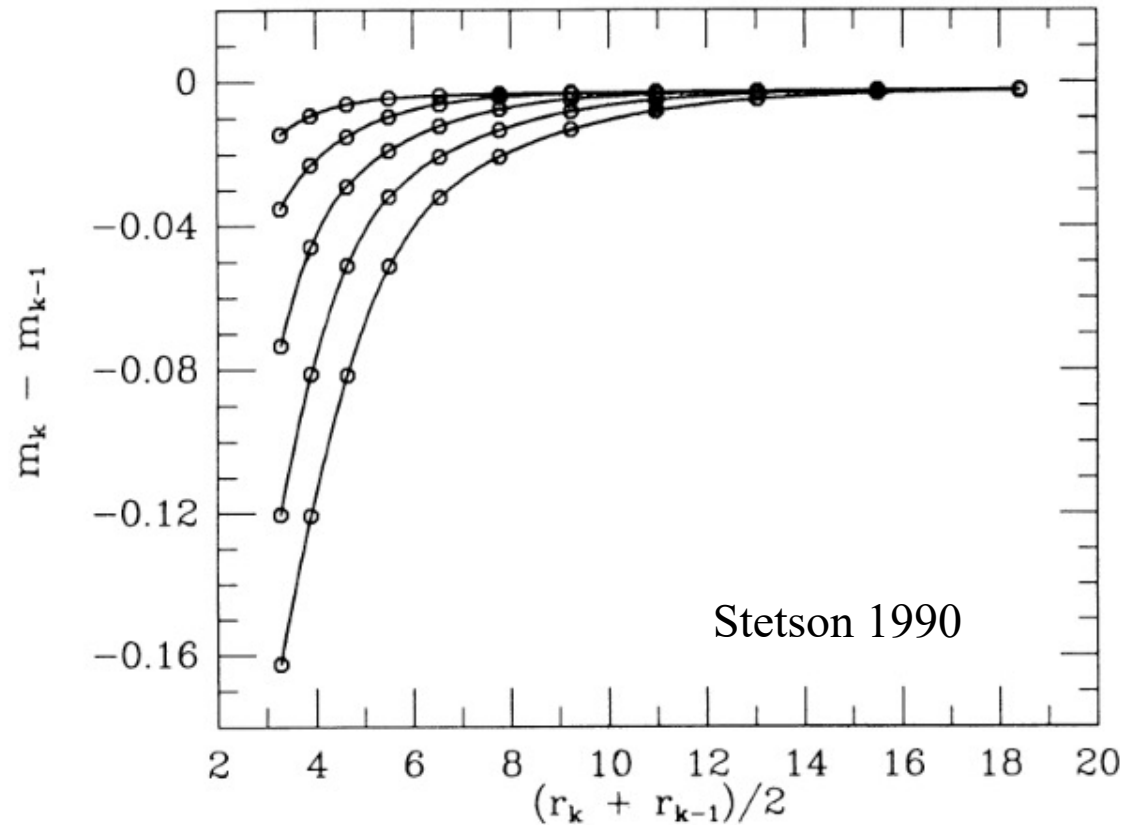


FIG. 6—S/N and photometric precision are plotted as functions of aperture radius for the same three point sources as before. The plots show that for a specific radius, which is fairly small, a point source has a maximum S/N and photometric precision. This maximum is not necessarily at the same radius for different objects. The symbols are ■, V = 14.2, △, V = 14.5, □, V = 16.1. The image scale is the same as in Figure 2.

天测与测光

Aperture Photometry



Aperture correction & growth curves

If stellar PSF Gaussian distribution:

0.85 FWHM = 2 sigma = 95.45%

1.27 FWHM = 3 sigma = 99.73%

1.70 FWHM = 4 sigma = 99.99%

2.12 FWHM = 5 sigma = ~100%

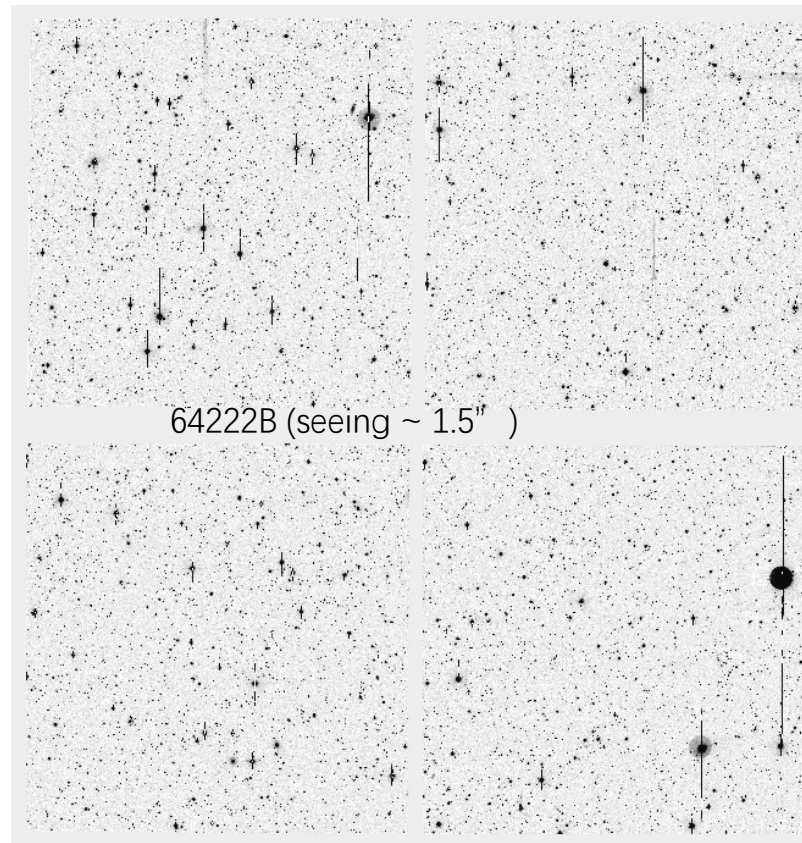
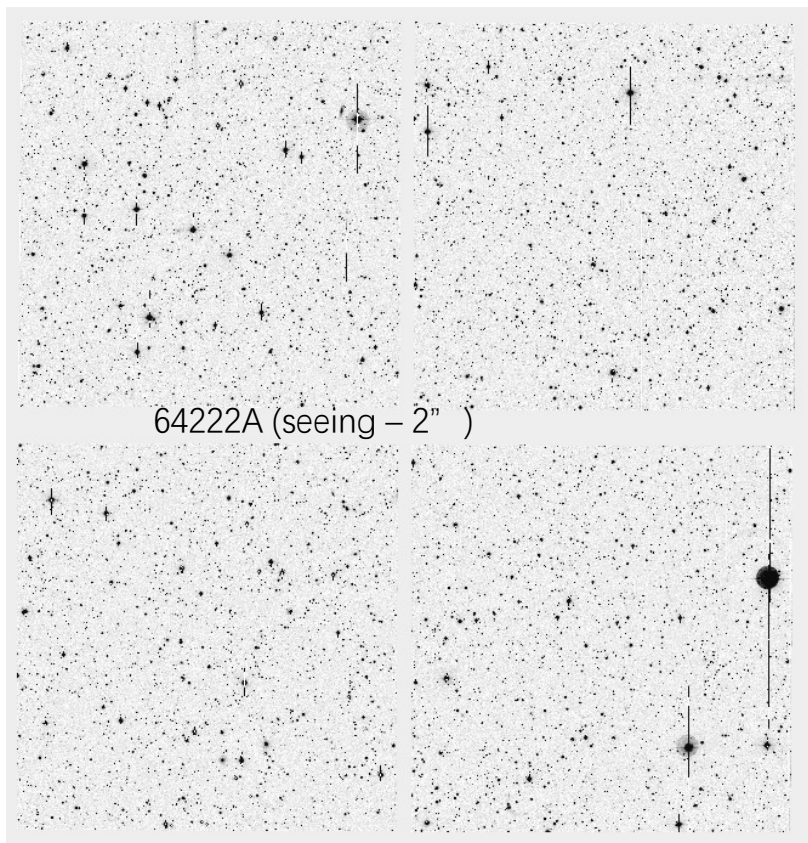
- Select a relative small aperture size (~1.5 FWHM)
- Construct growth curves using isolated and bright stars in the field
- Apply aperture corrections

天测与测光

BASS 64222 天区 r波段
RA : 06:14:35; Dec : 56:15:44
gl: 158.01138; gb: 17.461039

观测时间：20160203 163s 曝光

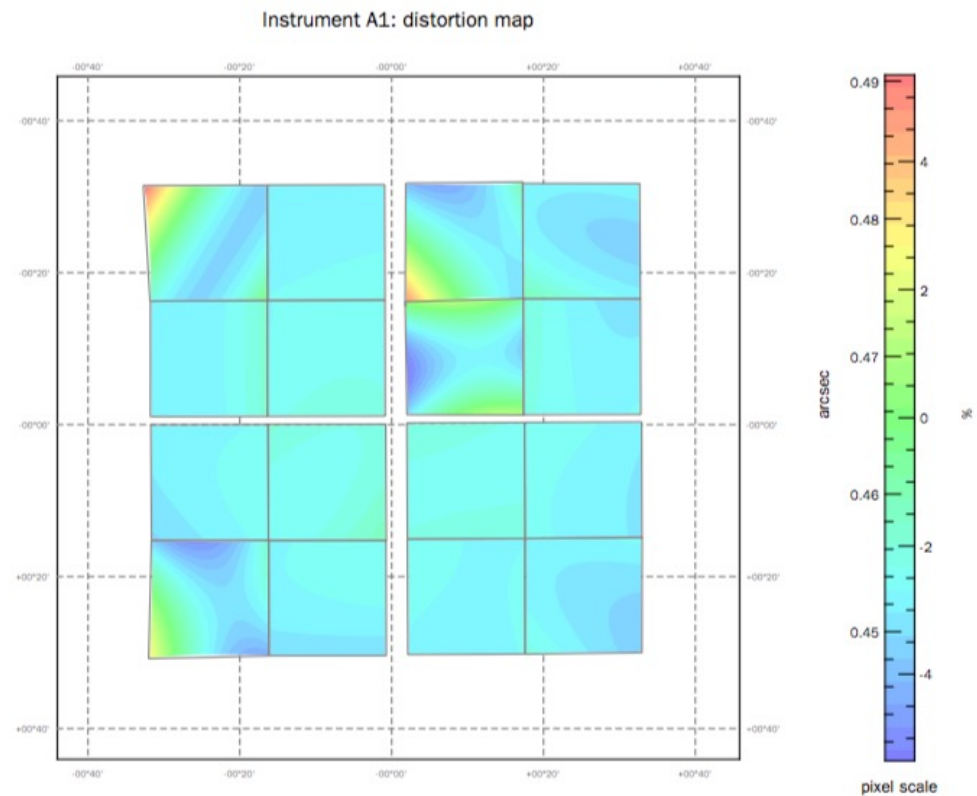
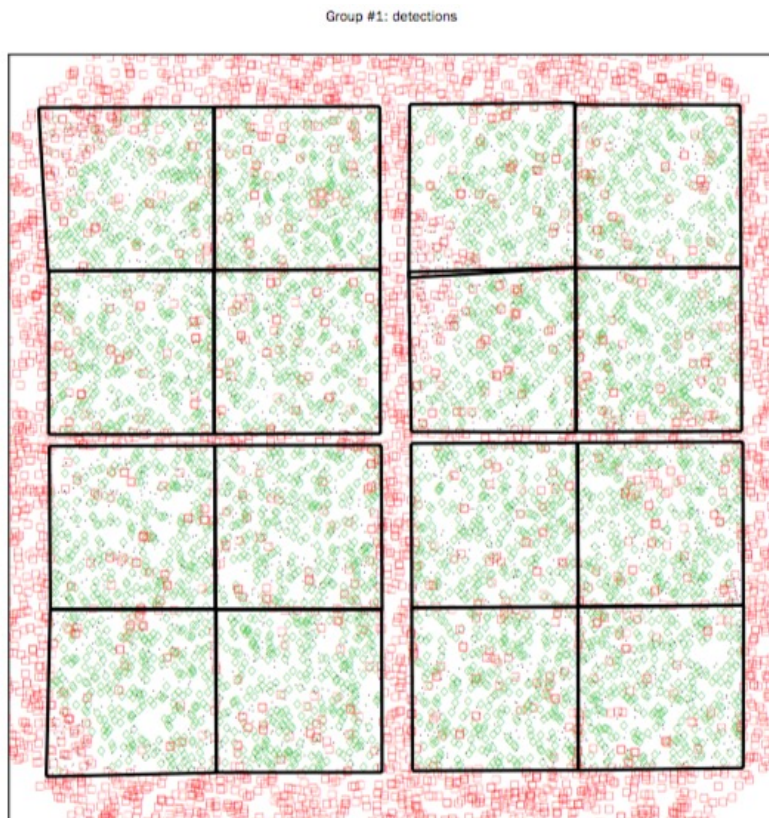
观测时间：20160203 212s 曝光



天测与测光

64222A
Ref: Gaia EDR3

Scamp

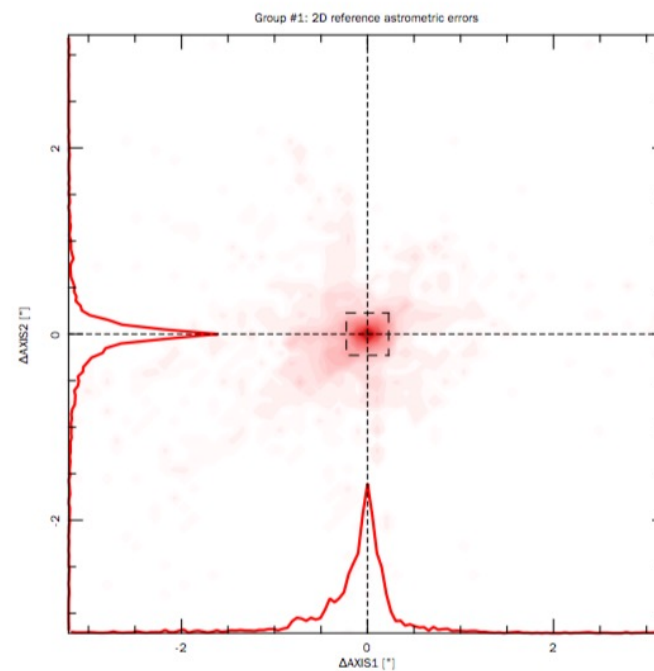
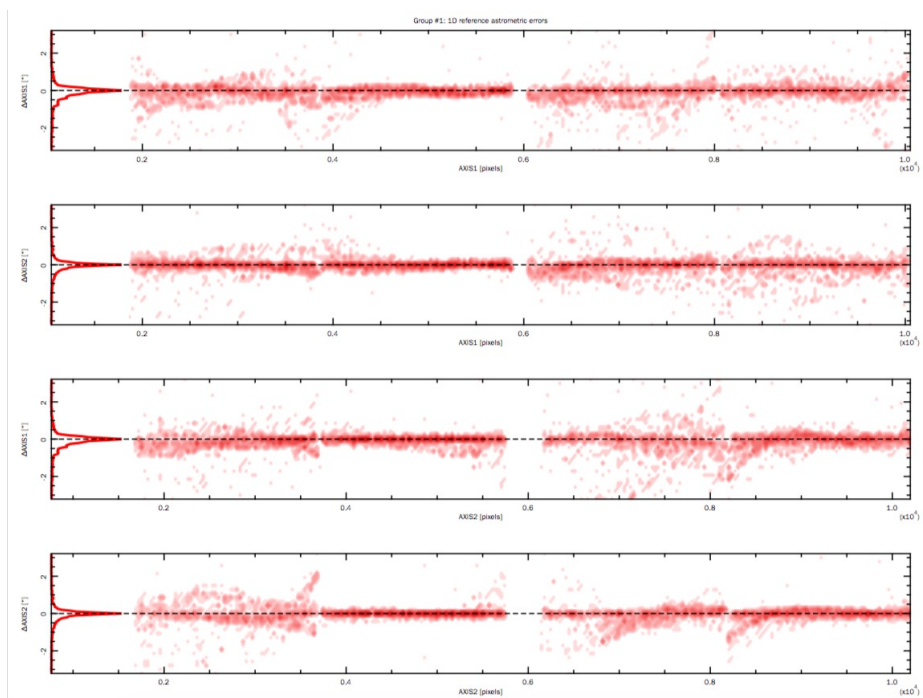


First solution: Run SExtractor of reduced image with initial WCS solution from pointing model from the telescope

天测与测光

64222A
Ref: Gaia EDR3

Scamp

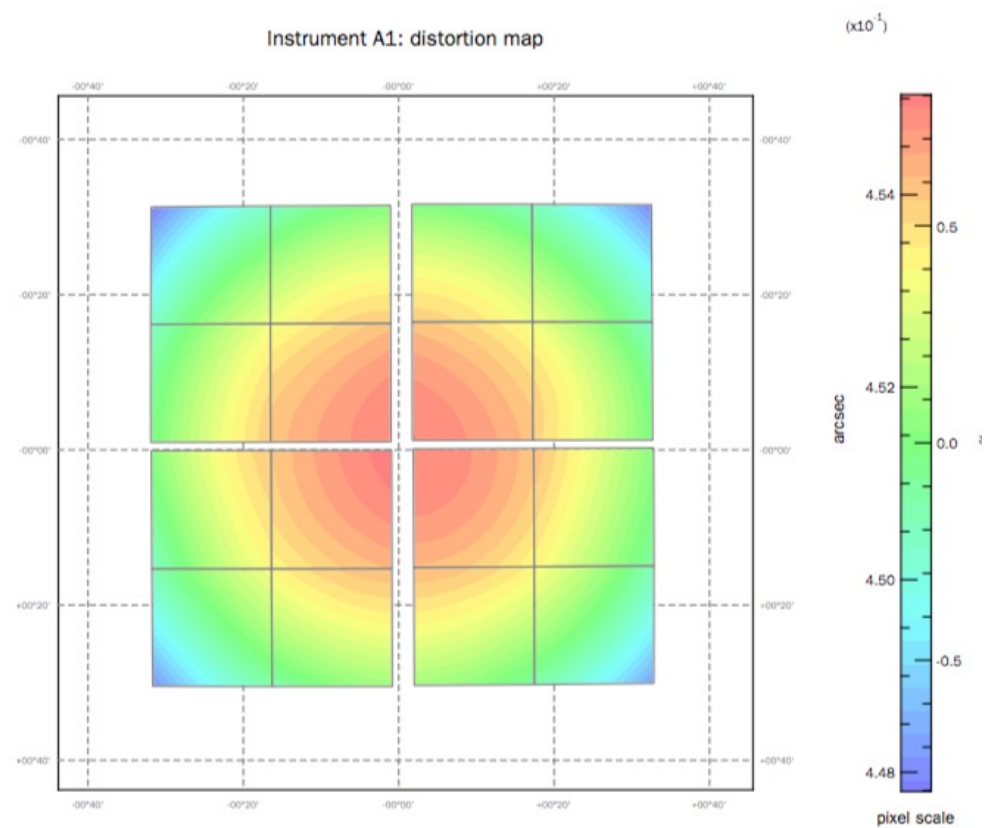
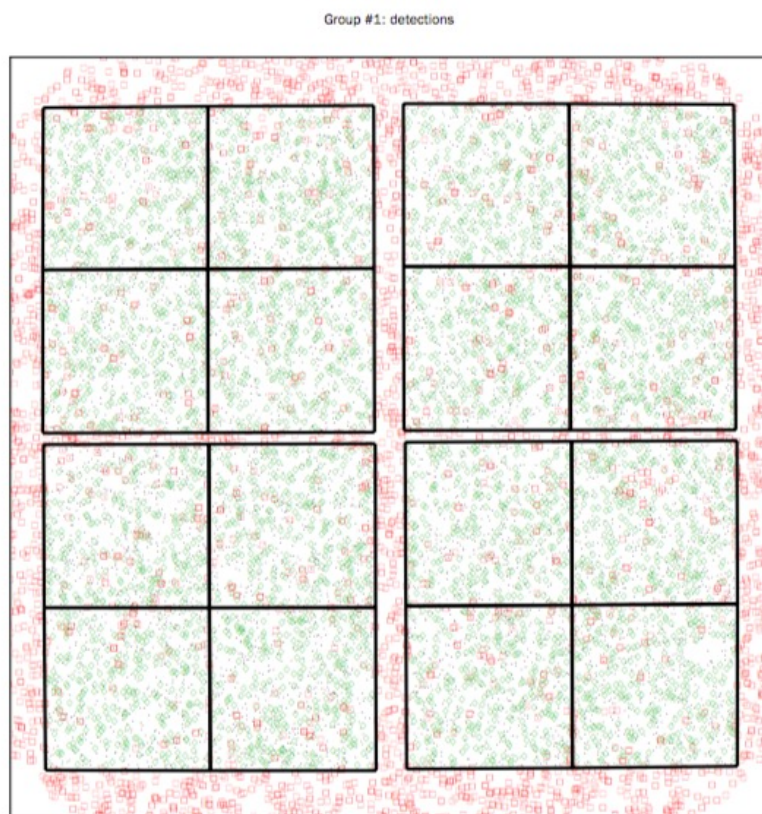


First solution: Run SExtractor of reduced image with initial WCS solution from pointing model from the telescope

天测与测光

64222A
Ref: Gaia EDR3

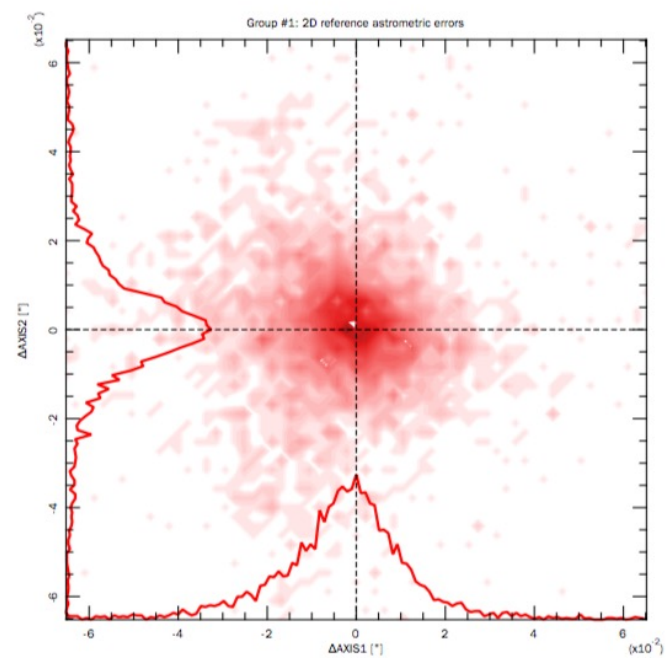
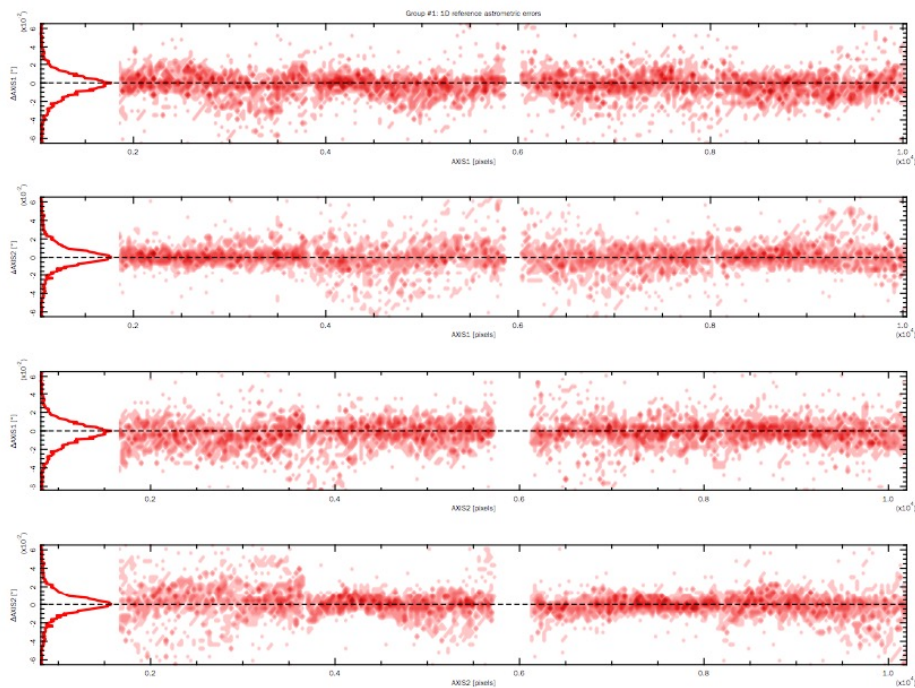
Scamp



天测与测光

64222A
Ref: Gaia EDR3

Scamp

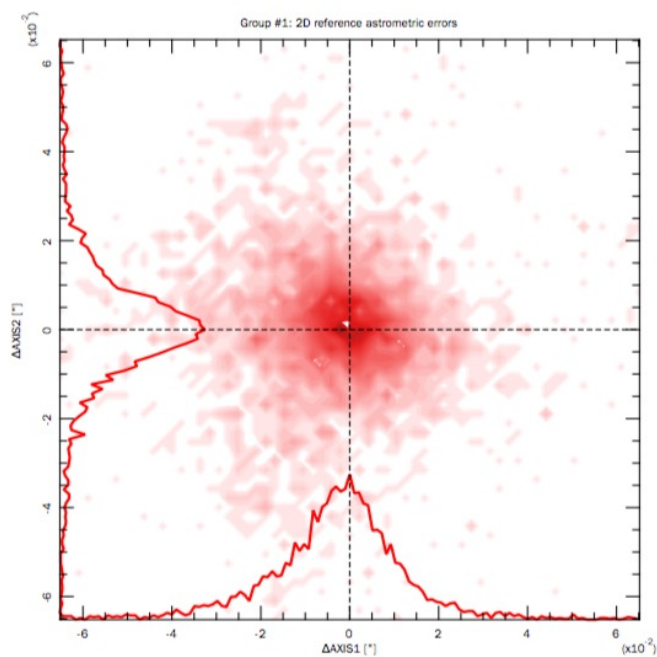


天测与测光

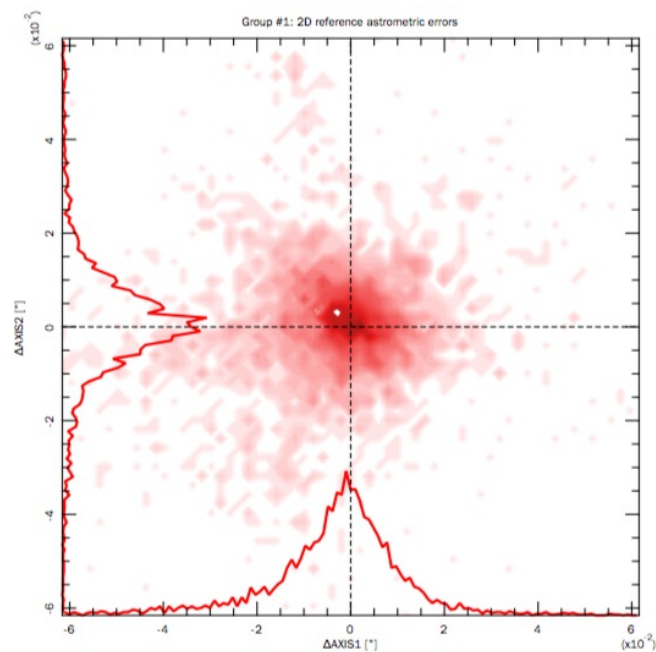
Scamp

64222A

64222B



sigma (RA) \sim 22 mas
sigma (Dec) \sim 24 mas

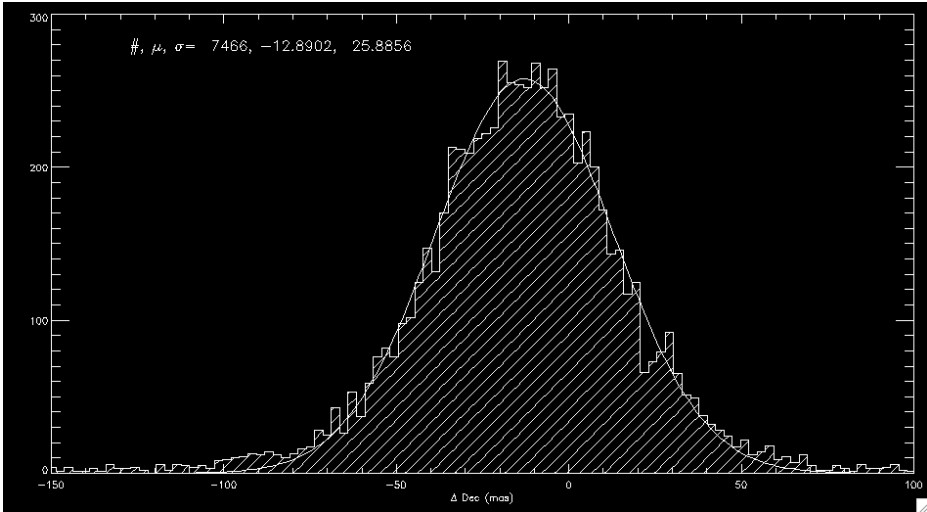
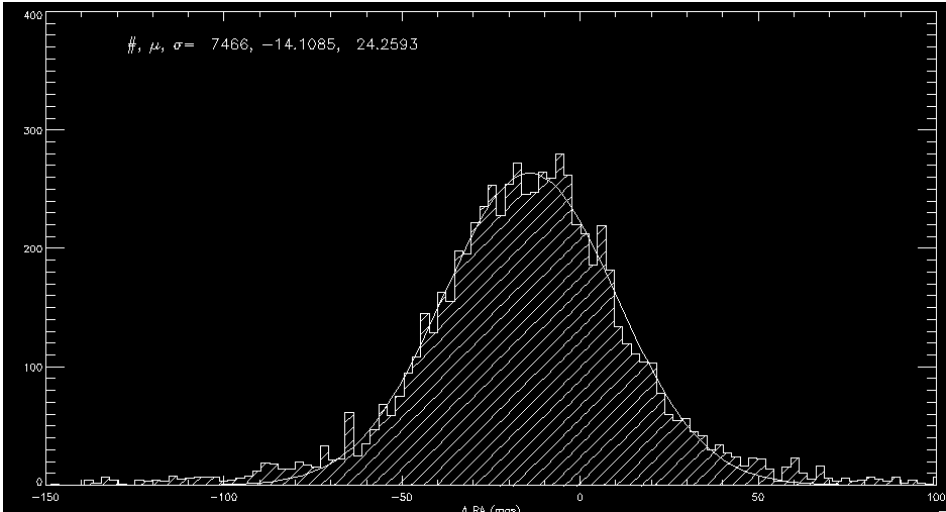


sigma (RA) \sim 20 mas
sigma (Dec) \sim 22 mas

天测与测光

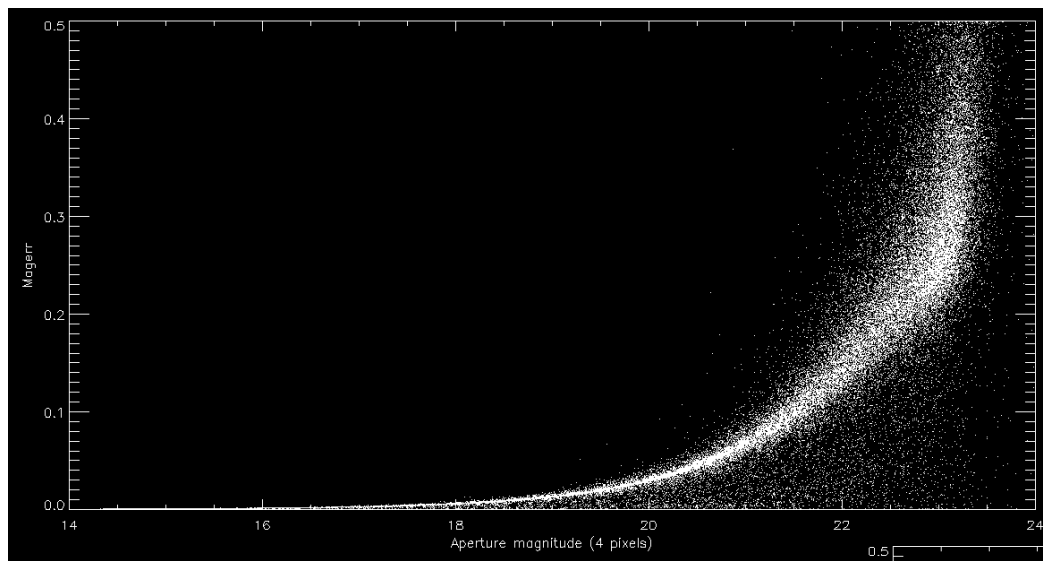
Scamp

64222 A v.s. B



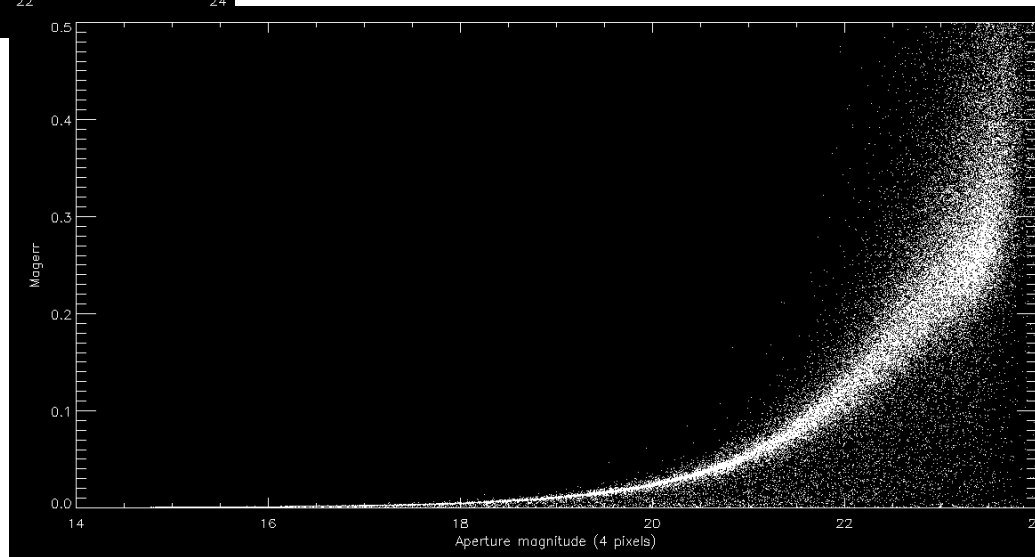
天测与测光

64222 A



Aperture magnitude
(4 pixels)

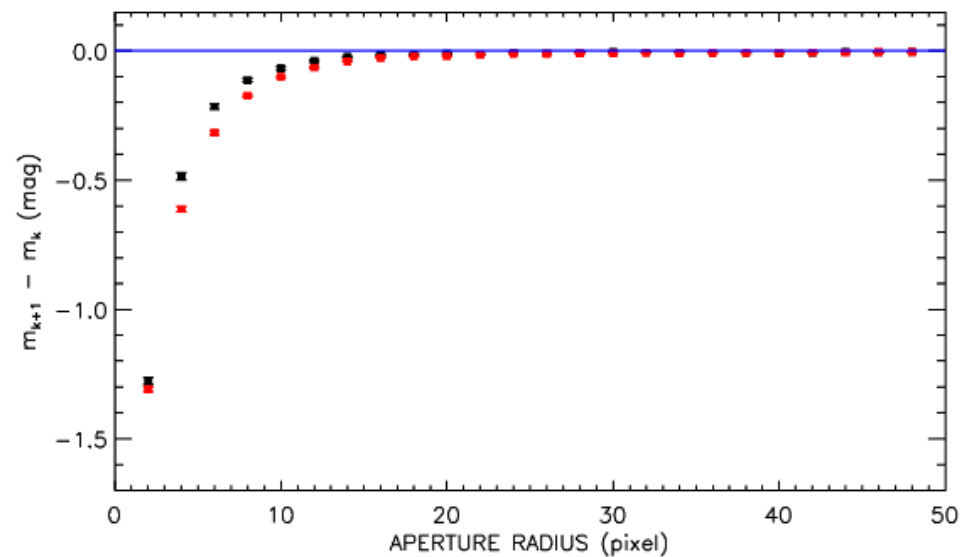
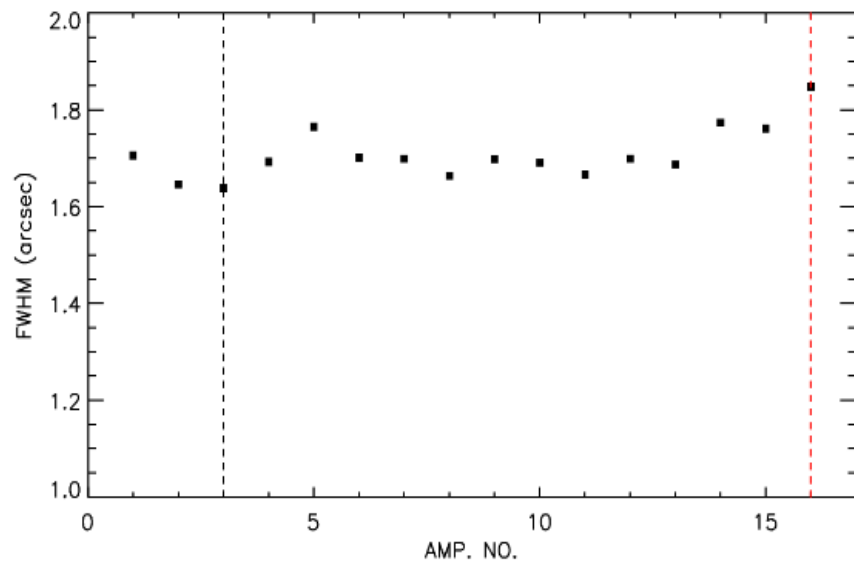
64222 B



SExtractor + PSFEx

天测与测光

Aperture correction:

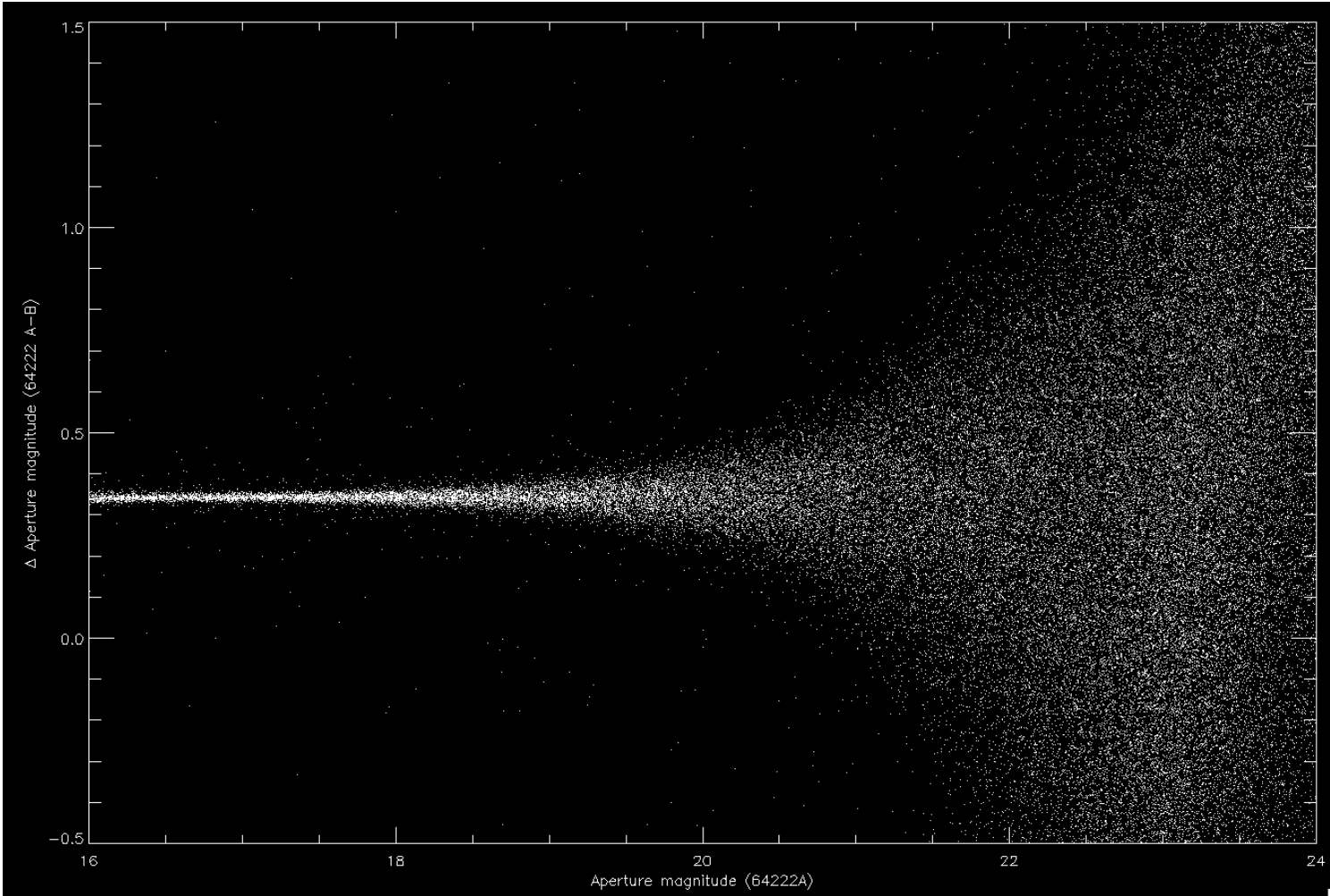


SExtractor + PSFEx

天测与测光

SExtractor + PSFEx

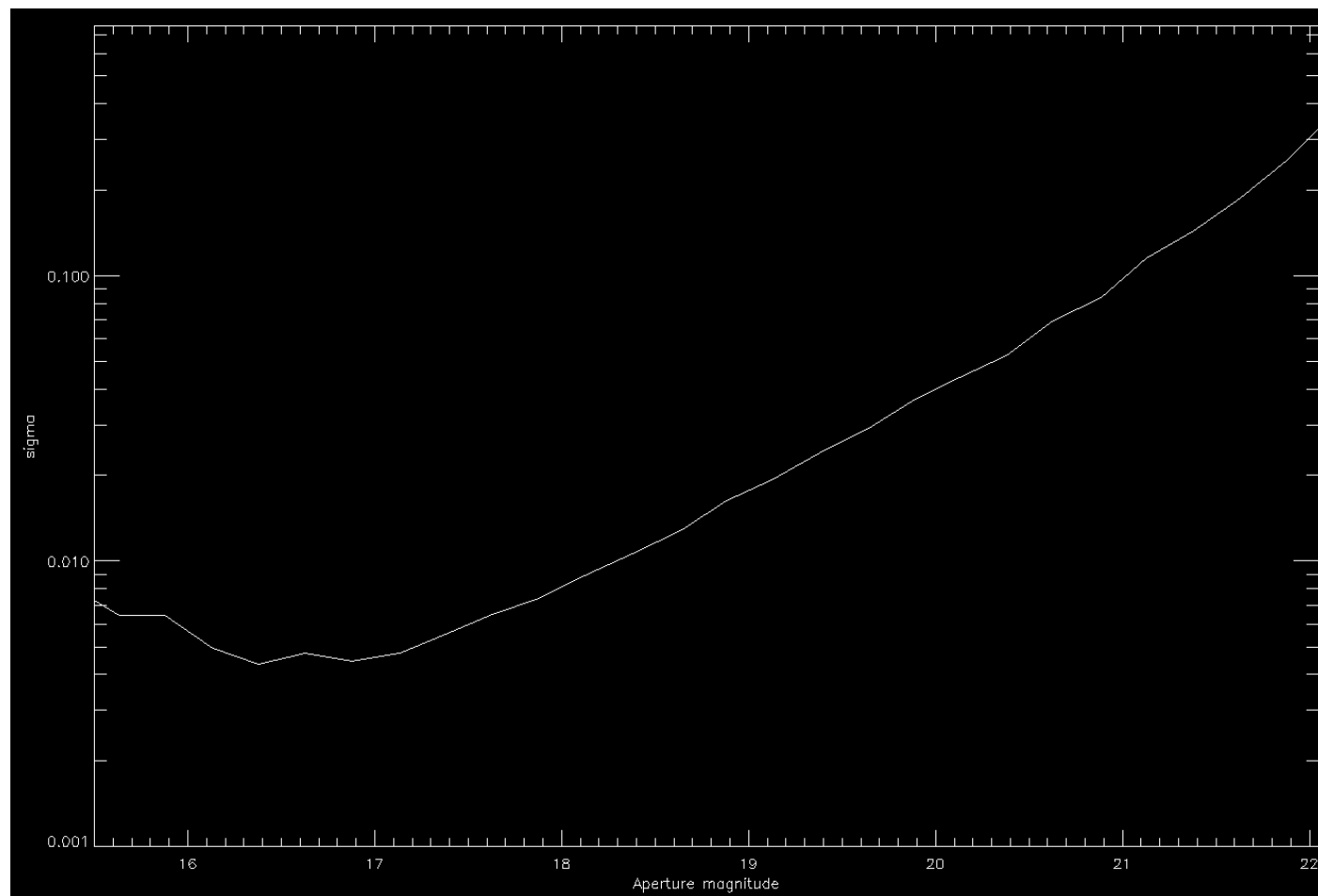
64222 A versus B



天测与测光

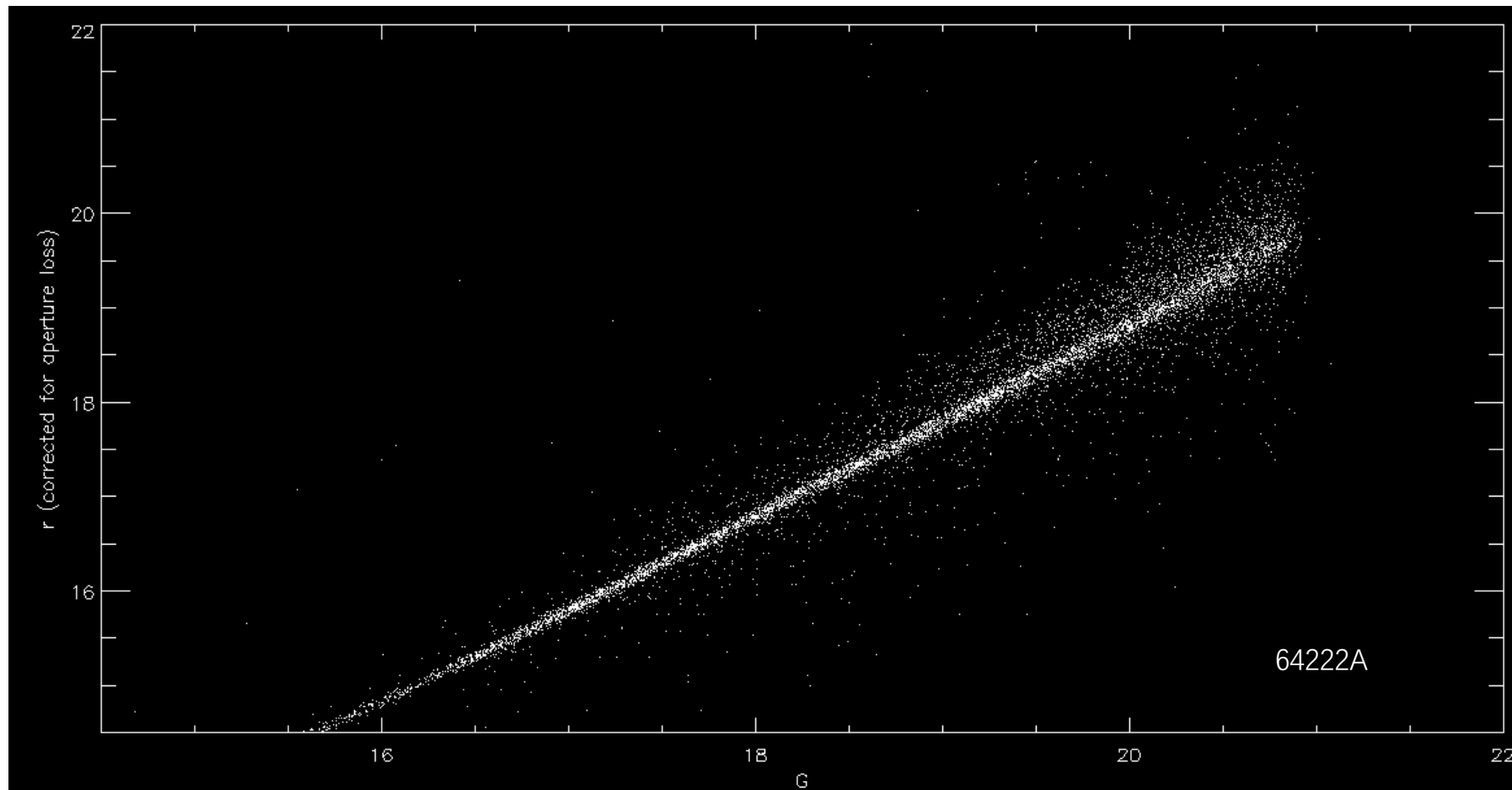
SExtractor + PSFEx

64222 A versus B



天测与测光

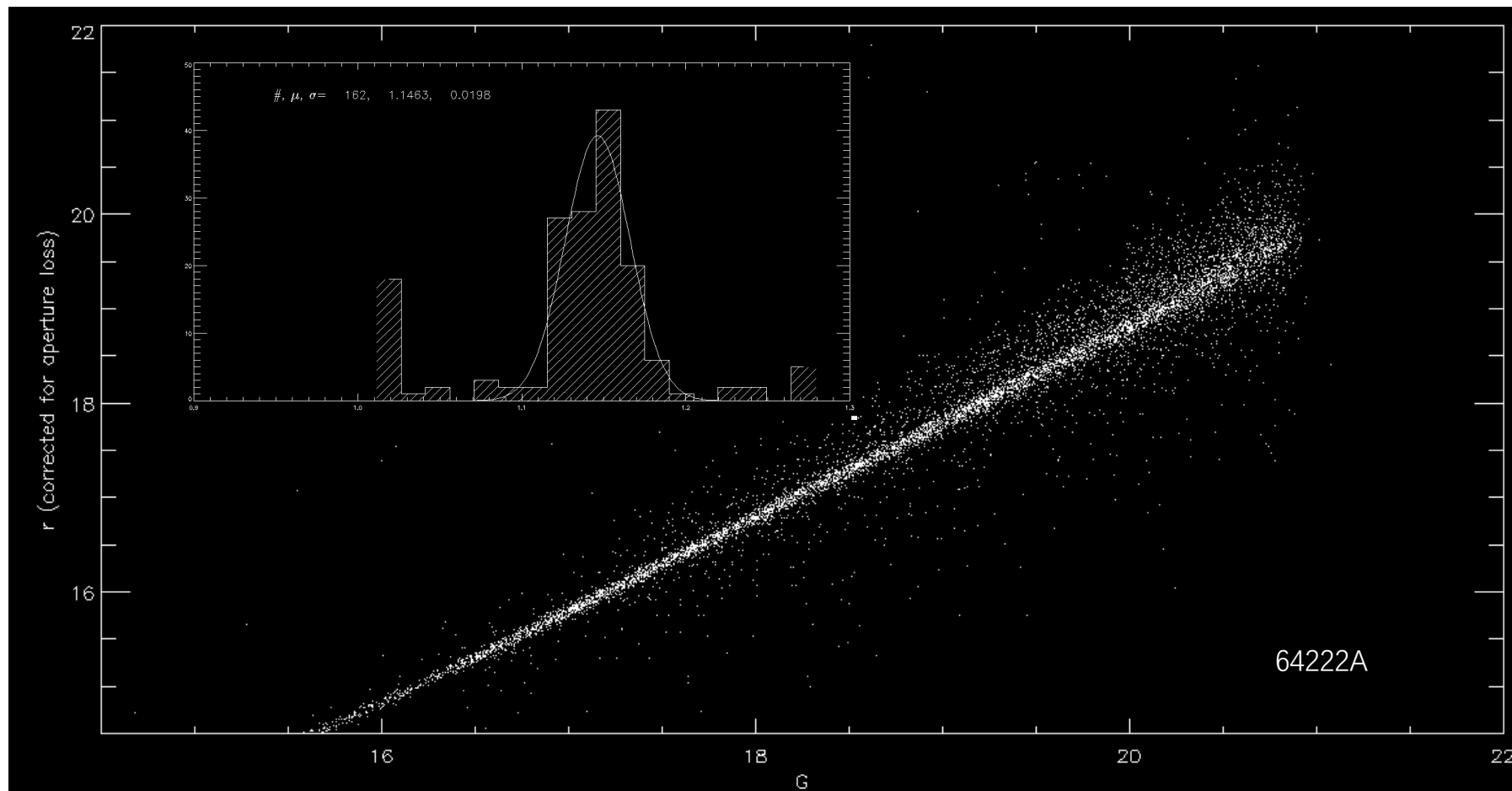
SExtractor + PSFEx



Compared to Gaia G

天测与测光

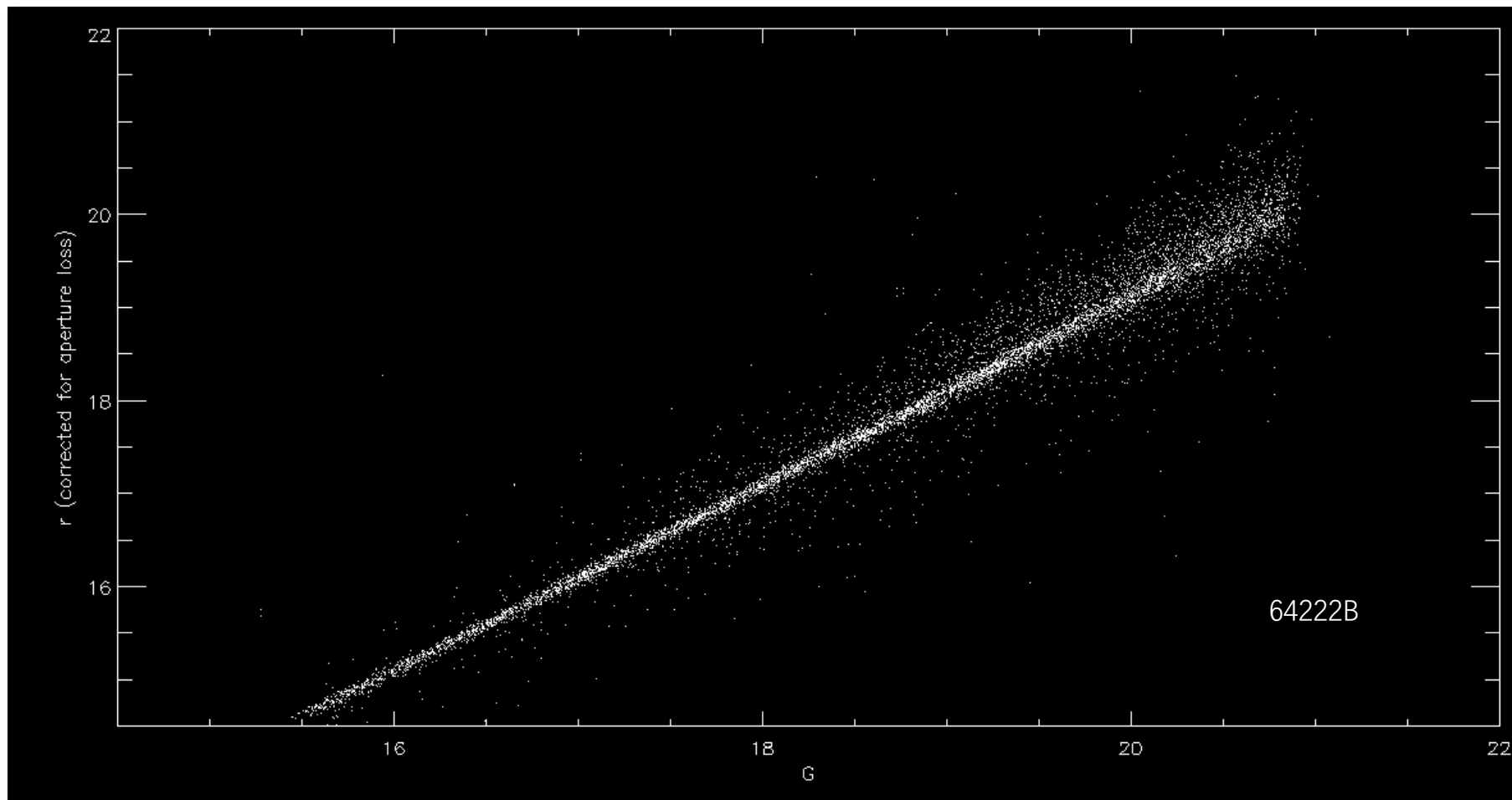
SExtractor + PSFEx



Compared to Gaia G

天测与测光

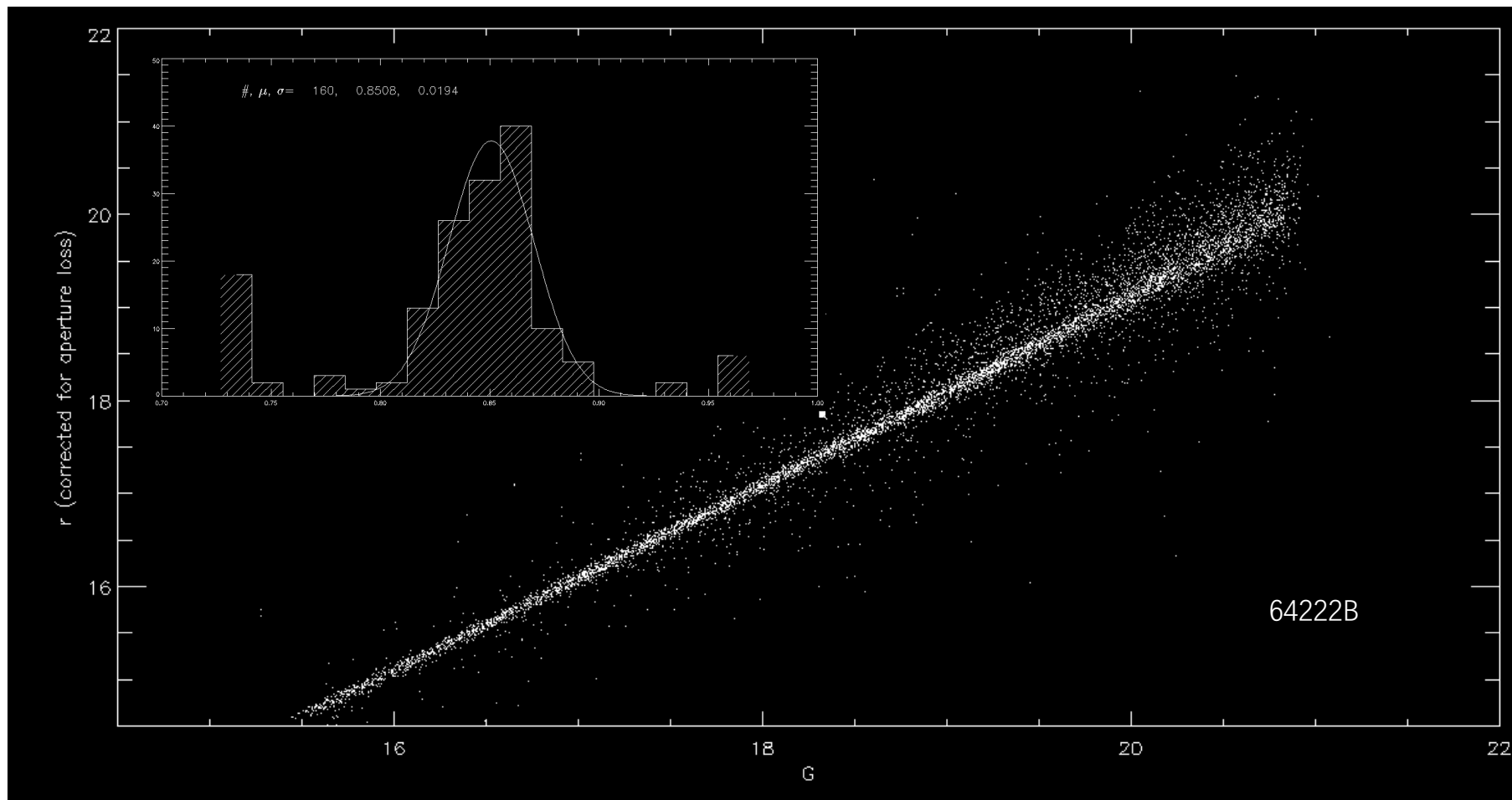
SExtractor + PSFEx



Compared to Gaia G

天测与测光

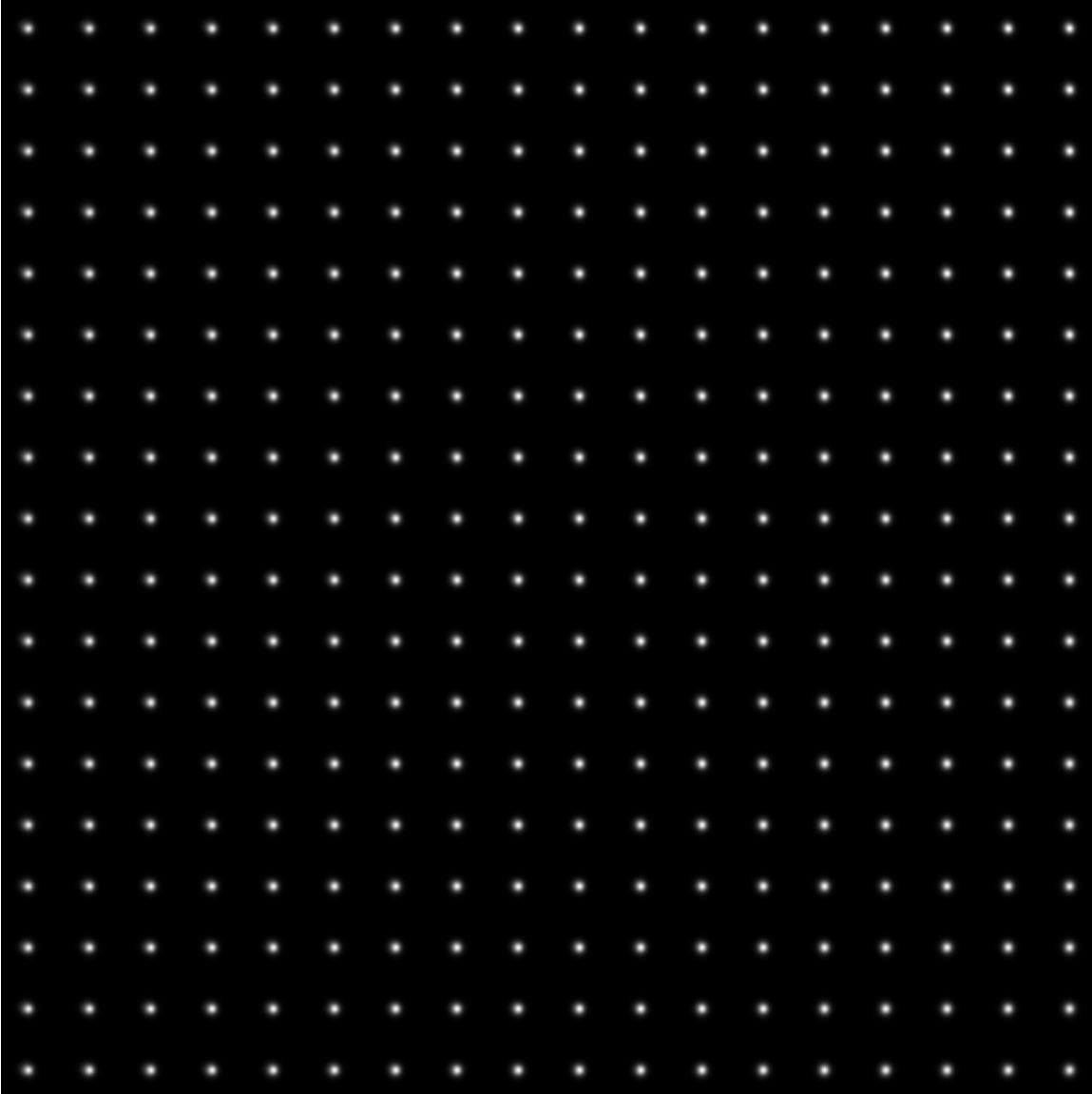
SExtractor + PSFEx



Compared to Gaia G

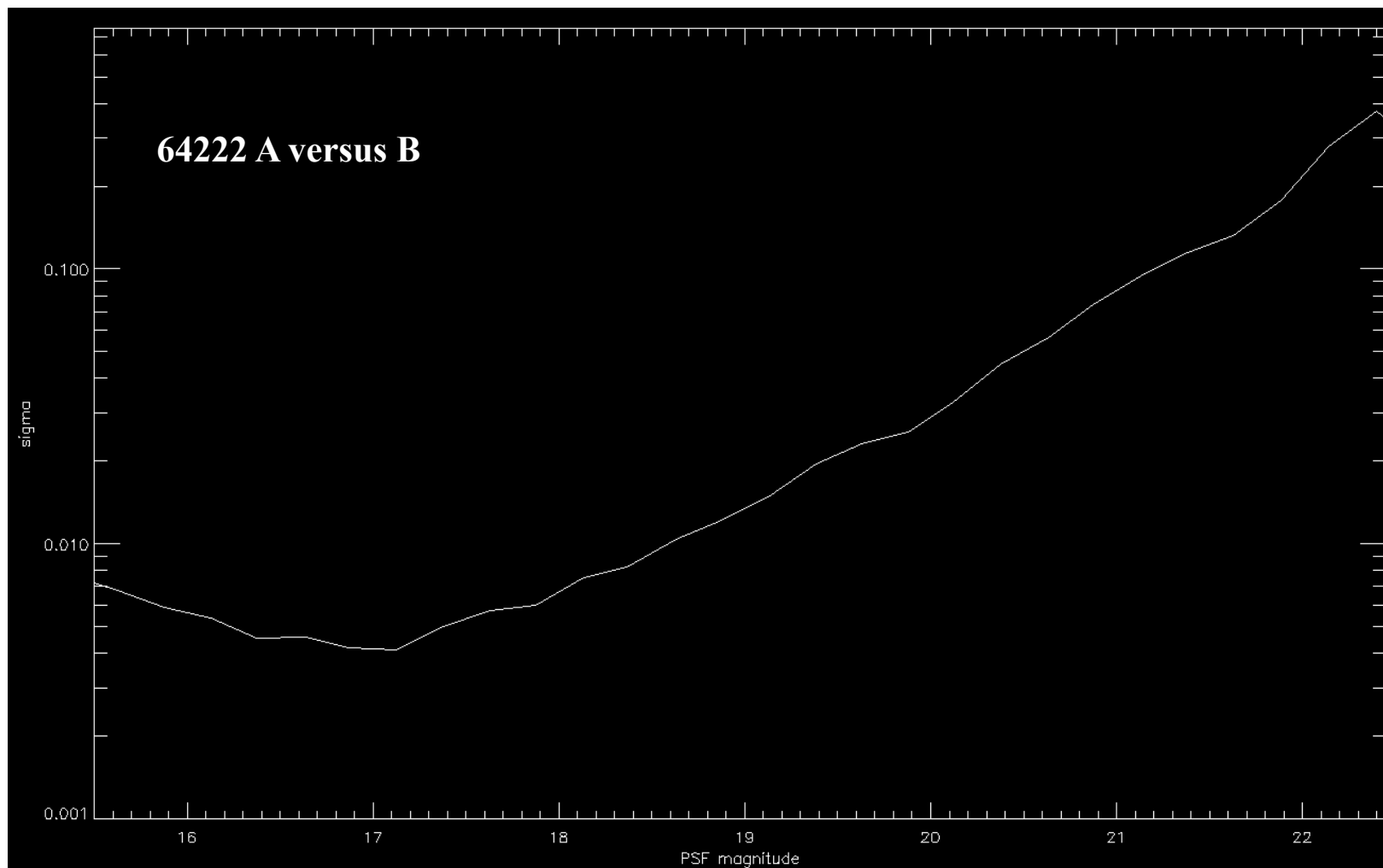
天测与测光

SExtractor + PSFEx



天测与测光

SExtractor + PSFEx



天测与测光

```
IDL> help,cc,/str
** Structure <1909200>, 58 tags, length=5376, data length=5362, refs=1:
NUMBER          LONG              1
FLUX_APER       FLOAT             393.838
FLUXERR_APER    FLOAT             58.7346
MAG_APER        FLOAT             Array[25]
MAGERR_APER     FLOAT             Array[25]
FLUX_AUTO       FLOAT             1286.83
FLUXERR_AUTO    FLOAT             306.742
MAG_AUTO        FLOAT             22.2262
MAGERR_AUTO     FLOAT             0.258870
MAG_PETRO       FLOAT             22.2262
MAGERR_PETRO    FLOAT             0.258870
SNR_WIN         FLOAT             8.77429
KRON_RADIUS     FLOAT             3.50000
BACKGROUND      FLOAT             -1.15763
FLUX_MAX        FLOAT             185.181
ISOAREA_IMAGE   LONG              19
ISOAREAF_IMAGE  LONG              39
X_IMAGE         FLOAT             5671.70
Y_IMAGE         FLOAT             269.411
ALPHA_J2000     DOUBLE            94.699654

DELTA_J2000     DOUBLE            56.413619
A_IMAGE        FLOAT             1.70247
B_IMAGE        FLOAT             1.37093
THETA_IMAGE    FLOAT             -10.0369
XWIN_IMAGE     DOUBLE            5671.6857
YWIN_IMAGE     DOUBLE            269.47892
ALPHAWIN_J2000 DOUBLE            94.699639
DELTAWIN_J2000 DOUBLE            56.413617
AWIN_IMAGE     FLOAT             1.04540
BWIN_IMAGE     FLOAT             0.563749
THETAWIN_IMAGE FLOAT             3.29667
ERRAWIN_IMAGE  FLOAT             0.217656
ERRBWIN_IMAGE  FLOAT             0.214979
ERRTHETAWIN_IMAGE
                FLOAT             7.22742
MU_MAX         FLOAT             22.6163
FLAGS          INT              0
FLAGS_WEIGHT   INT              0
FWHM_IMAGE     FLOAT             4.83339
FWHM_WORLD    FLOAT             0.000609545
ELONGATION     FLOAT             1.24184
ELLIPTICITY   FLOAT             0.194745
CLASS_STAR     FLOAT             0.834779
VIGNET         FLOAT             Array[35, 35]
FLUX_RADIUS    FLOAT             1.52044
FWHMPSF_IMAGE  FLOAT             2.25000
FWHMPSF_WORLD  FLOAT             0.000283750
XPSF_IMAGE     DOUBLE            5671.6660
YPSF_IMAGE     DOUBLE            269.47564
XPSF_WORLD     DOUBLE            56.413615
YPSF_WORLD     DOUBLE            94.699640
ALPHAPSF_J2000 DOUBLE            94.699640
DELTAPSF_J2000 DOUBLE            56.413615
FLUX_PSF       FLOAT             1658.84
FLUXERR_PSF    FLOAT             197.511
MAG_PSF        FLOAT             21.9505
MAGERR_PSF     FLOAT             0.129305
NITER_PSF      INT              0
CHI2_PSF       FLOAT             1.18686e-09
```

IDL>

流量定标

$$f_{\text{ADU}} = \kappa f$$

f : the flux of an object at earth (above the atmosphere)

f_{ADU} : the detected instrumental flux

κ depends on the exposure time, detector efficiency, filter responses, the telescope optical system, the optical path through the atmosphere, the SED of the objects in question

$$m_{\text{ADU}} = m - 2.5 \log_{10} (\kappa)$$

$$-2.5 \log_{10} (\kappa) = a(i, j; t) + k(t)x + f(i, j; t) + \dots$$

流量定标

$$f_{\text{ADU}} = \kappa f$$

f : the flux of an object at earth (above the atmosphere)

f_{ADU} : the detected instrumental flux

κ depends on the exposure time, detector efficiency, filter responses, the telescope optical system, the optical path through the atmosphere, the SED of the objects in question

$$m_{\text{ADU}} = m - 2.5 \log_{10} (\kappa)$$

$$-2.5 \log_{10} (\kappa) = a(i, j; t) + k(t)x + f(i, j; t) + \dots$$

**The optical response of the
telescope and detectors**

流量定标

$$f_{\text{ADU}} = \kappa f$$

f : the flux of an object at earth (above the atmosphere)

f_{ADU} : the detected instrumental flux

κ depends on the exposure time, detector efficiency, filter responses, the telescope optical system, the optical path through the atmosphere, the SED of the objects in question

$$m_{\text{ADU}} = m - 2.5 \log_{10} (\kappa)$$

$$-2.5 \log_{10} (\kappa) = a(i, j; t) + k(t)x + f(i, j; t) + \dots$$

Atmospheric extinction

流量定标

$$f_{\text{ADU}} = \kappa f$$

f : the flux of an object at earth (above the atmosphere)

f_{ADU} : the detected instrumental flux

κ depends on the exposure time, detector efficiency, filter responses, the telescope optical system, the optical path through the atmosphere, the SED of the objects in question

$$m_{\text{ADU}} = m - 2.5 \log_{10} (\kappa)$$

$$-2.5 \log_{10} (\kappa) = a(i, j; t) + k(t)x + f(i, j; t) + \dots$$

Detector flat fields

流量定标

Traditional methods: standard stars

Landolt standards (Landolt 1983; 1992): provide magnitudes accurate to $< 1\%$ in the *UBVRI* bands for 500 stars in the *V* magnitude range 11.5-16.

Stetson standards (Stetson 2000; 2005): extend Landolt's work to fainter magnitudes and provided the community with $\sim 1\text{-}2\%$ accurate magnitudes in the *BVRI* bands for $\sim 15,000$ stars in the magnitude range $V < 20$.

Ivezic standards (2007): present 1.01 million nonvariable unresolved objects from the equatorial stripe 82 with $< 1\%$ accurate magnitudes in *ugriz* bands in the *V* band magnitude range 14-22.

流量定标

Relative calibrations:

- **Ubercalibration (Ivezic et al. 2007; Padmanabhan et al. 2008)**
- **Stellar locus/color regression (SLR/SCR; High et al. 2009; Yuan et al. 2015)**
 - **Purely based on photometry (High et al. 2009)**
 - **Spectroscopy+photometry (Yuan et al. 2015)**



谢谢!

LAMOST与银河 ©Jin Ma 2012

2012.08.22 Nikon D90 + 10-24mm, F3.5, 14x30s, ISO2500

WWW.KARAJIN.COM